LAMINAR FREE CONVECTION THROUGH A POROUS MEDIUM

A Thesis Submitted
in Partial Fulfilment of the Requirements
for the degree of

DOCTOR OF PHILOSOPHY

by

ABHA RANI

to the

DEPARTMENT OF MATHEMATICS
INDIAN INSTITUTE OF TECHNOLOGY KANPUR
DECEMBER 1989

To

MY PARENTS

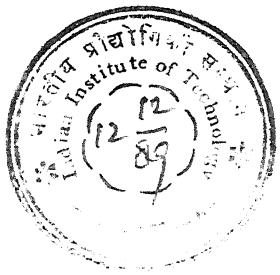

CERTIFICATE

This is to certify that the matter embodied in the thesis entitled 'LAMINAR FREE CONVECTION THROUGH A POROUS MEDIUM' by Abha Rani for the award of degree of Doctor of Philosophy of the Indian Institute of Technology, Kanpur, is a record of bonafide research work carried out by her under our supervision and guidance. The thesis has, in our opinions, reached the standard fulfilling the requirements of the Ph.D. degree. The results embodied in this thesis have not been submitted to any other University or Institute for the award of any degree or diploma.

(T. Sundararajan)
Assistant Professor
Mechanical Engineering Department
Indian Institute of Technology
Kanpur 208 016

(Punyatma Singh)
Professor
Department of Mathematics
Indian Institute of Technology
Kanpur 208 016

December, 1989

ACKNOWLEDGEMENTS

I hereby take an opportunity to express my sincere gratitude and thanks to my thesis supervisors, Prof. Punyatma Singh and Dr. T. Sundararajan for their valuable guidance during the period of present work.

I am extremely grateful to Profs. B.L. Dhoopar, J.B. Shukla, M.R.M. Rao and Dr. Manjul Gupta for encouraging me at my difficult moments.

I am indebted to my parents and my husband Shri Ajay Kumar Singh for their unfailing affection, solving my problems and leading me over many troubled spots.

I sincerely acknowledge the co-operation and moral support given to me by Puneet, Kalika, Shubhra and Dr. D.S. Pandey in the preparation of the present thesis.

I am thankful to all my friends, in particular to Ibha, Smita and Dr. J.K. Mishra for their splendid company during my stay at IIT Kanpur.

Finally, I thank to Swami Anand Chaitanya for his extensive patience in excellent typing of this thesis.

Abha Rani

December, 1989

SYNOPSIS

The work reported in the present thesis deals with the problems of flow and heat transfer through a porous medium.

In recent years, considerable interest has been envinced towards the study of natural convective flow phenomena within a fluid-saturated porous medium; such studies are of intrinsic importance and relevance to the various applications in the areas of petroleum engineering, chemical engineering, biomechanics, and geophysics.

For the modelling of flow through isotropic and homogeneous porous materials, the basic constitutive relation which has been widely used so far is the Darcy's law which relates the seepage velocity to the pressure gradient. In many practical situations, however, the porous medium is bounded by impermeable walls and has a high permeability, which render the Darcy's equation inapplicable for flow modelling. The inclusion of viscous stress terms in the Darcy's equation giving rise to a boundary layer type of flow near the impermeable wall, results in the so-called Brinkman model. A further extension of Darcy's law which takes into account the convective acceleration effects along with the viscous shear in the fluid is termed as the generalised Darcy's law.

The objective of the present work is to study two-dimensional

using generalised Darcy's law as the

idary layer situations as well as

nerical techniques have been used to

n-linear governing equations.

In the first chapter, an overview of the structure and properties of a porous medium is presented along with the conservation equations of mass, momentum and energy. Various flow models available for a fluid-saturated porous medium have been described. A brief survey of the published literature related to the present work is also presented.

In the second chapter, the existence of similarity solutions for free convection along a vertical plate immersed in a porous medium is analysed. Necessary and sufficient conditions are obtained in a porous medium described by generalised Darcy's law, the Brinkman model or the Darcy's law. The approach consists of defining an independent variable and two dependent similarity functions corresponding to the velocity and temperature solutions in terms of generalised transformation functions. Substituting these generalised transformation functions into the boundary layer equations, a set of ordinary differential equations will result only if the coefficients of all the terms are made constants. The minimum set of conditions to be satisfied for making these coefficients constant are referred to as similarity conditions. For the particular situation with wall temperature varying as a power function of distance, numerical solution has been obtained using the shooting technique. Velocity and temperature profiles have been presented for different permeability parameters and Prandtl numbers. It is found that in the boundary layer, the flow is weak and the temperature profile is less steep, when the voidage of the medium is small. Prandtl number is seen to have strong influence upon the temperature and

velocity profiles due to its effect upon heat penetration into the fluid.

The third chapter deals with the problem of conjugate free convection between a vertical fin and a saturated porous medium. The governing equations are based on the generalised Darcy's model and are solved iteratively within the framework of boundary layer approximations by a highly-implicit finite difference scheme. A variable mesh size is used in the direction normal to the fin surface in order to obtain the flow and heat transfer characteristics inside the boundary layer accurately. It is observed that the fin cooling is more effective at higher Grashof number or permeability parameter due to stronger convection effects. The local Nusselt number increases with the Grashof number, permeability parameter and Prandtl number and it decreases slightly with the conduction-convection parameter.

Unsteady natural convection in a rectangular enclosure is presented in fourth chapter. The enclosure consists of two isothermal vertical walls and two adiabatic horizontal walls. A general parametric study in terms of the Rayleigh, Darcy and Prandtl numbers has been presented. . The flow and temperature field solutions are obtained using the finite difference technique. The upwind procedure is applied for convection terms along with the central differences for the diffusion terms for spatially discretizing the governing equations. The timewise discretization is performed using a fully implicit scheme. The resulting equations are solved using line-by-line technique coupled with the tridiagonal matrix algorithm. Streamlines and isotherms have been plotted for analysing the flow and heat

transfer inside the enclosure at different times. The transient variation of average Nusselt number at the hot wall is also obtained for highlighting the rate of heat transfer between the wall and the fluid trapped inside the porous matrix. The flow is found to be unicellular and governed by the modified Rayleigh number; the product of the Rayleigh and Darcy numbers.

The last chapter deals with the problem of free convection over a moving vertical plate in a porous medium. The problem has an exact solution for the values of Prandtl number greater than or equal to unity. However, for Prandtl number less than unity, there is no exact result. Therefore, for Prandtl number less than unity the problem is solved here analytically by the momentum integral method and numerically by finite difference method. The results obtained by the two methods agree well. The fluid velocity at a point decreases with Grashof number and Prandtl number.

CONTENTS

CHAPTER I

INTRODUCTION

1.1 GENERAL BACKGROUND

The study of processes involving fluid flow and heat transfer through saturated porous media has evoked immense research interest in recent years. A broad range of applications including geothermal systems, crude oil production, ground water pollution, fibre and granular insulation, filtration and storage of nuclear waste material etc. have been modelled as porous media systems. In such processes the intersticial fluid trapped in the pores is subjected to vapourization, condensation and heat or mass transport due to the prevailing temperature or concentration gradients.

Most of the analytical and numerical works in this area accept Darcy's law [1] as the macroscopic equation of motion, which states that (seepage) velocity is proportional to the applied pressure gradient and that flow resistance is directly proportional to fluid viscosity and inversely proportional to the permeability of the medium. However, the Darcy's law becomes inapplicable when the porous medium has a high permeability and is bounded by impermeable walls. In these cases, due consideration needs to be given to factors such as inertial effects in the fluid. Later generalizations of the Darcy's law have focussed attention on some of these factors.

The inclusion of viscous shear stress terms in the flow equations and the consideration of a velocity field which

satisfies no slip at impermeable walls, have been proposed by Brinkman [2]. This is the so-called Brinkman's extension, which accounts for the flow resistance due to the fluid viscosity itself. Yamamoto and Iwamura [3] proposed a flow model in which the effects of inertia are taken into account via convection terms in the momentum equations. Obviously this is an important correction which has to be considered at higher flow rates through the porous medium. Yet another approach to handle the inertial effects was proposed by Forchheimer [4], which approximately accounts for the losses in the pressure due to flow separation in the pores, by the inclusion of an additional term in the flow equations. With all these extensions, the flow models for porous media situations have more or less the same general structure as that of Navier-Stokes equations for free fluid flows.

Most of the studies available at present on porous medium applications do not consider a generalized Darcy's law. In the present work, this generalized Darcy's model is taken as the equation of motion to study two-dimensional natural convection problems with and without the use of boundary layer approximations. The governing partial differential equations for these problems are non-linear, which are amenable to analytical study only in some limited cases. In the present work, full numerical solutions have been obtained using finite differences or shooting techniques, along with analytical solutions where available. Detailed velocity and temperature distributions and Nusselt numbers signifying the overall heat transfer rates, have been presented. Comparisons with previous works have also been provided where possible.

1.2 DESCRIPTION OF THE STRUCTURE OF A POROUS MEDIUM

Examples of porous materials are numerous. A few commonly encountered porous materials are soil, porous or fissured rocks, ceramics, filter paper and a loaf of bread. Somewhat less obvious examples, but still a part of this group, are large geological formations where open passages may be of substantial size and far apart. All of these examples have some properties in common that permit them to be grouped together as porous media.

A porous medium may loosely be described as a 'solid with holes'. However, a solid block with isolated holes or pores would not normally be classified as a porous medium for modelling flow through the block. However, the same block may be acceptable as a porous solid in connection with thermal insulation. In flow applications, the definitions may be somewhat improved by stipulating that the pores be interconnected by several continuous paths from one side of the medium to the other with an even distribution (in either a regular or random manner) of holes and paths over the entire porous medium domain.

Summarising these preliminary observations, the porous medium is defined [5] as:

(i) A portion of space occupied by heterogeneous or multiphase matter. It should include a solid phase and atleast another phase which is not a solid but may be a gas or liquid. The solid phase is called the solid matrix. That space within the porous medium domain which is not a part of the solid matrix, is referred to as the void space (or pore space).

(ii) The void space should be evenly distributed throughout the porous medium and should be present inside each representative

elementary volume. An essential characteristic of the porous medium is that the specific surface of the solid matrix (defined as the total interstitial surface area of pores per unit bulk volume of the porous medium) is relatively high. In many respects, this characteristic determines the interaction between the solid matrix and the fluid in porous media. Another basic feature of a porous medium is that the pores comprising the void space are relatively narrow.

(iii) At least some of the pores should be interconnected. The interconnected pore space is sometimes referred to as the effective pore space. As far as the flow through porous medium is concerned, the unconnected pores may be considered as part of the solid matrix. Certain portions of the interconnected pore space may, in fact, also be ineffective with regard to the flow through the medium. For example, pores may be dead-ended so that no flow occurs through them. Another way to define this pore interconnection characteristic of a porous medium is by requiring that any two points within the effective pore space be connected by many curves with an arbitrary maximal distance between them. For a finite porous medium domain, this maximal distance is a macroscopic property which is dictated by the dimensions of the domain.

1.3 DEFINITION OF POROUS MEDIUM PROPERTIES

1.3.a Porosity

Porosity is defined as the fraction of the bulk volume of material which is occupied by voids. Thus, the porosity ϕ is given by

$$\phi = \frac{V_P}{V_B} = \frac{\text{Volume of pores}}{\text{Bulk volume}} \quad , \qquad (1.1)$$

Since the portion of bulk volume not occupied by pores is occupied by solid grains or the matrix of the material, it follows that,

$$1 - \phi = \frac{V_S}{V_B} = \frac{\text{Volume of solids}}{\text{Bulk volume}} \quad . \qquad (1.2)$$

From the above definitions, it is evident that ϕ is a macroscopic property. Two classes of porosity can be defined, namely, the absolute or total porosity and the effective porosity. Absolute porosity is the fractional void space with respect to the bulk volume, regardless of the pore connections. Effective porosity is the fraction of bulk volume constituted by interconnecting pores. Many naturally occurring rocks such as lava and other igneous rocks, have a high total porosity but essentially zero effective porosity. Effective porosity is an indication of permeability of the porous medium but not a measure of it [6].

1.3.b Permeability

Permeability is that property of porous material which characterises the ease with which the fluid may be made to flow through the material by an applied pressure gradient. Permeability can also be thought of as fluid conductivity of the porous material.

The value of permeability is determined by the structure of the porous material. It has the dimensions of the square of length and is roughly a measure of the mean-square of the pore diameter in the material. Many porous materials have a directional quality in their structure. As a consequence, the permeabilities measured with flow perpendicular to each face of a cube may not be equal. Such materials are termed as anisotropic.

1.4 GOVERNING EQUATIONS

The analysis of flow and heat transfer in a porous medium is based on transport equations resulting from the differential balance laws. In many situations, detailed information of the velocity and temperature field is required to predict global effects such as flow resistance or heat flux from a given object. The flow and temperature fields, in turn, are extracted from the solution of the associated transport equations subject to pertinent boundary conditions. When flow occurs through a complex structure such as a porous medium, the transport equations are still valid inside the pores, but geometric complexity prevents general solutions of the detailed velocity and temperature fields. Since it is impossible to know what is happening in each of the many pores, at best one can attempt to predict the statistical average of the physical quantities over certain representative volumes of the system. This aspect has been investigated in detail by Slattery [7,8] and Whitaker [9]. They have considered a representative volume that is large compared to the pore size of the materal but small compared with the characteristic length of the object.

Here, we shall define the characteristics of an idealized porous medium which is often employed in the modelling of porous media flows. It is assumed that the medium is isotropic and consists of fine particles which are uniformly scattered and fixed in space. Shrinking and swelling of the porous medium during the flow is neglected and the density of the particles is assumed to be constant. Any suitable microscopic volume of the medium contains both solid and fluid phases. In other words, the matter

in any infinitesimal volume of the system under consideration will always be a solid-fluid mixture. For the fluid phase, a single liquid or gas is considered. Thus the state of an infinitesimal volume of the phases will be defined by the properties of the individual phases for the sake of simplicity in modelling. These properties are called intrinsic or actual properties. It is sometimes assumed that each of the pores occupies the entire control volume at any given point in the system. It is, therefore, necessary to modify some of the properties of the phases by appropriate volume averaging. These modified properties are called the bulk properties. From the above considerations, it is evident that for applying thermodynamic and hydrodynamic equations to an infinitesimal volume of the system, it will be necessary to use bulk properties of the phases [10].

1.4.a Conservation of Mass

As discussed above, an infinitesimal volume of the system at any point is assumed to contain both the phases and each phase is assumed to occupy the entire volume. The velocity of the fluid phase is therefore defined as the fluid mass flow rate per unit area of the system (usually called the mean filter velocity) at a given point divided by the bulk density of the fluid at that point. Since a continuum model is considered, in general, for a three-dimensional averaged flow the mass conservation statement reads as :

$$\frac{\partial \rho}{\partial t} + \nabla.\rho\underline{v} = 0, \qquad (1.3)$$

where, $\underline{v}$ is the volume averaged velocity vector. For an incompressible fluid, one may write,

$$\nabla.\underline{v} = 0 \qquad (1.4)$$

1.4.b Conservation of Momentum

Darcy's Model

Most of the available analytical work on fluid flow and heat transfer through porous media are based on Darcy's law. This law was established in 1856 by Darcy empirically, and since then has been verified experimentally by numerous investigators for Newtonian fluid motion in porous media at low flow rates. It states that for an isothermal fluid moving with a slow steady velocity u under a pressure gradient $\frac{dP}{dx}$ through a porous homogeneous and isotropic bed,

$$u = -\frac{K}{\mu}\frac{dP}{dx}, \qquad (1.5)$$

where, μ is the fluid viscosity and K is an empirical constant called the permeability of the medium. Originally the Darcy's law was established to obtain the average or apparent flow rates of fluids through porous media in one-dimensional flow. Later researchers, assuming the fluid velocity to be a continuous function of space co-ordinates have given Darcy's law for flow fields in two or three dimensions. The extension of Darcy's law to multi-dimensional flow including the body force term is expressed as,

$$\underline{v} = \frac{K}{\mu}[-\nabla P + \underline{f}], \qquad (1.6)$$

where, $\underline{f}$ is the body force vector given by the weight of the fluid per unit volume. It is to be noted, however, that Darcy's law is established empirically and it can not be derived analytically, by performing a momentum balance on a small element of the porous medium. It is merely a constitutive relation which does not yield much information about the permeability of the porous medium. The

drawbacks of Darcy's law are that it does not satisfy the no slip condition and is not valid for high flow rates.

Non-Darcy Models

There is enough evidence to indicate that Darcy's law is valid as long as Reynolds number ($R = \frac{uK^{1/2}}{\nu}$) is small compared to unity. The frictional resistance offered to flow by the solid matrix, is the predominant factor in this flow regime. As the velocity of the flow increases, a region of gradual transition is observed from laminar flow with dominant viscous forces, to still a laminar flow with inertial forces governing the flow. Often the value of Reynolds number R = 100 is mentioned as the upper limit of this transition region in which Darcy's law completely breaks down. Some researchers explain this deviation from the linear law by the separation of flow from the walls of the solid matrix caused at large Reynolds number by inertial effects.

(i) Forchheimer's Model

There is no universally accepted non-linear law which is valid for Reynolds number greater than unity. Many such relationships appear in the literature. The more general law follows from Forchheimer's modification [11] of the Darcy's law which may be written as

$$-\nabla P = \frac{\mu}{K}\underline{v} + b\,\rho|\underline{v}|\underline{v} \qquad (1.7)$$

where, b is another empirical constant. Ergun [12] and Ward [13] suggested a similar equation of motion.

(ii) Brinkman Model

In Darcy's law the term representing the viscous stresses in the fluid is not considered. This may lead to significant errors

near an impermeable solid boundary where a boundary layer with large velocity gradients may exist due to the no slip condition at the wall. Thus, for accurate modelling one has to take into account the viscous shear stresses, in addition to the Darcy resistance, however small they may be in the bulk of the fluid flow. Such an approach was postulated for the first time by Brinkman [2], for which a rigorous theoretical justification was given later by Tam [14] and Lundgren [15]. Their contention was that at the rigid boundary the no slip condition must be applied and this is inconsistent with the use of the usual Darcy equation. Based on these considerations, the momentum equation proposed by Brinkman is of the form:

$$\nabla P = -\frac{\mu}{K}\underline{v} + \mu \nabla^2 \underline{v}, \qquad (1.8)$$

where, μ is the viscosity of the fluid.

(iii) Generalised Darcy's Law

In situations such as the flow through porous filters used for separating suspended particles from a gas stream, the inertial terms are quite important. Several studies [16-20] have been made to analyse such flows on the basis of a generalised Darcy's law which bears a lot of similarity to the Navier-Stokes equations for the free fluid.

Most porous filters are made of fibrous materials and their porosity is close to unity [21,22]. In order to accurately predict the flow in such a highly porous medium under non-isothermal conditions, the buoyancy effects needs to be taken into consideration. Also, while accounting for the viscous stresses in the fluid due to velocity gradients in the flow, the form of the viscous term may be taken as in the case of a pure

fluid. Thus, the fundamental equations for an incompressible flow through a medium of high porosity are given by:

$$\rho \left[\frac{\partial \underline{v}}{\partial t} + (\underline{v}.\nabla)\,\underline{v} \right] = -\nabla P + \mu \nabla^2 \underline{v} + \rho \underline{g} - \frac{\mu}{K}\,\underline{v}. \qquad (1.9)$$

When Reynolds number R << 1, the convection terms can be safely neglected and equation (1.9) reduces to the one proposed by Brinkman. Also if the porosity of the medium is low, the Darcy term will dominate and it will chiefly account for the pressure drop. Thus, equation (1.9) may be taken as the generalized momentum equation which boils down to the equations corresponding to the other models in the appropriate range of parameters.

1.4.c Conservation of Energy

The energy equation for a fluid-saturated porous medium was obtained by Wooding in 1957 [23]. For an isotropic homogeneous porous medium in three-dimensional flow, this equation can be written as:

$$\frac{\partial T}{\partial t} + (\underline{v}.\nabla)\,T = \alpha \nabla^2 T \qquad (1.10)$$

where, T is the temperature and α is the thermal diffusivity of the fluid-saturated porous medium. In this equation, the viscous dissipation effect and the internal heat generation have been neglected. It is to be noted, however, that the above form of energy equation for a porous medium is derived by averaging the energy equations for fluid and solid parts over an elementary volume.

1.5 LITERATURE SURVEY AND THE PRESENT WORK

Early theoretical and experimental studies of convective flow of a fluid in a porous medium were reported in connection with the salt in subterranean sand layers [24-27]. Study of the motion of underground water with particular reference to geothermal

phenomena was presented by Wooding [23,28-33], Elder [34-37] and McNabb [38]. The results were presented on the structure of flow field and the corresponding heat transfer rates for convection of fluid in a porous medium owing to heat generation from below. The criterion for the onset of convective flow was predicted theoretically by Lapwood [39], while Wooding [33] and McNabb [38] introduced the concept of boundary layers in porous media.

Boundary layer analysis has been applied to the problem of free convection in a porous medium about a vertical flat plate, when the wall temperature is taken to be a power function of distance from the leading edge, by Cheng and Minkowycz [40]. They obtained similarity solutions for the problem. In a subsequent paper Cheng [41] used the Karman-Pohlhausen integral method to obtain the local Nusselt number for a number of convective heat transfer problems in a porous medium. It was found that the approximate solutions for the Nusselt number obtained from the integral method with different assumed profiles are in good agreement with those obtained by similarity solutions. The problem of natural convection adjacent to a vertical or horizontal heated surface with a power law variation in the wall temperature was studied by Cheng and Chang [42]. The results were obtained by the perturbation method where the first approximation gives the boundary layer solutions. A numerical solution for free convective flow past a vertical semi-infinite flat plate embedded in a highly saturated porous medium with a non-uniform temperature or a non-uniform heat flux distribution on the surface was developed by Na [43]. Both local heat transfer rate and excess surface temperature as a function of distance along the plate were

tabulated for a few cases of prescribed wall temperature and heat flux distributions. A study of the flow and heat transfer along a vertical flat plate which is placed in a saturated porous medium and at an arbitrary distance above the horizontal wall was performed by Ingham and Pop [44]. The first and second order boundary layer equations and the corresponding outer invicid flow equations were studied to find the effects of large,but finite values of Rayleigh numbers. Results were obtained when the plate is maintained at either constant temperature or uniform heat flux. An approximate series solution was found for free convection boundary layer flow past a vertical plate in a porous medium, over a wide range of wall temperature and injection velocity conditions, by Govindarajulu and Molarvizthi [45]. Although the treatment was similar to that of Merkin [46] the governing equations and boundary conditions were different.

The problem of conjugate heat transfer from a downward projecting fin was studied by Pop et al. [47, 48]. In such problems, inclusion of the coupling between the surrounding fluid and the fin makes the analysis very different from that of a vertical plate. Similarity solutions of the appropriate boundary layer equations were presented .

The buoyancy induced boundary layer flow adjacent to horizontal impermeable surfaces in a saturated porous medium was performed by Cheng and Chang [49]. Similarity solutions were obtained for the convective flow above a heated surface or below a cooled surface, where the wall temperature is a power function of distance from leading edge. Applications of the problem to convective flow in a liquid dominated geothermal reservoir were

also discussed. Steady free convection in a porous medium adjacent to a horizontal impermeable surface with prescribed wall temperature distribution was investigated by Chang and Cheng [50], using the method of matched asymptotic expansions. Similarity solutions for buoyancy induced flow in a saturated porous medium adjacent to a horizontal impermeable surface were given by Chandrasekhara [51]. The analysis incorporates the variation of permeability from the wall. An analytical study was presented by Ingham and Pop [52] for moderately high Darcy-Rayleigh numbers for steady free convection adjacent to a horizontal upward-facing, heated surface which is bounded by a vertical wall. The solution of the governing equations was obtained by the method of matched asymptotic expansions.

The transient free convection about a vertical flat plate embedded in a porous medium adjacent to a semi-infinite flat plate with a step increase in the wall temperature and the surface heat flux was initiated by Cheng and Pop [53]. The governing equations are first order partial differential equations of hyperbolic type and these have been solved exactly by the method of integral relations. Similarity conditions and similarity equations for steady and unsteady natural convection adjacent to a semi-infinite inclined flat plate in a porous medium were examined by Johnson and Cheng [54]. Similarity solutions were obtained by Cheng [55] for mixed convection over a horizontal impermeable surface in a porous medium. The problems of free and forced convection boundary layer flows in porous media, have been dealt by Cheng [56] on the basis of boundary layer approximations. Similarity solutions were obtained for the special case when the far-stream

velocity and the wall temperature distributions vary according to the same power function of distance. The free convection boundary layer on a semi-infinite heated flat plate which is inclined at a small angle to the horizontal was considered using the series method by Ingham et al. [57].

The analysis dealing with the onset of convection in a fluid saturated porous box, heated from below was performed by Lowell [58]. In an experimental study of natural convection in liquid-saturated confined porous medium, Kaneko et al. [59] had shown that the mode and intensity of convective motion are affected by the angle of inclination of the medium and the properties of the fluid. The true critical Rayleigh number for the case of a convective flow of a fluid in a rectangular box of porous material heated from below was found for various box geometries by Beck [60]. The preferred cellular mode of the motion at Rayleigh number just above the critical value was determined and the invalidity of Darcy's law in determining the stability of flow was also discussed. Natural convection in a confined porous medium was investigated experimentally and numerically by Holst and Aziz [61, 62].

Buoyancy-driven convection inside a porous cavity due to heating in the horizontal direction was analysed by Walker and Homsy [63]. The solutions were obtained over a range of the dimensionless parameters of Darcy-Rayleigh number and the cavity aspect ratio. Finite amplitude cellular convection in cubic boxes containing fluid- saturated porous material were reported by Strauss [64] for Rayleigh number as large as 150. Steady natural convection in a slightly inclined rectangular box filled with a

porous medium was studied by Walch and Dulieu [65] using the Galerkin technique. Exact solutions were developed by Philip [66] for small cavities of various shapes due to a uniform temperature gradient normal to the gravitational field. Exact solutions were presented in detail for rectangular and elliptical cavities for arbitrary aspect ratios and also for equilateral triangular cavities. Simple exact solutions have been found to exist for cavities of other shapes also. The finite difference technique was used to investigate finite amplitude convection in a porous container with a fault - like geometry. The principal purpose was to determine the role of boundary conditions and the initial perturbation to the subsequent flow pattern. The results were compared with data from naturally occuring geothermal systems by Lowell [67]. The thermally driven flows inside a two-dimensional rectangular cavity filled with a fluid saturated porous medium was considered in the large Rayleigh number limit, when the applied temperature gradient is perpendicular to the gravity vector. Bounds on the extent of various flow regimes in the parameter space were deduced by Blythe et al.[68]. A numerical and experimental study of two-dimensional steady free convection was presented for various thermal conditions on the walls of a rectangular cavity by Prasad et al.[69-71].

Buoyancy-driven convection in a differentially-heated vertical porous layer was studied theoretically by Gill [72] and Weber [73]. The model was of finite extent and the temperature difference between the vertical walls was assumed to be large. Satisfactory agreement with experiment was obtained for the interior temperature distribution and the Nusselt number. Gill

developed a modified Oseen technique and Weber, in his study, extended the method to include some effects of kinematic viscosity. Bejan [74] altered Gill's theory by calculating the net flow of energy (conduction and convection) in the vertical direction and setting it equal to zero at the top and bottom ends. In a further study Bejan [75] modified Weber's theory for convection in a vertical porous layer by combining Weber's boundary layer solution with zero energy flux boundary conditions at the top and bottom surfaces of the slab. Results were also obtained by Bejan and Tien [76] to consider the corner effects particularly in shallow cavities. Several vertical layers with different permeabilities were studied by Poulikakos and Bejan [77]. A fundamental study of natural convection in a fluid saturated porous layer differentially-heated in the horizontal direction, when the fluid exhibits a density maximum was presented by Poulikakos [78]. Results were obtained in [79-82] for the various porous layer problems with different conditions. Convection in a tilted layer was studied by Weber [83] while Blythe and Simpkins [84] studied the convection for a temperature dependent viscosity.

Forchheimer extension of Darcy's equation of motion was first used by Plumb and Huenefeld [85] to study free convection from a vertical plate embedded in a porous medium. Bejan and Poulikakos [86] reconsidered the problem and presented boundary layer solutions for the intermediate and non-Darcy flow regimes to supplement the boundary layer analysis of Cheng and Minkowycz [40] for Darcy flow. Their results indicate that the slope of the curve of Nusselt number versus Rayleigh number decreases when the

flow regime changes from Darcy to non-Darcy behaviour . Poulikakos and Bejan [87], Poulikakos [88] and Prasad and Tuntomo [89] also used the Forchheimer model to study non-Darcy natural convection in a vertical cavity for isothermal and constant heat flux conditions on the side walls. They have shown that, a new dimensionless parameter called the Forchheimer number governs the non-Darcy flow through porous media and the overall Nusselt number decreases with an increase in Forchheimer number.

It is noteworthy that with a few exceptions, most of the published theoretical work on convective heat transfer use Darcy's law as the momentum equation. Mathematically, since the order of Darcy's law is lower than the Navier-Stokes equations, the no slip boundary condition can not to be imposed on the impermeable boundary. For flow through a porous medium with a high permeability, the Brinkman model was used by Chan et al. [90] to study convective heat transfer in an enclosed, gas-filled, porous medium. It was also used by Katto and Masuoka [91] as well as by Walker and Homsy [63], to study the onset of convection of a liquid in a porous medium bounded between parallel plates and heated from below. The Brinkman model was employed by Hsu and Cheng [92] to study the natural convection about a semi-infinite vertical plate in a porous medium. Flow of a viscous fluid at small Reynolds number past a porous body was investigated by Yamamoto [93]. Sen [94] studied natural convection in a porous cavity .

Recently several works have been published using the generalised Darcy's law, in which the convective acceleration and the viscous stresses are also taken into account [19, 95]. This

generalized Darcy's law was used by Raptis et al. [96] to analyse the steady free convection and heat transfer in a porous medium bounded by a vertical infinite plate. The solution was obtained by the series method when the surface temperature has a constant suction velocity. Chawla and Singh [97] studied the oscillatory flow past a porous bed. Raptis [98] analysed the unsteady free convective flow through a porous medium bounded by an infinite vertical plate, when the temperature of the plate is oscillating with time about a constant non-zero mean. Analytical expressions for the velocity and temperature fields are derived by using the series method. In a subsequent paper, Raptis and Singh [99] obtained numerical solutions of unsteady free convective flow along a moving vertical wall embedded in a porous medium.In a recent paper Raptis and Perdikis [100] have studied combined free and forced convection through a porous medium.

The present work concentrates on the analysis of two-dimensional free convective flows with and without boundary layer approximations. The generalized Darcy's law is considered as the equation of motion. Since the governing equations are non-linear and there exists a mutual coupling between them, the solutions are obtained with the help of numerical techniques.

The first problem considered here, deals with the possible similarity solutions for free convective flow on a semi-infinite vertical plate embedded in a saturated porous medium. The necessary and sufficient conditions are obtained for similarity to exist, based on a generalised similarity method. Numerical solutions using the shooting method are obtained for a particular case and the corresponding velocity and temperature distributions

are presented.

The third chapter discusses the problem of conjugate free convection about a rectangular fin embedded in a porous medium. The governing equations are solved by using a highly-implicit finite difference scheme with a variable mesh-size in the direction normal to the fin. Wall temperature distributions and the local Nusselt numbers are obtained and plotted for various parameters of the problem.

A parametric study has been presented in chapter four for unsteady free convection inside a rectangular enclosure with two isothermal vertical and two adiabatic horizontal walls. The velocity and temperature distributions are obtained using the finite difference technique. The upwind-differencing procedure is followed for convective terms to get the spatial discretization of the governing equations. A fully implicit scheme is used to get the timewise discretization and the resulting algebraic equations are solved by the line-by-line procedure coupled with the tridiagonal matrix solver algorithm.

The last chapter deals with free convection about a moving vertical wall embedded in a porous medium. The problem is solved analytically by the momentum integral method and numerically by the semi-implicit finite difference method . The results obtained by the two methods are in good agreement. The velocity distribution and skin-friction at the wall are obtained.

REFERENCES

[1] Darcy, H., Les fontaines publiques de la ville de Dijon, Dalmont, Paris, 1856.

[2] Brinkman, H.C., A calculation of viscous force exerted by a flowing fluid on a dense swarm of particles, Appl. Sci. Res., 1, 27, 1947.

[3] Yamamoto, K. and Iwamura, N., Flow with convective acceleration through a porous medium, J. Engng. Maths., 10, 41, 1976.

[4] Forchheimer, P., Wasserbewegung durch Bodem, Z. Ver. Deutsch. Ing. 45, 1782, 1901.

[5] Bear, J., Dynamics of fluids in porous media, American Elsevier Pub. Co., New York, 1972.

[6] Collins, R.E., Flow of fluids through porous materials, Reinhold Pub. Co., New York, 1961.

[7] Slattery, J.C., Amer. Inst. Chem. Engng. J. 16, 866, 1969.

[8] Slattery,J.C., Momentum, Energy and Mass Transfer in Continua, McGraw-Hill, New York, 1972.

[9] Whitaker, S., Amer. Inst. Chem. Engng. J., 13, 420, 1967.

[10] Rudraiah, N.,Veerabhadriah,R., Chandrasekara, B.C. and Nagraj,S.T., Some Flow Problems in porous media,PGSAM Series,Central College , Banglore , 1979.

[11] Bear, J., Hydraulics of ground water, McGraw-Hill , 1979.

[12] Ergun, S., Fluid flow through packed columns, Chem. Engng. Prog. 48, 89, 1952.

[13] Ward, J.C., Turbulent flow in porous media, Proc. Soc. Civ. Engrs. 90 (HY5), 1, 1964.

[14] Tam, C.K.W.,The drag on a cloud of spherical particles in low Reynolds number flow, J. Fluid Mech., 38, 537, 1969.

[15] Lundgren,T.S., Slow flow through stationary random beds and suspension of spheres, J. Fluid Mech.,51, 273, 1972.

[16] Hamel, G., Uber Grundwasserstromung, Z. angew. Math. Mech., 14, 129, 1934.

[17] Yih, C.S., Dynamics of Nonhomogeneous Fluids, Macmillan Co., New York, 1965.

[18] Raats, P.A.C., The role of interia in hydrodynamics of porous media, Arch. Rational Mech. Anal. 44, 267, 1972.

[19] Yamamoto, K. and Yoshida, Z., Flow through a porous wall with convective acceleration, J. Phys. Soc. Japan, 37, .414, 1974.

[20] Prasad,V.,Kulacki,F.A. and Keyhani,M.,Natural convection in porous media ,J.Fluid Mech. ,150, 80, 1985.

[21] Davis, C.N., Air Filteration, Academic Press, London, 1973.

[22] Scheidegger, A.E., The Physics of Flow Through Porous Media, Univ. Toronto Press, 1957.

[23] Wooding, R.A., Steady state free thermal convection of water in saturated permeable material, J. Fluid Mech., 2, 273, 1957.

[24] Horton, C.W. and Rogers, F.T. Jr., Convective currents in a porous medium, J. Appl. Phys. 16, 367, 1945.

[25] Morison,H.L.,Rogers,F.T.Jr. and Horton, C.W., Convective Currents in porous media II, observation of conditions at onset of convection, J. Appl. Phys., 20, 1027, 1949.

[26] Rogers, F.T. Jr. and Morison, H.L., Convective currents in a porous medium III, Extended theory of critical gradients, J. Appl. Phys. 21, 1177, 1949.

[27] Rogers, F. T., Schilbeig, L. E. and Morison,H.L.,Convective currents in a porous media-IV, Remarks on the theory, J. Appl. Phys., 22, 1476, 1951.

[28] Wooding, R.A., The stability of a viscous liquid in a vertical tube containing porous material, Proc. of Royal Soc., London, Series A, 252, 120, 1949.

[29] Wooding, R.A., An experiment on free thermal convection of water in saturated permeable material, J. Fluid Mech., 3, 582, 1958.

[30] Wooding, R.A., Rayleigh instability of a thermal boundary layer in flow through a porous medium, J. Fluid Mech., 9, 183, 1960.

[31] Wooding, R.A., Instability of a viscous liquid of variable density in natural Hele-Shaw cell, J. fluid Mech., 7, 501, 1960.

[32] Wooding, R.A., Free convection of a fluid in a vertical tube filled with porous material, J. fluid Mech., 13, 129, 1962.

[33] Wooding, R.A., Convection in a saturated porous medium at large Rayleigh number or Peclet number, J. Fluid Mech., 15, 527, 1963.

[34] Elder, J.W., Laminar/turbulent free convection in a vertical slot, J. Fluid Mech., 29, 77, 1965.

[35] Elder, J.W., Numerical experiments with free convection in a vertical slot, J. Fluid Mech., 24, 823, 1966.

[36] Elder, J.W., Steady free convection in a porous medium heated from below, J. Fluid Mech., 27, 29, 1967.

[37] Elder, J.W., Transient convection in a porous medium, J. fluid Mech., 27, 609, 1967.

[38] McNabb A., On convection in a saturated porous medium, Proc. of 2nd Australian Conference on Hydraulics and fluid mechanics, University of Auckland, N.Z., C161, 1965.

[39] Lapwood, E.R., Convection of fluid in a porous medium, Proc. of the Camb. phil. Soc. 44, 508, 1948.

[40] Cheng, P. and Minkowycz, W.J., Free convection about a vertical flat plate embedded in a porous medium with application to heat transfer from a dike, J. Geophys. Res. 82, 2040, 1977.

[41] Cheng, P., convective heat transfer in a porous layer by integral methods, Letters in Heat Mass Transfer, 5, 243, 1978.

[42] Cheng, P. and Chang, I.D., Convection in a porous layer as a singular perturbation problem, Letters in Heat Mass Transfer, 6, 253, 1979.

[43] Na, T.Y., Free convection flow past a vertical flat plate embedded in a saturated porous media, Int. J. Engng. Sci., 21, 617, 1983.

[44] Ingham, D.B. and Pop, I., Free convection from a semi-infinite vertical surface bounded by a horizontal wall in a porous medium, Int. J.Heat Mass Transfer, 30,1615, 1987.

[45] Govindrajulu, T. and Malarvizthi,G., A note on the solution of free convection boundary layer flow in a saturated porous media, Int.J.Heat Mass Transfer, 30, 1769, 1987.

[46] Merkin, J.H., A note on the solution of a differential equation arising in boundary layer theory, J. Engng. Maths., 18, 31, 1984.

[47] Pop, I., Sunda, J.K., Cheng, P. and Minkowycz, W.J., Conjugate free convection from long vertical plate fins embedded in a porous media at high Rayleigh numbers, Int. J. Heat Mass Transfer, 28, 1629, 1985.

[48] Pop., I., Ingham, D.B., Heggs, P.J. and Gardner, D., Conjugate heat transfer from a downward projecting fin immersed in a porous medium, Proc. Heat Transfer Conference, 2635, 1986.

[49] Cheng, P. and Chang, I.D., Buoyancy induced flow in a saturated porous media adjacent to impermeable horizontal surface, Int. J.Heat Mass Transfer, 19, 1267, 1976.

[50] Chang, I.D. and Cheng, P., Matched asymptotic expansions for free convection about an impermeable horizontal surface in a porous medium, Int. J.Heat Mass Transfer, 26, 163, 1983.

[51] Chandrasekhara, B.C., Namboodiri, P.M.S. and Hanumanthappa, A.R., Similarity solutions for buoyancy induced flows in a saturated porous medium adjacent to impermeable horizontal surfaces, Wärme-und-Stoffübertragung, 18, 17, 1984.

[52] Ingham, D.B. and Pop, I., Darcian free convection flow about an impermeable horizontal surface, Int. J. Engng. Sci. 25, 373, 1987.

[53] Cheng, P. and Pop. I., Transient free convection about a vertical flat plate embedded in a saturated porous medium, Int. J. Engng. Sci. 22, 253, 1984.

[54] Johnson, C.H. and Cheng, P., Possible similarity solutions for free convection boundary layers adjacent to flat plates in porous media, Int. J.Heat Mass Transfer, 21, 669, 1978.

[55] Cheng, P., Similarity solutions for mixed convection from horizontal impermeable surfaces in a porous medium, Int. J.Heat Mass Transfer, 20, 893, 1977.

[56] Cheng, P., Combined free and forced convection boundary layer flows about inclined surfaces in a porous medium, Int. J.Heat Mass Transfer, 20, 806, 1977.

[57] Ingham, D.B., Merkin, J.H. and Pop, I., Natural convection from a semi-infinite flat plate inclined at a small angle to the horizontal in a saturated porous medium, Acta Mechanica 57, 183, 1985.

[58] Lowell, R.P., and Shyu, C.T., On the onset of convection in a water saturated porous box: effect of conducting wall, Letters in Heat Mass Transfer, 5, 371, 1978.

[59] Kaneko, T. and Mohtadi,M.F., and Azid, K., An experimental study of natural convection in inclined porous media, Int. J.Heat Mass Transfer, 17, 485, 1974.

[60] Beck, J.L., Convection in a box of porous material saturated with fluid, Phys. Fluids, 15, 1377, 1972.

[61] Holst, P.H. and Aziz, K., A theoretical and experimental study of natural convection in a confined porous medium, Can. J. Chem. Engng. 50, 232, 1972.

[62] Holst, P.H. and Aziz, K., *Transient three-dimensional convection in a confined porous medium, Int. J. Heat Mass Transfer, 15, 73, 1972.

[63] Walker, K.L. and Homsy, G.L., Convection in a porous cavity, J. Fluid Mech., 87, 449, 1978.

[64] Strauss, J.M. and Schubert, G., On the existence of 3-dimensional convection in a rectangular box containing fluid saturated porous material, J. Fluid Mech., 87, 385, 1978.

[65] Walch, J.P. and Dulieu, B., Convection naturalle dans une boite rectangulaire légérement inclineé contenant un milieu poroux, Int. J.Heat Mass Transfer, 22, 1607, 1979.

[66] Philip, J., Free convection at small Rayleigh number porous cavities of rectangular, elliptical, triangular, and other cross-sections, Int. J.Heat Mass Transfer, 25, 1503, 1972.

[67] Lowell, R.P. and Harnandez, Finite amplitude convection in a porous container with fault like geometry, effect of initial and boundary conditions, Int. J.Heat Mass Transfer, 25, 631, 1972.

[68] Blythe, P.A. and Simpkins, P.G., and Daniels, P.G., Thermal convection in a cavity filled with a porous medium; A classification of limiting behaviour, Int. J.Heat Mass Transfer, 26, 701, 1983.

[69] Prasad, V. and Kulacki, F.A., Natural convection in a rectangular porous cavity with constant heat flux on one vertical wall, J. Heat Transfer, 106, 152, 1984.

[70] Prasad, V. and Kulacki, F.A., Convective heat transfer in a rectangular porous cavity-effect of aspect ratio on flow structure and heat transfer, J. Heat Transfer, 106, 158, 1984.

[71] Prasad, V., Thermal convection in a rectangular cavity filled with a heat generating Darcy porous medium, J. Heat Transfer, 109, 697, 1987.

[72] Gill, A.E., The boundary-layer regime for convection in a rectangular cavity, J. Fluid Mech., 26, 515, 1966.

[73] Weber, J.E., The boundary layer regime for convection in a vertical porous layer, 18, 569, 1975.

[74] Bejan, A., J. Fluid Mech., 90, 561, 1979.

[75] Bejan, A., On the boundary layer regime in a vertical enclosure filled with a porous medium, Letters in Heat and Mass Transfer, 6, 93, 1979.

[76] Bejan, A. and Tien,C.L., Natural convection in a horizontal porous medium subject to an end to end temperature difference, J. Heat Transfer, 100, 191, 1978.

[77] Poulikakos, D. and Bejan, A., Natural convection in a vertically and horizontally layered porous media heated from below, Int. J.Heat Mass Transfer, 26, 1805, 1983.

[78] Poulikakos, D., Maximum density effects on natural convection in a porous layer differentially heated in the horizontal direction, Int. J.Heat Mass Transfer, 27, 2067, 1984.

[79] Bejan, A., Natural convection in an infinite porous media with concentrated heat sources, J. Fluid Mech., 89, 97, 1978.

[80] Bejan, A., The boundary layer regime with uniform heat flux from the side, Int. J. Heat Mass Transfer, 26, 1339, 1983.

[81] Bejan,A., Natural convection heat transfer in a porous layer with internal flow obstructions, Int. J. Heat Mass Transfer, 26, 815, 1983.

[82] Blake, K.R. Bejan, A. and Poulikakos,D., Natural convection near 4°C in water saturated porous layer heated from below, Int. J. Heat Mass Transfer, 27, 2355, 1984.

[83] Weber, J.E., Thermal convection in a tilted porous layer, Int. J. Heat Mass Transfer, 18, 474, 1985.

[84] Blythe, P.A. and Simpkins, P.G., Convection in a porous layer for a temperature dependent viscosity, Int. J. Heat Mass Transfer, 24, 497, 1981.

[85] Plumb, O.A. and Hunefeld, J.C., Non-Darcy natural convection from heated surfaces in saturated porous media, Int. J. Heat Mass Transfer, 24, 765, 1981.

[86] Bejan, A. and Poulikakos, D., The non-Darcy regime for vertical boundary layer natural convection in a porous medium, Int. J. Heat Mass Transfer, 27, 717, 1984.

[87] Poulikakos, D. and Bejan, A., The departure from Darcy flow in natural convection in a vertical porous layer, Phys. Fluids, 28, 3477, 1985.

[88] Poulikakos, D., A departure from the Darcy model in boundary layer natural convection in a vertical porous layer with uniform heat flux from side, J. Heat Transfer, 107, 716, 1985.

[89] Prasad, V. and Tuntomo, A., Inertia effects on natural convection in a vertical porous cavity, Num. Heat Transfer, 11, 295, 1987.

[90] Chan, B.K.C., Ivey, C.M. and Barry, J.M., Natural convection in enclosed porous media with rectangular boundaries, J. Heat Transfer, 92, 21, 1970.

[91] Katto, Y. and Masuoka, T., Criterian for the onset of convective flow in a fluid in a porous media, Int. J. Heat Mass Transfer, 10, 297, 1967.

[92] Hsu, C.T. and Cheng, P., The Brinkman model for natural convection about a semi-infinite vertical flat plate in a porous medium, Int. J. Heat Mass Transfer, 28, 688, 1985.

[93] Yamamoto, K., Flow of viscous fluid at small Reynolds numbers past a porous body, J. Phys. Soc. Japan, 34, 814, 1973.

[94] Sen, A.K., Natural convection in a shallow porous cavity-Brinkman model, Int. J. Heat Mass Transfer, 30, 855, 1987.

[95] Varshney, C.L., Indian J. Pure Appl. Maths., 10, 1558, 1979.

[96] Raptis, A., Perdikis, C. and Tzivanidis, G., Free convection flow through a porous medium bounded by a vertical surface, J. Phys. D: Appl. Phys., 14, L99, 1981.

[97] Chawla, S.S. and Singh, S., Acta Mech., 34, 205, 1979.

[98] Raptis, A.A., Unsteady free convective flow through a porous medium, Int. J. Engng. Sci., 21, 345, 1983.

[99] Raptis, A. and Singh, A.K. Free-convection flow past an impulsively started vertical plate in a porous medium by finite difference method, Astrophysics and Space Science, 112, 259, 1985.

[100] Raptis, A. and Perdikis, C., Combined free and forced convection through a porous medium, Int. J. Energy Res. 12, 557, 1988.

CHAPTER II

POSSIBLE SIMILARITY SOLUTIONS FOR FREE CONVECTIVE FLOW ALONG A VERTICAL PLATE IMMERSED IN A POROUS MEDIUM

2.1 INTRODUCTION

There has recently been considerable interest in the study of free convective flows in porous media because of their applications to many physical and engineering problems. Theoretical studies in this area leading to exact solutions, chiefly pertain to the linear stability analysis of the onset of free convection [1-3] and the prediction of velocity and temperature distributions for free convective flows near heated surfaces [4,5].

The problem of natural convection in a free fluid has been investigated by many researchers and notably among them are Stewartson [6], Gill et al. [7], Rotem and Clausen [8], Pera and Gebhart [9] and Blanc and Gebhart [10]. In the above investigations, similarity solutions have been obtained using boundary layer approximations. For flow through a porous medium also, Wooding [11] and McNabb [12] showed that the convection takes place in a thin layer around the heated surface and the boundary layer approximations are valid.

A large volume of literature exists on thermal boundary layer studies for natural convection inside a saturated porous medium using Darcy's law as the momentum equation. Cheng and Minkowycz [13] have considered the idealized problem of a vertical flat plate embedded in an isotropic porous medium with the wall

temperature prescribed as a power function of height. Within the framework of boundary layer approximations the similarity solutions were obtained. In another paper Cheng and Chang [14] have obtained the similarity solution near a horizontal plate. The similarity solution for combined free and forced convection about an inclined surface in a saturated porous medium were analysed by Cheng [15]. Considering the effects of lateral injection or withdrawal of fluid through the wall, Cheng [16] has analysed possible similarity solutions for power law type variation of wall temperature. In a subsequent publication [17], he has also found the similarity solution for mixed convection over a horizontal impermeable surface in a saturated porous medium.

Na and Pop [18] have investigated steady natural convection heat transfer between an impermeable vertical surface and a porous medium, when a non-uniform heat flux condition is prescribed at the wall. They have shown that the governing equations possess a similarity solution for only a limited class of wall temperature or heat flux distributions. Transient boundary layer flow in a porous medium is dealt by Johnson and Cheng [19]. Similarity solutions have been obtained for specific variations of wall temperature with time and position. Plumb and Huenefeld [20] and Bejan and Poulikakos [21] considered a non-Darcy model to study free convection from heated surfaces in a porous medium. They have shown that only for the case of a vertical isothermal surface similarity exists. All of the above theoretical solutions based on Darcy or non-Darcy models, do not take into account viscous force

acting along the impermeable surface and hence the no slip condition at the boundary is not satisfied by them.

The objective of the present work is to obtain the necessary and sufficient conditions under which similarity is possible for free convection adjacent to a vertical plate, in a porous medium described by the generalized Darcy law. The generalized similarity method which was earlier used by Yang [22], Cheesewright [23], Gebhart [24] and Johnson and Cheng [19], has been adopted here. The approach consists of defining an independent similarity variable η and two dependent similarity functions of η corresponding to the velocity and temperature solutions, in terms of generalized transformation functions. When these variables are substituted into the boundary layer equations they can be reduced to a set of ordinary differential equations only if the coefficients of all the terms are made constant. The minimum set of conditions to be satisfied for making these coefficients into constants are referred to as similarity conditions. In general, the similarity conditions contain derivatives of the transformation functions and are thus differential equations themselves. Any set of solutions to these differential equations which will result in explicit forms for the transformation functions, can be used to transform the boundary layer equations of the problem into a similarity form.

The first part of the present chapter deals with the theoretical discussion and the derivation of the similarity equations. In the later part, the numerical solution of the situation with the wall temperature varying as a power function of distance, has been obtained.

2.2 GOVERNING EQUATIONS

To simplify the mathematical analysis, the following assumptions are made:

(1) The fluid and the porous medium are homogeneous and isotropic.

(2) The porous medium is fully saturated.

(3) The equations of motion are based on generalized Darcy's model.

(4) The Boussinesq approximation is valid, i.e. the fluid density can be taken as constant except in the buoyancy force term.

(5) Other fluid and porous medium properties are constant.

With the above assumptions the boundary layer equations for laminar free convection on a vertical plate are given as:

$$\frac{\partial u}{\partial x} + \frac{\partial v}{\partial y} = 0, \tag{2.1}$$

$$\frac{\partial u}{\partial t} + u\frac{\partial u}{\partial x} + v\frac{\partial u}{\partial y} = g\beta\,(T-T_\infty) + \nu\frac{\partial^2 u}{\partial y^2} - \frac{\nu u}{K_1}, \tag{2.2}$$

$$\frac{\partial T}{\partial t} + u\frac{\partial T}{\partial x} + v\frac{\partial T}{\partial y} = \alpha\frac{\partial^2 T}{\partial y^2}, \tag{2.3}$$

where, u and v are components of velocity in the tangential and normal directions to the plate, g is the acceleration due to gravity, β is the coefficient of volume expansion, ν is the kinematic viscosity, T is the temperature of the fluid, T_∞ is the ambient fluid temperature, K_1 is the permeability of the medium and α denotes the thermal diffusivity. The variables x and y denote space co-ordinates in the horizontal and vertical directions. The physical geometry of the problem is given in figure 1.

The situation, considered for the present analysis corresponds to T_w greater than T_∞. By a simple change in co-ordinate system, one can get the results for the case when T_w is smaller than T_∞ also, from the present result. The initial conditions, depend on the problem under consideration, while the boundary conditions are as follows:

$$y = 0 : \quad u = v = 0, \quad T = T_w\ (x,t), \tag{2.4}$$

$$y \to \infty : \quad u = 0, \quad T = T_\infty\ (\text{constant}), \tag{2.5}$$

and the boundary conditions at the leading edge are:

$$x = 0 : u = v = 0, \quad T = T_\infty. \tag{2.6}$$

Introduce the following dimensionless quantities,

$$x = \frac{x}{L}, \quad y = \frac{y}{L}, \quad u = \frac{uL}{\nu}, \quad v = \frac{vL}{\nu}, \quad t = \frac{\nu t}{L^2}, \quad G = \frac{g\beta L^3 (T-T_\infty)}{\nu^2}$$

$$K = \frac{K_1}{L^2}, \quad Pr = \nu/\alpha, \tag{2.7}$$

where, L is the characteristic length, Pr is the Prandtl number and G is the generalised Grashof number.

In terms of the dimensionless quantities of equation (2.7), the equations (2.1)-(2.3) reduce to the following non-dimensional system:

$$\frac{\partial u}{\partial x} + \frac{\partial v}{\partial y} = 0, \tag{2.8}$$

$$\frac{\partial u}{\partial t} + u\frac{\partial u}{\partial x} + v\frac{\partial u}{\partial y} = G + \frac{\partial^2 u}{\partial y^2} - \frac{u}{K} \tag{2.9}$$

$$\frac{\partial G}{\partial t} + u\frac{\partial G}{\partial x} + v\frac{\partial G}{\partial y} = \frac{1}{Pr}\frac{\partial^2 G}{\partial y^2}. \tag{2.10}$$

The boundary conditions transform to

$$y = 0 : \quad u = v = 0, \quad G = G_w\ (x,t), \tag{2.11}$$

$$y \to \infty : \quad u = 0, \; G = 0, \tag{2.12}$$

$$x = 0 : \quad u = 0, \; G = 0. \tag{2.13}$$

The continuity equation (2.8)is automatically satisfied when a dimensionless stream function ψ is introduced such that,

$$u = \frac{\partial \psi}{\partial y} , \quad v = - \frac{\partial \psi}{\partial x} . \tag{2.14}$$

We shall choose a similarity variable η in the following form,

$$\eta = y \, \phi_1 \, (x,t) \tag{2.15}$$

and the corresponding dependent variables $f(\eta)$ and $\theta(\eta)$ as,

$$f(\eta) = \frac{\psi(x,y,t)}{\phi_2(x,t)} \quad \text{and} \quad \theta(\eta) = \frac{G(x,y,t)}{G_w(x,t)} . \tag{2.16}$$

The present problem of finding the conditions for the existence of similarity, therefore, reduces to that of determining the functions $\phi_1(x,t)$, $\phi_2(x,t)$ and $G_w(x,t)$ such that the equations (2.9) and (2.10) are transformed into ordinary differential equations for $f(\eta)$ and $\theta(\eta)$ with appropriate boundary conditions for these variables. Combining equations (2.15) and (2.16), we get,

$$u = \frac{\partial \psi}{\partial y} = \phi_1 \, \phi_2 \, f' \tag{2.17}$$

$$v = - \frac{\partial \psi}{\partial x} = - \left[\left(\frac{\partial \phi_2}{\partial x} \right) f + \frac{\phi_2}{\phi_1} \left(\frac{\partial \phi_1}{\partial x} \right) \eta \, f' \right] \tag{2.18}$$

and

$$G = G_w \theta. \tag{2.19}$$

Substituting these expressions in equations (2.9) and (2.10), the following generalised similarity equations are obtained:

$$f''' - a_2 \eta \, f'' - (a_2+a_3+a_8) \, f' + a_5 \, f \, f'' - (a_4+a_5) \, f'^2 + a_1 \, \theta = 0 \tag{2.20}$$

and

$$\frac{1}{Pr} \theta'' - (a_2 \eta - a_5 f) \, \theta' - (a_6 + a_7 f') \, \theta = 0 \tag{2.21}$$

where, prime denotes derivative with respect to η. Also,

$$a_1 = \frac{G_w}{\phi_1^3 \phi_2} , \tag{2.22}$$

$$a_2 = \frac{1}{\phi_1^3} \left(\frac{\partial \phi_1}{\partial t} \right) , \tag{2.23}$$

$$a_3 = \frac{1}{\phi_1^2 \phi_2} \left(\frac{\partial \phi_2}{\partial t} \right) , \tag{2.24}$$

$$a_4 = \frac{\phi_2}{\phi_1^2} \left(\frac{\partial \phi_1}{\partial x} \right) , \tag{2.25}$$

$$a_5 = \frac{1}{\phi_1} \left(\frac{\partial \phi_2}{\partial x} \right) , \tag{2.26}$$

$$a_6 = \frac{1}{G_w \phi_1^2} \left(\frac{\partial G_w}{\partial t} \right) , \tag{2.27}$$

$$a_7 = \frac{\phi_2}{G_w \phi_1} \left(\frac{\partial G_w}{\partial x} \right) , \tag{2.28}$$

$$a_8 = \frac{1}{\phi_1^2 K(x,t)} . \tag{2.29}$$

It may be noted from equation (2.29) that the permeability parameter, K may be a function of space and time both. The boundary conditions for the variables f and θ are:

$$f(0) = f'(0) = 0 , \quad f'(\infty) = 0 \tag{2.30}$$

$$\theta(0) = 1 , \quad \theta(\infty) = 0 . \tag{2.31}$$

It is clear from equations (2.20) and (2.21) that the similarity solutions are possible if and only if a_1, a_2, a_3, a_4, a_5, a_6, a_7 and a_8 are constants. Consequently, equations (2.22) - (2.29) may be regarded as the necessary and sufficient conditions for similarity solutions. Since there are more conditions than unknowns, the constants are not all arbitrary. For example, the

following relations can be easily verified,

$$a_6 = 3a_2 + a_3 \qquad (2.32)$$

$$a_7 = 3a_4 + a_5 \qquad (2.33)$$

A general method for the determination of the unknown functions ϕ_1, ϕ_2 and G_w, is to solve for ϕ_1 and ϕ_2 first from the equations (2.23) - (2.26), and then solve for the surface temperature variation from equation (2.22).

2.3 SIMILARITY SOLUTIONS

Case - 1: Steady free convection with constant surface temperature.

For this case, $a_2 = a_3 = a_6 = a_7 = 0$ and $a_5 = -3a_4$. By eliminating ϕ_2 from equations (2.24) and (2.25), we have

$$\frac{1}{\phi_1^5}\frac{d\phi_1}{dx} = \frac{a_4\ a_1}{G_w} \quad , \qquad (2.34)$$

the general solution of the equation (2.34) is

$$\phi_1 = \left(a_9 - \frac{4a_4\ a_1\ x}{G_w}\right)^{-1/4} \quad , \qquad (2.35)$$

where, a_9 is the constant of integration. Equation (2.22) yields,

$$\phi_2 = \frac{G_w}{a_1}\left(a_9 - \frac{4a_4\ a_1\ x}{G_w}\right)^{3/4} \qquad (2.36)$$

The constant of integration a_9 can be chosen to be zero and convenient values may be chosen for the arbitrary constants a_1, a_4 and a_8. Thus, if we assume $a_1 = 1$, $a_4 = -1$, $a_8 = K_o$ and $a_9 = 0$, the expressions for ϕ_1, ϕ_2 and K are given by:

$$\phi_1 = \left(\frac{4x}{G_w}\right)^{-1/4}, \qquad (2.37)$$

$$\phi_2 = G_w\left(\frac{4x}{G_w}\right)^{3/4} \quad \text{and} \qquad (2.38)$$

$$\frac{1}{K} = K_o \left(\frac{4x}{G_w} \right)^{-1/2}, \qquad (2.39)$$

respectively. Finally, the governing equations reduce to

$$f''' + 3 ff'' - 2f'^2 - K_o f' + \theta = 0$$

$$\frac{1}{Pr} \theta'' + 3f\theta' = 0 \qquad (2.40)$$

with boundary conditions specified by the equations (2.11), (2.12) and (2.13). Thus, for steady free convection along a semi-infinite vertical wall with a constant surface temperature, similarity exists if K, the permeability parameter, varies as $x^{1/2}$.

Case - II: Steady free convection with surface temperture varying as a power of a linear function of x.

Since the flow is steady, $a_2 = a_3 = a_6 = 0$. It is possible to obtain the general solution of equations (2.25) and (2.26) for the present case.

A combination of (2.25) and (2.26) yields,

$$\frac{1}{\phi_2} \frac{d\phi_2}{dx} = \frac{\epsilon}{\phi_1} \frac{d\phi_1}{dx} \qquad (2.41)$$

where, $\epsilon = a_5/a_4$. The general solution of this equation is,

$$\phi_2 = a_{10} \phi_1^{\epsilon} \qquad (2.42)$$

where, a_{10} is the constant of integration. Using (2.42), (2.25) and (2.26), the expressions for ϕ_1 and ϕ_2 are obtained as,

$$\phi_1 = \left(a_{11} + \frac{a_4}{a_{10}} (\epsilon-1)\, x \right)^{1/(\epsilon-1)} \qquad (2.43)$$

$$\phi_2 = a_{10} \left(a_{11} + \frac{a_4}{a_{10}} (\epsilon-1)\, x \right)^{\epsilon/(\epsilon-1)}. \qquad (2.44)$$

We first discuss the case when $\epsilon \neq 1$. G_w is obtained from (2.22) with the help of (2.43) and (2.44),

$$G_w = a_1\, a_{10}\, (a_{11} + \frac{a_4}{a_{10}}\,(\epsilon-1)\; x\;)^{\frac{\epsilon+3}{\epsilon-1}}\,, \qquad (2.45)$$

The constants a_1, a_4, a_{10} and a_{11} are arbitrary. One can make a few simplifications here, without loss of generality. As can be seen from equation (2.45), a_1 can be chosen to be 1. By a similar reasoning, the value of a_4 may be chosen leaving ϵ, a_{10} and a_{11} as arbitrary. Let us put $n = \frac{\epsilon+3}{\epsilon-1}$ or $\epsilon = \frac{n+3}{n-1}$. From the definition of ϵ, it is clear that $a_4 = n-1$, $a_5 = n+3$ and $a_7 = 4n$, from equations (2.25), (2.26) and (2.33) respectively. The functions ϕ_1, ϕ_2, G_w and K take the following form:

$$\phi_1 = (a_{11} + \frac{4x}{a_{10}})^{\frac{n-1}{4}}\,, \qquad (2.46)$$

$$\phi_2 = (a_{11} + \frac{4x}{a_{10}})^{\frac{n+3}{4}}, \qquad (2.47)$$

$$G_w = a_{10}\,(a_{11} + \frac{4x}{a_{10}})^{n}, \qquad (2.48)$$

$$\frac{1}{K} = K_o\,(a_{11} + \frac{4x}{a_{10}})^{\frac{1-n}{2}} \qquad (2.49)$$

and the similarity equations reduce to

$$f''' + (n+3)\, ff'' - 2(n+1)\, f'^2 - K_o\, f' + \theta = 0, \qquad (2.50)$$

$$\frac{1}{Pr}\,\theta'' + (n+3)\, f\theta' - 4n\, f'\theta = 0, \qquad (2.51)$$

which are solved numerically by the shooting method with boundary conditions (2.11), (2.12) and (2.13) for various values of n.

The variation of physical variables within the boundary layer may now be expressed as:

$$u = a_{10}\,(a_{11} + \frac{4x}{a_{10}})^{\frac{n+1}{2}}\; f' \qquad (2.52)$$

$$v = -\left(a_{11} + \frac{4x}{a_{10}}\right)^{\frac{n+1}{4}} [(n+3)\, f + (n-1)\, \eta\, f'] \qquad (2.53)$$

$$G = a_{10} \left(a_{11} + \frac{4x}{a_{10}}\right)^{n} \theta. \qquad (2.54)$$

It may be noted here that for $n = a_{11} = 0$, the present case and case 1 are identical. It is also observed from the present analysis that the numerical results are applicable for all values of a_{11} and n (positive, negative or zero), although all the cases do not correspond to physically realistic situations.

The physical implication of non-zero a_{11} is that the surface temperature at the leading edge of the plate is different from that in the ambient, a more realistic feature, since it is difficult physically to heat the plate without raising the temperature of its leading edge. For non-zero a_{11}, the velocity component u is not identically zero along $x = 0$, but is zero only at $y = 0$ and $y = \infty$.

It can also be seen that when $n = 1$ and $a_{11} = 0$, a_4 becomes zero, indicating that the similarity variable, η is a function of y only and the plate surface temperature varies linearly with distance from the leading edge. The free stream velocity and the similarity variable for this situation are analogous to those of steady forced flow, in the neighbourhood of the stagnation point of a blunt-nosed cylinder.

Yet another simplication arises when $\epsilon = 1$. The general solution for this case is

$$\phi_2 = a_{10}\, \phi_1, \qquad (2.55)$$

Thus, from equation (2.25)

$$\phi_1 = a_{12} \exp \left(\frac{a_4}{a_{10}} x \right) \tag{2.56}$$

and $$G_w = a_1 a_{10} a_{12}^4 \exp \left(\frac{4a_4 x}{a_{10}} \right) \tag{2.57}$$

The constants of integration a_{10} and a_{12} are arbitrary.

The similarity equations are,

$$f''' + ff'' - 2f'^2 - K_o f' + \theta = 0, \tag{2.58}$$

$$\frac{1}{Pr} \theta'' + f\theta' - 4f' \theta = 0 \tag{2.59}$$

with boundary conditions (2.11), (2.12) and (2.13).

Unsteady Cases:

For unsteady cases we find that the expression of permeability becomes a function of space as well as time. We omit the discussion of such situations as permeability is generally not a function of time in real physical situations.

The above similarity equations derived for the generalized Darcy's model can be simplified to obtain the similarity form of equations for other formulations such as the Brinkman's model and the Darcy's model. A brief description of such simplifications is presented in the following sections.

2.4 SIMILARITY SOLUTIONS FOR BRINKMAN MODEL

Considering Brinkman model as the equation of motion, the generalized similarity equations (2.20) and (2.21) reduce to,

$$f''' - a_1 \theta - a_8 f' = 0, \tag{2.60}$$

$$\frac{1}{Pr} \theta'' - (a_2 \eta - a_5 f) \theta' - (a_6 + a_7 f') \theta = 0. \tag{2.61}$$

For the steady case, $a_2 = a_6 = 0$ and a_1, a_5, a_7 and a_8 are, in general, non-zero constants. Using (2.26) and (2.28), one gets,

$$G_w = A \phi_2^{\varepsilon}, \tag{2.62}$$

where, A is the constant of integration and $\epsilon = a_7/a_5$. The expressions for ϕ_1, ϕ_2, G_w and K may now be obtained from the equations (2.22), (2.26), (2.28), (2.29) and (2.62) as follows:

$$\phi_1 = A_1(A_4x + A_5)^{\frac{\epsilon-1}{4-\epsilon}}, \tag{2.63}$$

$$\phi_2 = (A_4x + A_5)^{\frac{3}{4-\epsilon}} \tag{2.64}$$

$$G_w = Aa_1 (A_4x + A_5)^{\frac{3\epsilon}{4-\epsilon}}, \tag{2.65}$$

$$\frac{1}{K} = a_8 A_1(A_4x + A_5)^{\frac{2(\epsilon-1)}{4-\epsilon}}, \tag{2.66}$$

where, $A_1 = (A/a_1)^{1/3}$ and A_4, A_5 are the constants of integration. Let us first consider the case for $\epsilon \neq 4$. On substituting $n = \frac{3\epsilon}{4-\epsilon}$, one can write,

$$\phi_1 = A_1 (A_4x + A_5)^{\frac{n-1}{4}}, \tag{2.67}$$

$$\phi_2 = (A_4x + A_5)^{\frac{n+3}{4}}, \tag{2.68}$$

$$G_w = Aa_1 (A_4x + A_5)^{n}, \tag{2.69}$$

$$\frac{1}{K} = a_8 A_1 (A_4x + A_5)^{\frac{n-1}{2}}. \tag{2.70}$$

It is observed from equations (2.67) - (2.70), that the transformation functions for steady flow using Brinkman model are the same as in the case of the generalized Darcy's law. The similarity equations are, however, different for the two models. For Brinkman model, one obtains:

$$f''' - \theta - K_o f' = 0, \tag{2.71}$$

$$\frac{1}{Pr}\theta'' + (3+n) f\theta' - 4n f'\theta = 0. \tag{2.72}$$

For the case of $\epsilon = 4$, the expressions for ϕ_1, ϕ_2, G_w and K are

obtained as,

$$\phi_1 = A_9 \, e^{A_7 x}, \tag{2.73}$$

$$\phi_2 = A_8 \, e^{A_7 x}, \tag{2.74}$$

$$G_w = A \, \phi_2^4, \tag{2.75}$$

$$\frac{1}{K} = a_8 \, A_9^2 \, e^{2 A_7 x}, \tag{2.76}$$

where, A_8, A_9 are the constants of integration.

2.5 SIMILARITY SOLUTIONS FOR DARCY'S LAW

If the Darcy's law is considered as the momentum equation the similarity equations (2.20) and (2.21) reduce to:

$$f' - Ka \, \theta = 0, \tag{2.77}$$

$$\frac{1}{Pr} \theta'' - (a_2 \eta - a_5 f) \theta' - (a_6 + a_7 f') \theta = 0, \tag{2.78}$$

where, $a = \dfrac{G_w}{\phi_1 \, \phi_2}$. (2.79)

For steady case $a_2 = a_6 = 0$. From the expressions (2.26) and (2.28), one gets,

$$G_w = A \, \phi_2^{\epsilon}, \tag{2.80}$$

where, A is the constant of integration and $\epsilon = a_7/a_5$.

From equations (2.26), (2.28), (2.79) and (2.80), one obtains:

$$\phi_1 = A_{12} \, (A_{10} x + A_{11})^{\frac{\epsilon - 1}{2 - \epsilon}}, \tag{2.81}$$

$$\phi_2 = (A_{10} x + A_{11})^{\frac{1}{2 - \epsilon}}, \tag{2.82}$$

$$G_w = a \, A_{12} \, (A_{10} x + A_{11})^{\frac{\epsilon}{2 - \epsilon}} \tag{2.83}$$

Here K is taken as a constant and the above expressions are vali

for $\epsilon \neq 2$. A_{10}, A_{11} and A_{12} are constants of integration. On substituting $n = \frac{\epsilon}{2-\epsilon}$, one gets,

$$\phi_1 = A_{12} (A_{10}x + A_{11})^{\frac{n-1}{2}}, \quad (2.84)$$

$$\phi_2 = (A_{10}x + A_{11})^{\frac{n+1}{2}}, \quad (2.85)$$

$$G_w = a A_{12} (A_{10}x + A_{11})^{n}. \quad (2.86)$$

If we choose a = 1, the above transformation functions are the same as those obtained by Johnson and Cheng [19] for a vertical plate embedded in a porous medium. The similarity equations (2.77) and (2.78) now reduce to the form:

$$f' - k\theta = 0 \quad (2.87)$$

$$\frac{1}{Pr}\theta'' + \left(\frac{1+n}{2}\right) f\theta' - n f'\theta = 0 \quad (2.88)$$

These equations have the same form as the similarity equations obtained by Cheng and Minkowycz [13] and Johnson and Cheng [19]. It may be noted, however, that the definition of the dimensionless temperature in the present work is different from those of [13, 19], which gives rise to an explicit appearance of Pr and K in the present formulation.

The equations (2.81)-(2.83) are valid for $\epsilon \neq 2$. For the case $\epsilon = 2$, one gets the exponential variation of the form,

$$\phi_1 = A_{13} e^{A_{14}x}, \quad (2.89)$$

$$\phi_2 = A_{15} e^{A_{14}x}, \quad (2.90)$$

$$G_w = A \phi_2^{2}, \quad (2.91)$$

where, A_{13}, A_{14}, A_{15} are the constants of integration.

2.6 Method of Solution

The numerical solution procedure for steady free convection wi wall temperature varying as a power function of x is presented here.

Let us consider the similarity equations (2.50) and (2.51) along with boundary conditions (2.11), (2.12) and (2.13). We employ the shooting method for solving these system of ordinary differential equations which reduces the solution of a boundary value problem to the iterative solution of an initial value problem. In this method the generalized similarity equations (2.50) and (2.51) are reformulated into a system of first order ordinary differential equations and solved. The solution procedure is briefly discussed below. Let,

$$F_1 = f,$$

$$F_2 = f',$$

$$F_3 = f'',$$

$$F_4 = \theta,$$

$$F_5 = \theta',$$

$$\frac{dF_1}{d\eta} = F_2, \tag{2.92}$$

$$\frac{dF_2}{d\eta} = F_3 , \tag{2.93}$$

$$\frac{dF_3}{d\eta} = -(n+3)\, F_1 F_3 + 2(n+1)\, F_2^{\,2} + K_o\, F_2 - F_4, \tag{2.94}$$

$$\frac{dF_4}{d\eta} = F_5, \tag{2.95}$$

$$\frac{dF_5}{d\eta} = -Pr\ (n+3)\, F_1 F_5 + 4n\ Pr\ F_2\, F_4 . \tag{2.96}$$

The boundary conditions in terms of the new variables are:

At $\eta = 0$: $F_1 = 0$, $F_2 = 0$, $F_4 = 1$, (2.97)

At $\eta = \eta_{max}$: $F_2 = 0$, $F_4 = 0$. (2.98)

The conditions at $\eta = 0$ are the prescribed initial conditions The other required initial conditions (i.e. F_3 and F_5 which ar not specified at $\eta = 0$) are assumed and the resulting initia value problem is solved by the Fourth-Order Runge Kutta method The assumed initial conditions are improved by the Newton-Raphso procedure until a solution which satisfies the known boundar conditions at far stream is obtained. The iterativ Newton-Raphson process can be set up as follows:

Let, $F_3|_{\eta=0} = \alpha_1$ and $F_5|_{\eta=0} = \alpha_2$ and assume that

$F_2|_{\eta=\eta_{max}} = G_1\ (\alpha_1, \alpha_2)$ and $F_4|_{\eta=\eta_{max}} = G_2\ (\alpha_1, \alpha_2)$.

The aim is now to solve for the roots of two numerically define functions Y_1 and Y_2 which imply the satisfaction of the far strea conditions, as given below:

$$G_1\ (\alpha_1, \alpha_2) - F_2\ (\eta_{max}) = Y_1\ (\alpha_1, \alpha_2) = 0, \quad (2.99$$

$$G_2\ (\alpha_1, \alpha_2) - F_4\ (\eta_{max}) = Y_2\ (\alpha_1, \alpha_2) = 0. \quad (2.10$$

Using the generalized Newton-Raphson scheme for finding the root of the non-linear algebraic system

$$\underline{Y}\ (\underline{\alpha}) = 0, \quad (2.101$$

where, both the dependent variable $\underline{Y}$ and $\underline{\alpha}$ are vectors. Knowin the value of $\underline{\alpha}$ at the nth iteration, the (n+1)th iteration gues value can be obtained by the expression:

$$\underline{\alpha}^{n+1} = \underline{\alpha}^{n} - [J]^{-1} \cdot \underline{Y}\ (\underline{\alpha}^{n}), \quad (2.102$$

where, [J] is the Jacobian $\frac{d\underline{Y}}{d\underline{\alpha}}$.

Since the functions are not known analytically, to calculate the Jacobian the guess values of α_1 and α_2 are slightly perturbed (for instance, as $\alpha_1' = 1.0001\ \alpha_1$ and $\alpha_2' = 1.0001\ \alpha_2$) and numerical differentiation is used to find the derivatives.

2.7 RESULTS AND DISCUSSION

There are no detailed numerical results available in the literature for similarity problems with free convection in porous media using generalized Darcy's law. Therefore, for limiting values of parameters K_o and n, the present results have been compared with those of Ostrach [26], which correspond to free convection over a vertical plate with constant wall temperature. Setting $K_o = 0$ and $n = 0$ in the present formulation, the results for the situation studied by Ostrach can be obtained.

The comparison between our results and those of [26], has been presented for $Pr = 1.0$ and $Pr = 0.72$. The velocity and temperature distributions, are shown in tables 1 – 4.

Table 1: Velocity Distribution for Pr = 1.0.

η	Present Values	Values in Ref. [26]
0.2	0.10918	0.1092
0.4	0.18328	0.1833
1.0	0.25012	0.2502
2.0	0.13987	0.1400
3.0	0.05205	0.0524
4.0	0.01468	0.0151
5.0	0.00309	0.0035
6.0	0.00000	0.0004

Table 2: Velocity Distribution for Pr = 0.72.

η	Present Values	Values in Ref. [26]
0.2	0.11581	0.1159
0.4	0.19606	0.1962
1.0	0.27543	0.2759
2.0	0.16867	0.1697
3.0	0.06443	0.0661
4.0	0.01919	0.0212
5.0	0.00415	0.0060
6.0	0.00000	0.0015

Table 3: Temperature Distribution for Pr = 1.0.

η	Present Values	Values in Ref. [26]
0.2	0.88666	0.8867
0.4	0.77421	0.7742
1.0	0.46382	0.4638
2.0	0.14220	0.1422
3.0	0.03382	0.0339
4.0	0.00712	0.0072
5.0	0.00125	0.0014
6.0	0.00000	0.0002

Table 4: Temperature Distribution for Pr = 0.72.

η	Present Values	Values in Ref. [26]
0.2	0.89913	0.8991
0.4	0.79886	0.7989
1.0	0.51682	0.5168
2.0	0.19435	0.1945
3.0	0.05953	0.0601
4.0	0.01618	0.0170
5.0	0.00357	0.0040
6.0	0.00000	0.0009

In figure 2, the velocity profile variation with permeability is depicted. It is seen that with increasing K_o (decreasing voidage) the velocity decreases in the boundary layer. This is because of the increased resistance to flow at higher K_o.

The velocity boundary layer is also thinner when the medium is less porous. For all values of K_o, the velocity profile shows a typical maximum around $\eta = 1$ as generally seen in natural convective boundary layers.

In figure 3, the variation in temperature profile with K_o is shown. It is seen that the temperature drop is less steep when the voidage in the medium is small. This is because the rate of heat transfer is less, when the flow is weak due to higher Darcy resistance. The thermal boundary layer thickness is only mildly influenced by the permeability parameter. Also, both the temperature and velocity profiles appear to be very sensitive to change in K_o, at higher values of K_o. Thus, at low permeabilities even a slight change could greatly affect the flow and heat transfer processes within the medium.

The effect of Pr upon the velocity and temperature profiles are presented in figures 4 and 5. In the purely Darcy model the effect of Prandtl number will not be felt because it does not make any explicit appearance in either energy or the momentum equation. It appears only in a combination of Rayleigh number for such a case. In the present work which focusses the non-Darcian effects, Prandtl number is seen to have strong influence upon both temperature and velocity profiles.

The effect of η is shown in figures 6 and 7 on temperature and velocity distributions.

REFERENCES

[1] Lapwood, E.R., Convection of fluid in a porous medium, Camb. Phil. Soc. Math. Phys. Sci. 44, 508, 1948.

[2] Beck, J.L., Convection in a box of porous material saturated with fluid, Phys. Fluids, 15, 1377, 1972.

[3] Bories, S.A. and Combarnous, M.A., Natural convection in a sloping porous layer, J. Fluid Mech., 57, 63, 1973.

[4] Elder, J.W., Steady free convection in a porous medium heated from below, J. Fluid Mech., 27, 29, 1967.

[5] Donaldson, I.G., Temperature gradient in the upper layers of earth's crust due to convective water flows, J. Geophysics, Res. 67, 3449, 1962.

[6] Stewartson, K., On the convection from a horizontal plate, Z. Angew. Maths. Phys. 9, 276, 1958.

[7] Gill, W.N., Zeh, D.W. and Casal, E.D., Free Convection on a Horizontal Plate, Z. Angew. Maths., Phys. 16, 539, 1965.

[8] Rotem, Z., and Claussen, I., Natural convection above unconfined horizontal surfaces, J. Fluid Mech. 38, 173, 1969.

[9] Pera, L. and Gebhart, B., Natural convection flows adjacent to horizontal surfaces resulting from the combined buoyancy effect of thermal and mass diffusion, Int. J. Heat Mass Transfer, 15, 269, 1972.

[10] Blanc, P. and Gebhart, B., Buoyancy induced flows adjacent to horizontal surfaces, in Proceeding of the 5th International Heat Transfer Conference, Tokyo, Japan, 1974, A.I.Ch. E., New York, 1974.

[11] Wooding, R.A., Convection in a saturated porous medium at large Rayleigh number or Peclet number, J. Fluid Mech. 15, 527, 1963.

[12] McNabb, A., On convection in a porous medium, in Proceeding of Second Australian Conference on Hydraulics and Fluid Mechanics, C161, University of Auckland, Auckland, New Zealand, 1965.

[13] Cheng, P. and Minkowycz, W.J., Free convection about a vertical flat plate embedded in a porous medium with application to heat transfer from a dike, J. Geophys. Res. 82, 2040, 1977.

[14] Cheng,P. and Chang, I. Dee., Buoyancy induced flows in a saturated porous medium adjacent to impermeable horizontal surfaces, Int. J. Heat Mass Transfer, 19, 1267, 1976.

[15] Cheng, P., Combined free and forced convection flow about inclined surfaces in porous media, Int. J. Heat Mass Transfer, Vol. 20, 807, 1977.

[16] Cheng, P., The influence of lateral mass flux on the free convection boundary layers in a saturated porous medium, Int. J. Heat Mass Transfer, 20, 201, 1977.

[17] Cheng, P., Similarity solutions for mixed convection from horizontal impermeable surface in saturated porous media, Int. J. Heat Mass Transfer, 20, 893, 1977.

[18] Na, T.A. and Pop, I., Free convection flow past a vertical flat plate embedded in a saturated porous medium, Int. J. Eng. Sci. 21, 517, 1983.

[19] Johnson, C.H. and Cheng, P., Possible similarity solutions for free convection boundary layers adjacent to flat plates in porous medium, Int. J. Heat Mass Transfer, 21, 709, 1978.

[20] Plumb, O.A. and Huenefeld, J. C., Non-Darcy natural convection from heated surfaces in saturated porous media., Int. J. Heat Mass Transfer, 24, 765, 1981.

[21] Bejan, A. and Poulikakos, D., The non-Darcy regime for vertical boundary layer natural convection in a porous medium, Int. J. Heat Mass Transfer, 26, 815, 1983.

[22] Yang, K.T., Possible similarity solutions for laminar free convection on vertical plates and cylinders, J. Appl. Mech., 27, 230, 1960.

[23] Cheesewright, R., Natural convection from a vertical surface in non-isothermal surroundings, Int. J. Heat Mass Transfer, 10, 1847, 1967.

[24] Gebhart,B., Natural convection flows and stability, Int. J. Heat Mass Transfer, 9, 273, 1973.

[25] M. Kaviany, Mittal, M., Natural convection heat transfer from a vertical plate to high permeability porous media: an experiment and an approximate solution, Int. J. Heat Mass Transfer, 30, 967, 1987.

[26] Ostrach, S., An analysis of laminar free-convection flow and heat transfer about a flat plate parallel to the direction of the generating body force, NACA, TN 2635.

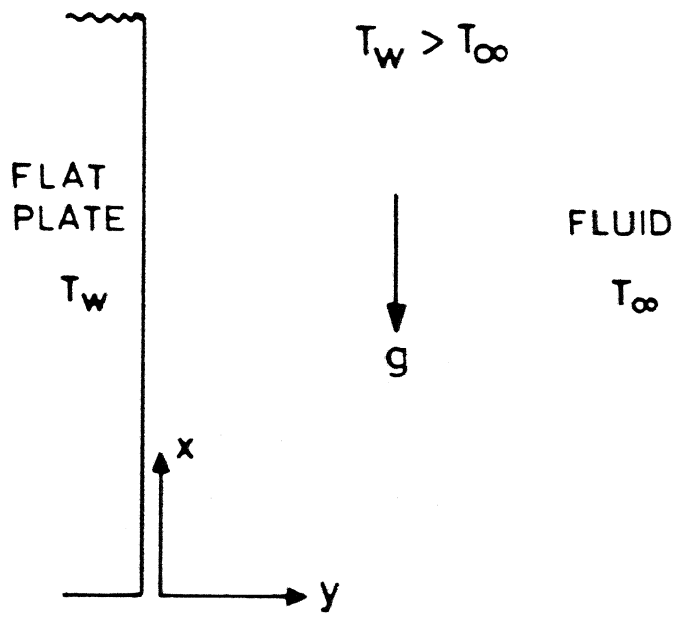

Figure 1 Physical geometry of the problem .

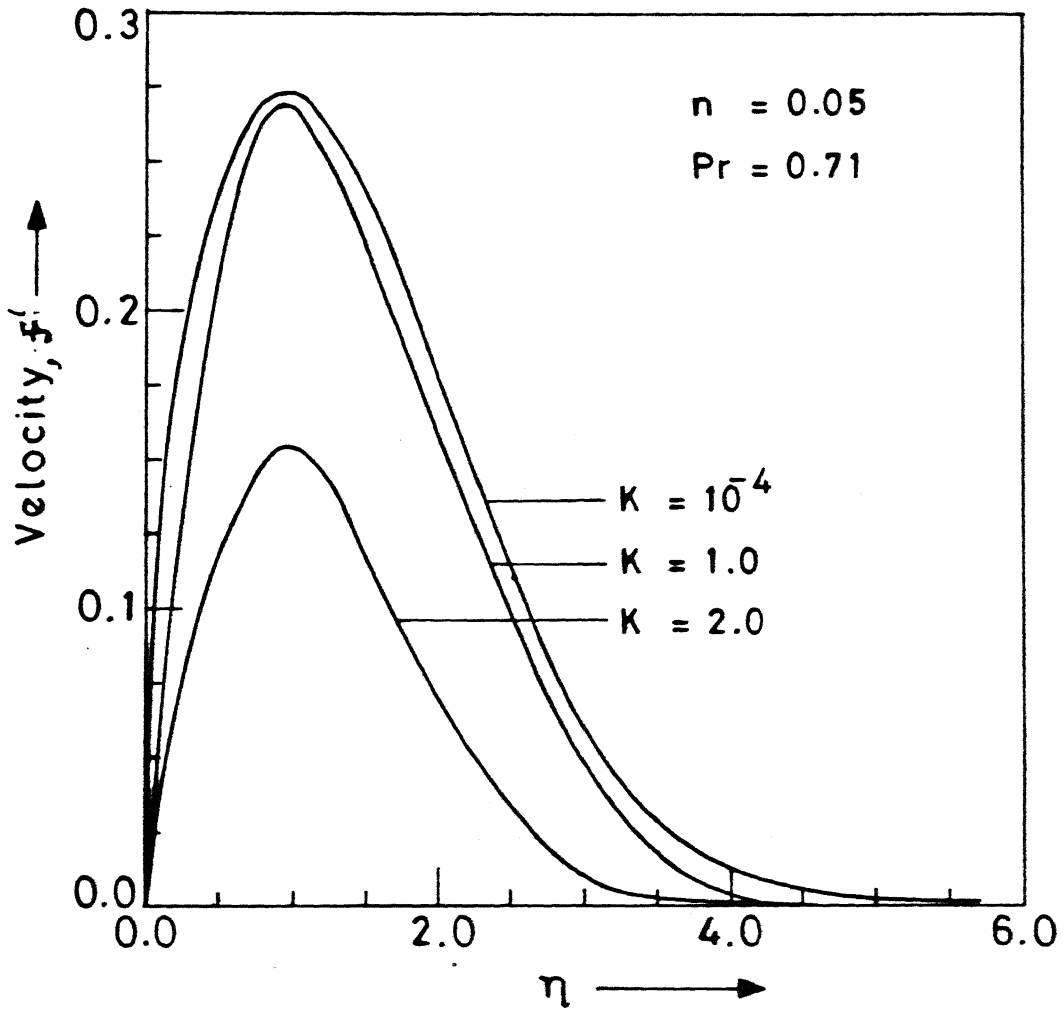

Figure 2 Velocity distribution

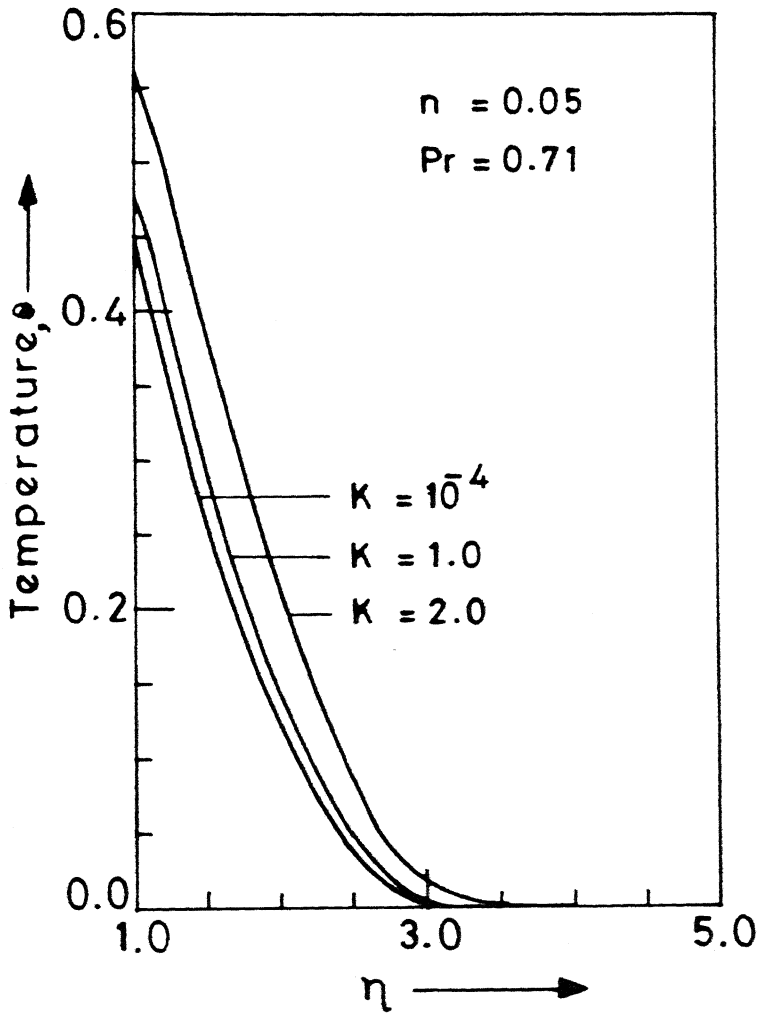

Figure 3 Temperature distribution

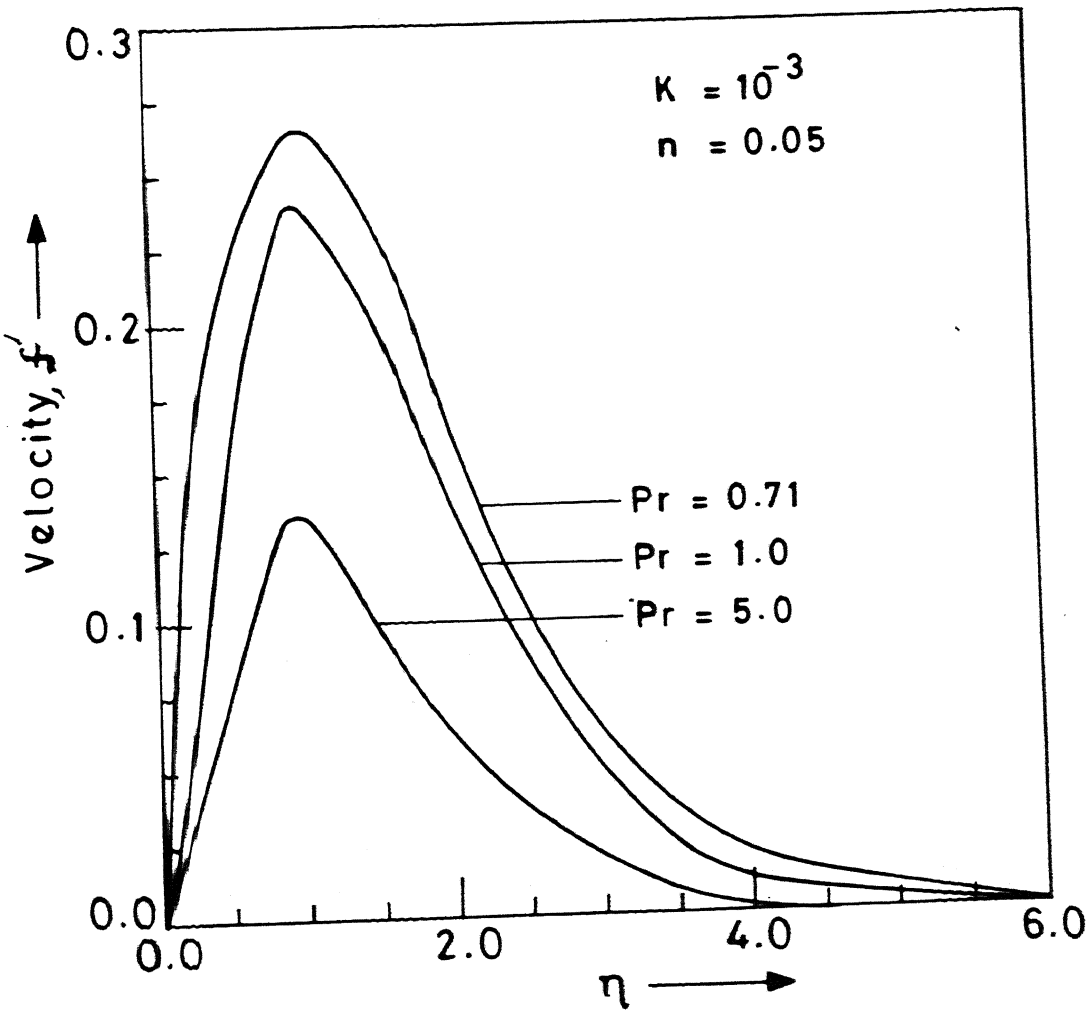

Figure 4 Velocity distribution

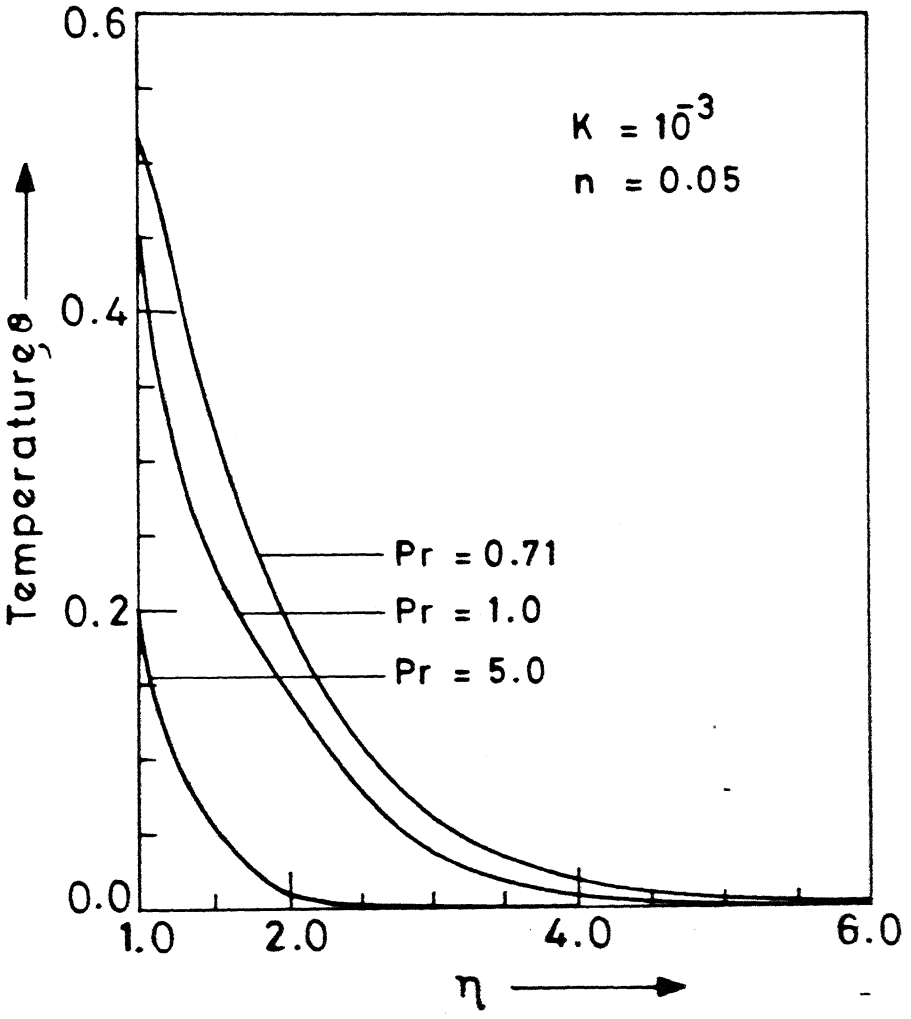

Figure 5 Temperature distribution

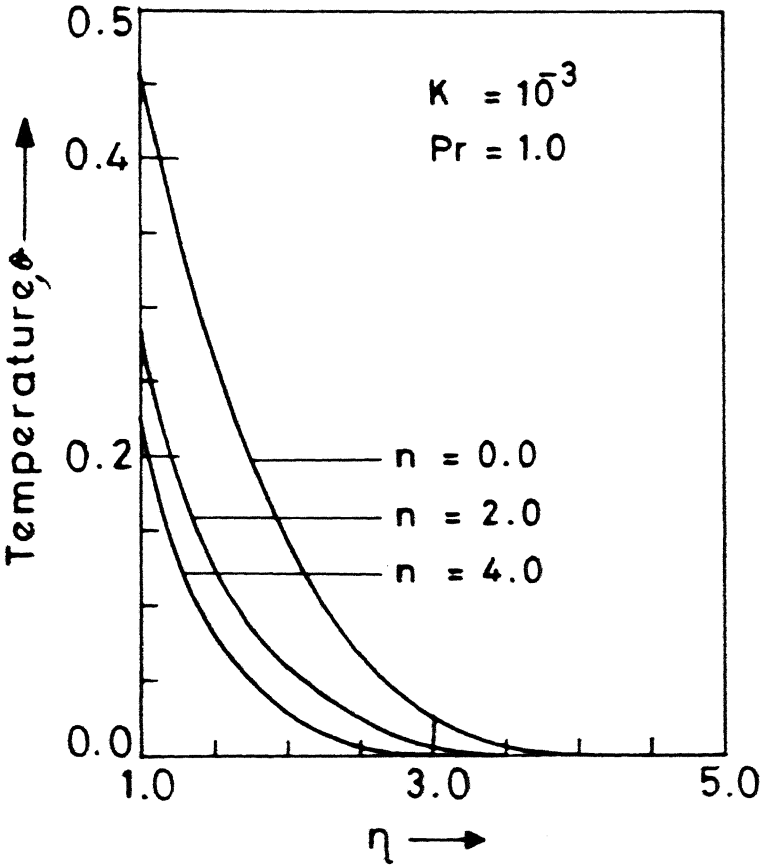

Figure 6 Temperature distribution

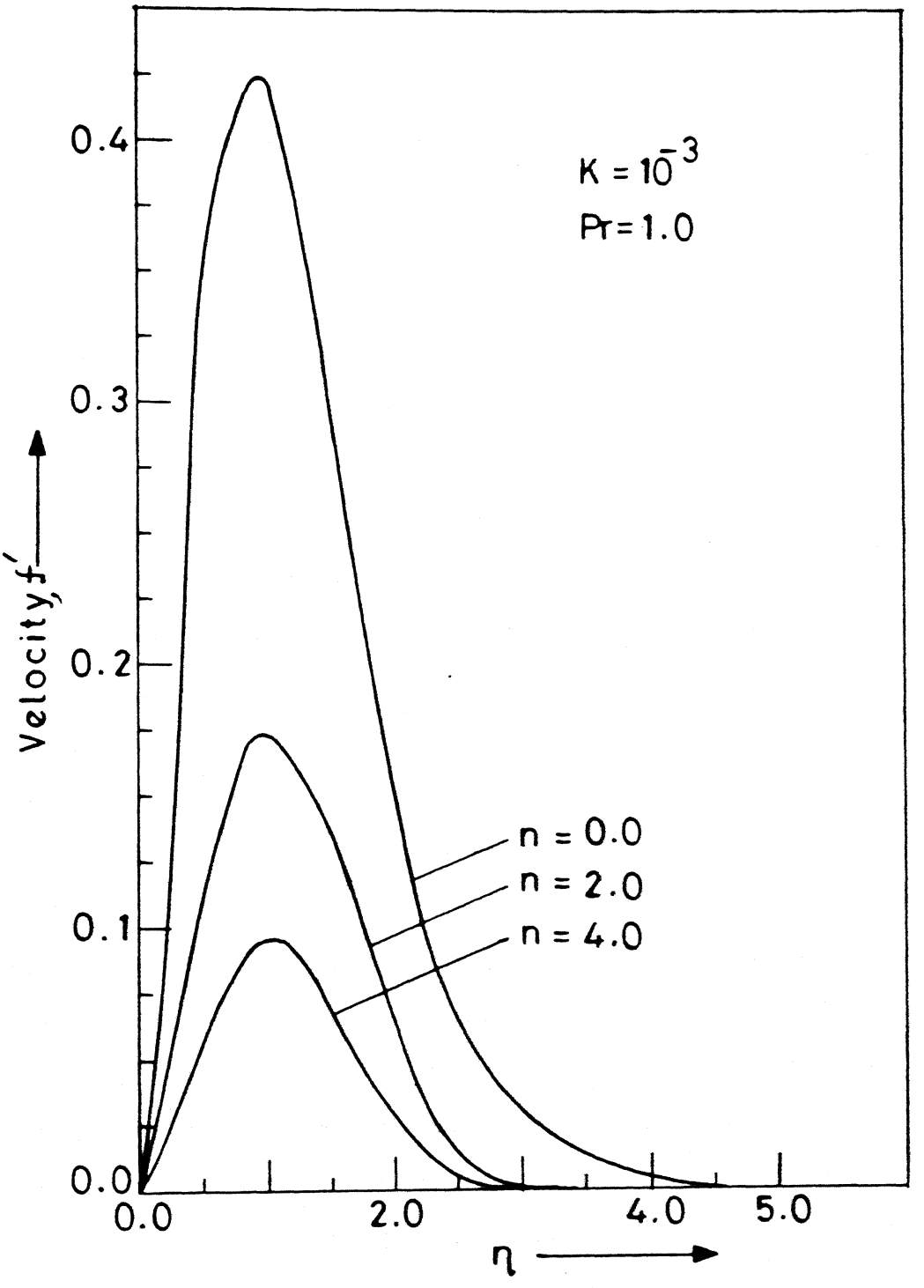

Figure 7 Velocity distribution

CHAPTER III

CONJUGATE FREE CONVECTION FROM A VERTICAL FIN EMBEDDED IN A POROUS MEDIUM

3.1 INTRODUCTION

The problem of conjugate heat transfer from a downward projecting fin immersed in a saturated porous medium is important in applications such as the extraction of geothermal energy and the design of insulating systems for energy conservation. The problem discussed in the present chapter deals with a vertical plate fin situated in a saturated porous medium. The coupled heat transfer between the fin and the fluid flow is analysed in detail and a generalized non-Darcian flow model is used to describe natural convective flow within the porous medium.

In the analysis of natural convective flows, it is possible to consider the fluid region alone exclusively, if the surrounding wall temperature is known. However, in several situations, especially for flows around slender bodies, a prescribed wall temperature distribution cannot be maintained. A majority of the available research studies dealing with heat transfer from submerged fins, assume that the convective heat transfer coefficient at the fin surface is uniform all along the fin. The fin heat conduction equation is then solved analytically using a uniform value of heat transfer coefficient [1,2]. However, the local fin heat transfer coefficient can, indeed, experience

substantial variation along the fin surface [3,4,5] due to nonuniformities in both the velocity and temperature fields in the fluid.

It is necessary, therefore, to solve the conductive - convective heat transfer as a coupled problem and thereby simultaneously analyse the flow and temperature fields on the fluid side and the temperature distribution in the fin. The continuity of heat flux and temperature at the solid-fluid interface is demanded, while solving the coupled heat transfer between the two phases. A problem of this kind is referred to as a conjugate heat transfer problem.

The application and theory of heat transfer by free convection from finned bodies has been studied for over half a century [6]. However, a study of conjugate heat transfer for natural convective flow was initiated by Lock and Gunn [3] in 1968, who have studied the boundary layer flow and heat transfer along a thin vertical fin. They have shown that similarity solutions exist for certain types of surface temperature variations. They also presented experimental results which agree with the theoretical predictions. Using a modified approach, Kuehn et al. [7] also obtained similarity solutions for the problem. More general solutions were obtained by Sparrow and Acharya [8] for natural convection about a vertical plate fin, with a portion of the fin-length heated by a plane heat source. Tolpadi and Kuehn [7] studied the problem of a vertical fin with a circular heat source. A numerical investigation of heat transfer between a rectangular fin and a combined forced and natural convective flow is presented by Sunden [9]. Anderson and Bejan [10,11] have

studied the conjugate heat transfer problems for an impermeabl wall adjacent to a porous medium or a free fluid. However, thes solutions are applicable only to symmetrical problems in which th Oseen linearization can be used.

The conjugate heat transfer for a fin embedded in a porou medium has been investigated by Pop et al. [12]. They considered the natural convective flow with a high Rayleigh number around a vertical fin. In another paper, Pop et al. [13] considered the mixed convection heat transfer along a vertical fin. They used similarity variables to transform the boundary layer equations and solved the resulting equations using a finite difference scheme based on central difference formulae. It is worthwhile to mention that all the above investigations treat the porous medium as purely Darcian.

The purpose of the present work is to study the conjugate heat transfer problem along a fin embedded in a fluid saturated porous medium. A generalized non-Darcian model is invoked to describe the flow. Inertial and viscous terms are taken into account in the momentum equations. The governing equations are solved iteratively within the framework of boundary layer approximations by a highly-implicit finite difference scheme described by Hornbeck [14]. A variable mesh size is used in the direction normal to the fin surface, in order to obtain accurate flow and heat transfer characteristics inside the boundary layer.

3.2 GOVERNING EQUATIONS

A slender rectangular fin of thickness 2b and length L, as shown in figure 1, is considered. The fin is placed vertically in a fluid saturated porous medium and the base temperature of the

fin is taken to be prescribed. A laminar boundary layer flow is assumed to exist around the fin surface. The fluid is incompressible and the density is assumed to be constant except in the buoyancy force term according to the Boussinesq approximation. Viscous dissipation effects are neglected due to low flow velocities and one-dimensional heat conduction within the fin is considered since 2b << L. The momentum equation is described by the generalized Darcy's law as proposed by Yamamoto and Iwamura. The governing equations for the fluid and the fin are therefore given by,

$$\frac{\partial u}{\partial x} + \frac{\partial v}{\partial y} = 0, \tag{3.1}$$

$$u \frac{\partial u}{\partial x} + v \frac{\partial u}{\partial y} = \nu \frac{\partial^2 u}{\partial y^2} + g\beta (T-T_\infty) - \frac{\nu u}{K_o}, \tag{3.2}$$

$$u \frac{\partial T}{\partial x} + v \frac{\partial T}{\partial y} = \alpha \frac{\partial^2 T}{\partial y^2}, \tag{3.3}$$

$$\frac{d^2 T_w}{dx^2} + \frac{k_f}{k_s b} \left[\frac{\partial T}{\partial y} \right]_w = 0. \tag{3.4}$$

The boundary conditions are,

$$\begin{aligned} &y = 0: \quad u = 0, \; v = 0, \; T = T_w, \\ &y \to \infty: \quad u \to 0, \quad T \to T_\infty \\ &x = 0: \quad u = 0, \; T = T_\infty, \; \frac{dT_w}{dx} = 0, \\ &x = L: \quad T_w = T_b, \end{aligned} \tag{3.5}$$

where, u and v are the horizontal and vertical velocity components, T is the fluid temperature and T_∞, T_w and T_b are the temperatures of the ambient fluid, the fin-surface and the fin-base respectively. Also, g is the acceleration due to gravity, ν, β, α are the kinematic viscosity, the coefficient of

volume expansion, and the thermal diffusivity of the fluid, K_o is the permeability of the porous medium and K_f, K_s are the thermal conductivities of the fluid and the fin. It may be noted that in the temperature boundary condition for the fluid at $y = 0$, the wall temperature T_w is unknown and needs to be solved through the heat conduction equation for the fin.

Introducing the following dimensionless quantities,

$$u = \frac{uL}{\nu}, \quad v = \frac{vL}{\nu}, \quad \theta = \frac{T-T_\infty}{T_b-T_\infty}, \quad \theta_w = \frac{T_w-T_\infty}{T_b-T_\infty}, \quad x = \frac{x}{L}, \tag{3.6}$$

$$y = \frac{y}{L}, \quad K = \frac{K_o}{L^2}, \quad Gr = \frac{g\beta\,(T_b-T_\infty)\,L^3}{\nu^2}, \quad CCP = \frac{k_f L}{k_s b} \text{ and } Pr = \frac{\nu}{\alpha}.$$

The governing equations (3.1) - (3.4) take the form:

$$\frac{\partial u}{\partial x} + \frac{\partial v}{\partial y} = 0, \tag{3.7}$$

$$u\frac{\partial u}{\partial x} + v\frac{\partial u}{\partial y} = \nu\frac{\partial^2 u}{\partial y^2} + Gr\,\theta - \frac{u}{K}, \tag{3.8}$$

$$u\frac{\partial \theta}{\partial x} + v\frac{\partial \theta}{\partial y} = \frac{1}{Pr}\frac{\partial^2 \theta}{\partial y^2}, \tag{3.9}$$

$$\frac{d^2\theta_w}{dx^2} + CCP\left[\frac{\partial \theta}{\partial y}\right]_w = 0, \tag{3.10}$$

where, Gr is the Grashof number, Pr is the Prandtl number, K is the permeability parameter and CCP is the conduction-convection parameter.

The equations (3.7) - (3.10) are to be solved with the following boundary conditions,

$$\begin{aligned} &y = 0: \quad u = 0, \; v = 0, \; \theta = \theta_w(x), \\ &y \to \infty: \quad u \to 0, \quad \theta \to 0, \\ &x = 0: \quad u = 0, \; \theta = 0, \; \frac{d\theta_w}{dx} = 0, \\ &x = 1: \quad \theta_w = 1. \end{aligned} \tag{3.11}$$

The boundary condition for θ_w at x = 0 is based on the following argument. If the fin is very long and thin, the amount of heat which passes from the tip of the fin to the fluid is negligible, compared to the heat loss through the lateral surface. In such a case the assumption of an adiabatic tip is justified and the temperature gradient in the fin at the tip is thus assumed to be zero [1,2].

It may be observed that in the foregoing description of the boundary conditions, no mention is made of the velocity condition at the base surface. This omission is required by the boundary layer equations. Once the conditions have been specified at the leading edge of the plate (x = 0), the solution yields the velocity field at all x > 0 and, therefore, does not permit the specification of velocity boundary condition at any x > 0. The non-accounting of hydrodynamic effects related to the presence of the base surface should not materially affect the fin heat transfer results provided that the fin length L is large compared with the boundary layer thickness at x = L [9].

3.3 METHOD OF SOLUTION

Equations (3.7)-(3.10) are now expressed in finite difference form. A highly-implicit numerical scheme [14] is used in which the non-linear coefficients are taken at (j + 1)th level, where the subscripts j and k correspond to x and y directions, repsectively. This form is necessitated by the zero velocity of the free stream, which will result in the classical implicit formulation being inconsistent. The difference equations are given as,

$$\frac{u_{j+1,k+1} - u_{j,k+1}}{\Delta x} + \frac{v_{j+1,k+1} - v_{j+1,k}}{\Delta y} = 0, \qquad (3.12)$$

$$u_{j+1,k} \frac{u_{j+1,k} - u_{j,k}}{\Delta x} + v_{j+1,k} \frac{u_{j+1,k+1} - u_{j+1,k-1}}{2(\Delta y)}$$

$$= \frac{u_{j+1,k-1} - 2u_{j+1,k} + u_{j+1,k+1}}{(\Delta y)^2} - \frac{u_{j+1,k}}{K} + Gr\ \theta_{j+1,k}, \qquad (3.13)$$

$$u_{j+1,k} \frac{\theta_{j+1,k} - \theta_{j,k}}{\Delta x} + v_{j+1,k} \frac{\theta_{j+1,k+1} - \theta_{j+1,k-1}}{2(\Delta y)}$$

$$= \frac{1}{Pr} \frac{\theta_{j+1,k-1} - 2\theta_{j+1,k} + \theta_{j+1,k+1}}{(\Delta y)^2}. \qquad (3.14)$$

Since the difference form is non-linear, an iterative scheme is required to obtain the solution. The difference equations given above can be written as,

$$\frac{u^{(i+1)}_{j+1,k+1} - u_{j,k+1}}{\Delta x} + \frac{v^{(i+1)}_{j+1,k+1} - v^{(i+1)}_{j+1,k}}{\Delta y} = 0, \qquad (3.15)$$

$$u^{(i)}_{j+1,k} \frac{u^{(i+1)}_{j+1,k} - u_{j,k}}{\Delta x} + v^{(i)}_{j+1,k} \frac{u^{(i+1)}_{j+1,k+1} - u^{(i+1)}_{j+1,k-1}}{2(\Delta y)}$$

$$= \frac{u^{(i+1)}_{j+1,k-1} - 2u^{(i+1)}_{j+1,k} + u^{(i+1)}_{j+1,k+1}}{(\Delta y)^2}$$

$$- \frac{u^{(i+1)}_{j+1,k}}{K} + Gr\ \theta^{(i)}_{j+1,k}, \qquad (3.16)$$

$$u^{(i+1)}_{j+1,k} \frac{\theta^{(i+1)}_{j+1,k} - \theta_{j,k}}{\Delta x} + v^{(i+1)}_{j+1,k} \frac{\theta^{(i+1)}_{j+1,k+1} - \theta^{(i+1)}_{j+1,k-1}}{2(\Delta y)}$$

$$= \frac{1}{Pr} \frac{\theta^{(i+1)}_{j+1,k-1} - 2\theta^{(i+1)}_{j+1,k} + \theta^{(i+1)}_{j+1,k+1}}{(\Delta y)^2}, \qquad (3.$$

where, the superscripts i and (i+1) indicate the values obtained at the ith and (i+1)th iterations, respectively. The iterative

scheme is applied for the above equations by solving one equation at a time in a sequential manner. For instance, the momentum equation can be handled in the following way. The simplified form of equation (3.16) is,

$$\left[-\frac{1}{(\Delta y)^2}-\frac{v^{(i)}_{j+1,k}}{2(\Delta y)}\right]u^{(i+1)}_{j+1,k-1}+\left[\frac{2}{(\Delta y)^2}+\frac{u^{(i)}_{j+1,k}}{\Delta x}+\frac{1}{K}\right]u^{(i+1)}_{j+1,k}$$

$$+\left[-\frac{1}{(\Delta y)^2}+\frac{v^{(i)}_{j+1,k}}{2(\Delta y)}\right]u^{(i+1)}_{j+1,k+1}$$

$$=\frac{u^{(i)}_{j+1,k}\,u_{j,k}}{\Delta x}+Gr\,\theta^{(i)}_{j+1,k}. \qquad (3.18)$$

The matrix form of the above equation (after incorporating the velocity boundary conditions) is as follows,

$$\begin{bmatrix} 1 & 0 & & & & & \\ A_2 & B_2 & C_2 & & & & \\ & A_3 & B_3 & C_3 & & & \\ & - & - & - & & & \\ & - & - & - & & & \\ & & - & - & - & & \\ & & & & A_{N-1} & B_{N-1} & C_{N-1} \\ & & & & & 0 & 1 \end{bmatrix} \begin{bmatrix} u^{(i+1)}_{j+1,1} \\ u^{(i+1)}_{j+1,2} \\ u^{(i+1)}_{j+1,3} \\ - \\ - \\ - \\ u^{(i+1)}_{j+1,N-1} \\ u^{(i+1)}_{j+1,N} \end{bmatrix} = \begin{bmatrix} 0 \\ D_2 \\ D_3 \\ - \\ - \\ - \\ D_{N-1} \\ 0 \end{bmatrix}$$

(3.19)

where,

$$A_k = -\frac{1}{(\Delta y)^2} - \frac{v^{(i)}_{j+1,k}}{2(\Delta y)} ,$$

$$B_k = \frac{2}{(\Delta y)^2} + \frac{u^{(i)}_{j+1,k}}{\Delta x} + \frac{1}{K} , \qquad (3.20)$$

$$C_k = -\frac{1}{(\Delta y)^2} + \frac{v^{(i)}_{j+1,k}}{2(\Delta y)} ,$$

$$D_k = \frac{u^{(i)}_{j+1,k}\, u_{j,k}}{\Delta x} + Gr\, \theta^{(i)}_{j+1,k} .$$

The discretized continuity equation (3.15) can be written as,

$$v^{(i+1)}_{j+1,k+1} = v^{(i+1)}_{j+1,k} - \frac{\Delta y}{\Delta x} (u^{(i+1)}_{j+1,k+1} - u_{j,k+1}) . \qquad (3.21)$$

Equation (3.21) is solved in an explicit fashion to obtain the velocity component v at all y locations starting from the wall. Now, the discretized energy equation (3.14) may be rearranged as,

$$\left[-\frac{1}{Pr(\Delta y)^2} - \frac{v^{(i+1)}_{j+1,k}}{2(\Delta y)}\right] \theta^{(i+1)}_{j+1,k-1} + \left[\frac{2}{Pr(\Delta y)^2} + \frac{u^{(i+1)}_{j+1,k}}{\Delta x}\right] \theta^{(i+1)}_{j+1,k}$$

$$+ \left[-\frac{1}{Pr(\Delta y)^2} + \frac{v^{(i+1)}_{j+1,k}}{2(\Delta y)}\right] \theta^{(i+1)}_{j+1,k+1} = \frac{u^{(i+1)}_{j+1,k}\, \theta_{j,k}}{\Delta x} . \qquad (3.22)$$

The above equation can be put in the matrix form, after incorporating the temperature boundary conditions as follows,

$$\begin{bmatrix} 1 & 0 & & & & & \\ A_2' & B_2' & C_2' & & & & \\ & A_3' & B_3' & C_3' & & & \\ & - & - & - & & & \\ & - & - & - & & & \\ & & - & - & - & & \\ & & & & A_{N-1}' & B_{N-1}' & C_{N-1}' \\ & & & & & 0 & 1 \end{bmatrix} \begin{bmatrix} \theta_{j+1,1}^{(i+1)} \\ \theta_{j+1,2}^{(i+1)} \\ \theta_{j+1,3}^{(i+1)} \\ - \\ - \\ - \\ \theta_{j+1,N-1}^{(i+1)} \\ \theta_{j+1,N}^{(i+1)} \end{bmatrix} = \begin{bmatrix} \theta_w \\ D_2' \\ D_3' \\ - \\ - \\ - \\ D_{N-1}' \\ 0 \end{bmatrix} \tag{3.23}$$

where,

$$A_k' = -\frac{1}{Pr\ (\Delta y)^2} - \frac{v_{j+1,k}^{(i+1)}}{2(\Delta y)},$$

$$B_k' = \frac{2}{Pr\ (\Delta y)^2} + \frac{u_{j+1,k}^{(i+1)}}{\Delta x}, \tag{3.24}$$

$$C_k' = -\frac{1}{Pr\ (\Delta y)^2} + \frac{v_{j+1,k}^{(i+1)}}{2(\Delta y)},$$

$$D_k' = \frac{u_{j+1,k}^{(i+1)}\ \theta_{j,k}}{\Delta x}.$$

The fin heat conduction equation (3.10) may be written in the difference form as,

$$\frac{\theta_{j-1}^w - 2\theta_j^w + \theta_{j+1}^w}{(\Delta x)^2} = -CCP\ \left[\frac{\partial\theta}{\partial y}\right]_{(j,0)} \tag{3.25}$$

where θ_j^w is the fin-surface temperature at location j. The above equations can be rearranged in the more convenient form,

$$\theta^{w}_{j-1} - 2\theta^{w}_{j} + \theta^{w}_{j+1} = - CCP\ (\Delta x)^2 \left[\frac{\partial \theta}{\partial y} \right]_{(j,0)} \qquad (3.26)$$

After incorporating the boundary conditions for the fin, the matrix equation corresponding to equation (3.26) can be obtained easily.

Due to the non-linearity and the mutual coupling between the equations (3.19), (3.21), (3.23) and (3.26), an iterative solution needs to be developed. The iterative process is complex since it involves an overall iteation loop between the fluid and the fin equations and a sub-iteration loop for the fluid phase equations. The basic steps of the procedure are summarised below:

(a) An initial guess for the fin temperature $\theta_w(x)$ is estimated. A parabolic variation, say $\theta_w(x) = x^2$ was found to be a good initial guess.

(b) The flow field and convective heat transfer equations in the fluid are solved with the guessed fin temperature distribution as the wall boundary condition.

(c) From the calculated fluid temperature field the heat flux $(\frac{\partial \theta}{\partial y})_w$ is estimated at every x-position.

(d) The fin heat conduction equation is solved with the prescription of the value of $(\frac{\partial \theta}{\partial y})_w$ as obtained above. The new guess for the fin temperature distribution $\theta_w(x)$ is evaluated and steps (b-d) are repeated until convergence is obtained. When acceptable convergence of the above mentioned iterative process is achieved and the conditions of continuity of heat flux and temperature at the fluid-solid interface are satisfied, all the relevant heat transfer characteristics can then be calculated.

The equations have been solved by using a constant step-size in x-direction and a variable mesh size in the y-direction. A finer mesh size is used in the region of rapid variation i.e. near the fin and a relatively coarse mesh is used for the region of slower variation.

There are many advantages of using the variable mesh technique over that of a uniform mesh-size over the entire region. Firstly, with a variable mesh-size, the number of simultaneous equations to be solved can be reduced, which is very important for an implicit formulation. Since the time required to solve the simultaneous linear equations increases with the number of equations, a considerable saving in computational time can be achieved. In addition, the round-off error accumulated while solving the large number of simultaneous equations is held to a minimum. Furthermore, since the boundary layer has zero thickness at the tip of the fin, a uniform discretization will have very few grid points near the fin tip. Hence the solution will not be accurate near the tip and these inaccuracies will be transmitted along the full length of the fin. In the present work a three-stage mesh size variation has been considered and due care has been taken to provide sufficient number of grid points within the boundary layer region near the fin tip.

3.4 RESULTS AND DISCUSSION

The temperature distribution in the fin and the porous medium are obtained along with the velocity distribution in the fluid, for a wide range of governing parameters of the problem, namely Gr, CCP, Pr and K. A constant step size of $\Delta x = 0.002$ is used in

the x-direction while a three-stage variable mesh size is used in the y-direction. The step size Δy varies as follows,

Δy = 0.002 for the first 51 steps from the wall,

Δy = 0.005 for the next 130 steps and

Δy = 0.01 for the last 6 steps.

The total y distance covered by these steps, (y_{max}), approximates the thickness of the boundary layer in the present calculations.

To establish the correctness of the present work, the results obtained by the finite difference method are compared with analytical results for a limiting case. The situation considered for this purpose corresponds to a low Grashof number for a free fluid ($K \to \infty$). For small Gr, the temperature solution in the fluid around the fin is dominated by one-dimensional conduction normal to the fin and the horizontal and vertical components of fluid velocity are very small so that the convective effects can be neglected from the energy equation. With these assumptions the energy equation reduces to,

$$\frac{d^2\theta}{dy^2} = 0 \ . \qquad (3.27)$$

The general solution of the above equation which satisfies the given boundary conditions is

$$\theta = \theta_w(x) \left(1 - \frac{y}{y_{max}}\right), \qquad (3.28)$$

where, $\theta_w(x) = \frac{\cosh m x}{\cosh m}$ and $m^2 = CCP/Y_{max}$, for $CCP \neq 0$. For CCP = 0, there is no heat loss from the fin and the entire fin can taken to be at base temperature. So, one can set $\theta_w(x) = 1$ for CCP = 0.

Neglecting the inertial and the Darcy resistance terms

equation of motion can be written in a simplified form as,

$$\frac{d^2u}{dy^2} + Gr\ \theta = 0. \qquad (3.29)$$

The solution of equation (3.29) with the given velocity boundary conditions is,

$$u = Gr\ \left(\frac{y^3}{6\ y_{max}} - \frac{y^2}{2} + \frac{y\ y_{max}}{3} \right). \qquad (3.30)$$

In Table 1 the results corresponding to the above described limiting case, obtained by finite difference method are tabulated with the exact analytical values.

Table 1

Temperature and velocity distribution for $K \to \infty$ (10^3), CCP = 0, Gr = 1.0, y_{max} = 0.81.

y	Temperature		Horizontal velocity	
	Numerical results	Analytical results	Numerical results	Analytical results
0.0	1.0000	1.0000	0.0000	0.0000
0.1	0.8780	0.8765	0.0225	0.0222
0.2	0.7560	0.7531	0.0363	0.0356
0.3	0.6340	0.6296	0.0425	0.0416
0.4	0.5120	0.5062	0.0423	0.0412
0.5	0.3901	0.3827	0.0371	0.0357
0.6	0.2681	0.2593	0.0279	0.0264
0.7	0.1462	0.1358	0.0160	0.0146

The good agreement between the numerical and the exact analytical solution indicates the correctness of the results obtained by the finite difference method.

The wall temperature variation with x is plotted for various Gr in figure 2. The analytical result obtained for small Gr is shown by a dotted line. It is found that as Gr decreases the temperature profile approaches the hyperbolic variation as suggested by the analytical solution (CCP ≠ 0 and Gr low). As Gr increases more heat is removed from the fin by fluid convection as indicated by the slope of wall temperature. In figure 3, the wall temperature variation for various permeability parameters is shown. It is seen that as the permeability parameter K approaches the value of zero, the wall temperature distribution moves closer to the analytical solution for pure conduction in fluid. This is to be expected, since for small K, the Darcy resistance to flow is very high which reduces the velocity of the fluid. The heat convection effect, therefore, becomes very small even at large Gr as K approaches zero. thus for increasing K the fin is cooled more.

In figure 4, the effect of the conduction-convection parameter, CCP, upon the wall temperature distribution is depicted. For each value of CCP, the numerical solution and the corresponding pure conduction solution have been plotted. From the figure, it is observed that wall temperature increases with CCP. This trend is easily understandable since higher CCP leads to more coupling between the solid and fluid phases and hence more heat loss from the fin. Both the analytical and numerical solutions exhibit similar variation with CCP, although a close match between the numerical and its corresponding analytical solution is not to be expected on account of the high Gr value used for the numerical solutions.

The variation of wall temperature distribution with Pr, Prandtl number is shown in figure 5. It is seen that the fin cooling is more effective at higher Prandtl number due to a thinner thermal boundary layer.

In figure 6 the fluid temperature variation in x-direction is shown for various Grashof numbers at a fixed value of y. The fluid temperature has a similar variation as the fin temperature with respect to x. As Grashof number increases the temperature of the fluid decreases. This trend is similar to that of the fin temperature. Although the total amount of heat removed from the fin is larger at higher Grashof number, the increase in the heat transfer coefficient is more rapid resulting in a smaller fluid temperature. Figure 7 and 8 show the variation of the velocity field and the temperature field in the y-direction, at various x-locations. As expected, for fixed values of other parameters, the values of velocity and temperature increase with x. The increase in the velocity values with x indicates that natural convection becomes more and more vigorous as fluid flows adjacent to the fin in x-direction. This is a direct consequence of the increased heat penetration into the fluid at higher values of x.

In figures 9, 10, 11 and 12, the local Nusselt number variation with the governing parameters Gr, K, CCP and Pr are shown. The Nusselt number increases with Gr, K and Pr and it decreases slightly with CCP. Since the heat loss from the fin is related to the slope of the wall temperature variation in x-direction and the Nusselt number characterises the heat loss from the fin, the observed variation of Nusselt number with various

parameters can be explained by considering the slope of θ_w in figures 2-5.

In figure 13, the wall temperature profile predicted by the present analysis is compared with that of Pop et al. [13] who have considered Darcy's model for flow. For smaller Grashof number the difference is not that significant. However, as expected, the non-Darcy effects play an important role at higher Grashof numbers.

REFERENCES

[1] Eckert, E.R.G. and Drake, E.M., Analysis of Heat and Mass Transfer, McGraw Hill, New York, 1972.

[2] Kern, D.Q. and Kraus, A.D., Extended surface heat transfer, McGraw Hill, New York, 1972.

[3] Lock, G.S.H. and Gunn, J.C., Laminar free convection from a downward projecting fin, Journal of Heat Transfer, 90, 63, 1968.

[4] Sparrow, E.M., Baliga, B.R. and Patankar, S.V., Forced Convection heat transfer from a shrouded fin array with and without tip clearence, Journal of Heat Transfer, 100, 572, 1978.

[5] Stachiewicz, J.W., Effect of variation of local film coefficient on fin performance, ASME Journal of Heat Transfer, 91, 21, 1969.

[6] Harper, W.P. and Brown, D.R., Mathematical equation for heat conduction in the fins of air cooled engines, N.A.C.A. Report, 158, 122.

[7] Kuehn, T.H., Kwon, S.S. and Tolpadi, A.K., Similarity solutions for conjugate natural convection heat transfer from a long vertical fin, Int. J. Heat Mass Transfer, 26, 1718, 1983.

[8] Sparrow, E.M. and Acharya, S.A., Natural convection fin with a solution determined non-monotonically varying heat transfer coefficient, J. Heat Transfer, 103, 218, 1981.

[9] Sunden, B., Conjugate mixed convection heat transfer from a vertical rectangular fin, Int. Com. Heat Mass Transfer, 10, 267, 1983.

[10] Anderson, R., and Bejan, A., Natural convection on both sides of a vertical wall separating fluids at different temperatures, J. Heat Transfer, 102, 630, 1980.

[11] Bejan,A., and Anderson, R., Heat transfer across a vertical impermeable partition embedded in a porous medium, Int. J. Heat Transfer, 24, 1237, 1981.

[12] Pop, I., Sunda, J.K., Cheng, P. and Minkowycz, W.J., Conjugate free convection from a long vertical plate fins embedded in a porous medium at high Rayleigh numbers, Int. J.H.T., 28, 1629, 1985.

[13] Pop, I., Ingham, B., Heggs, P.J. and Gardner, D., Conjugate heat transfer from a downward projecting fin immersed in porous med. Proceeding Heat Transfer, 2635, 1986.

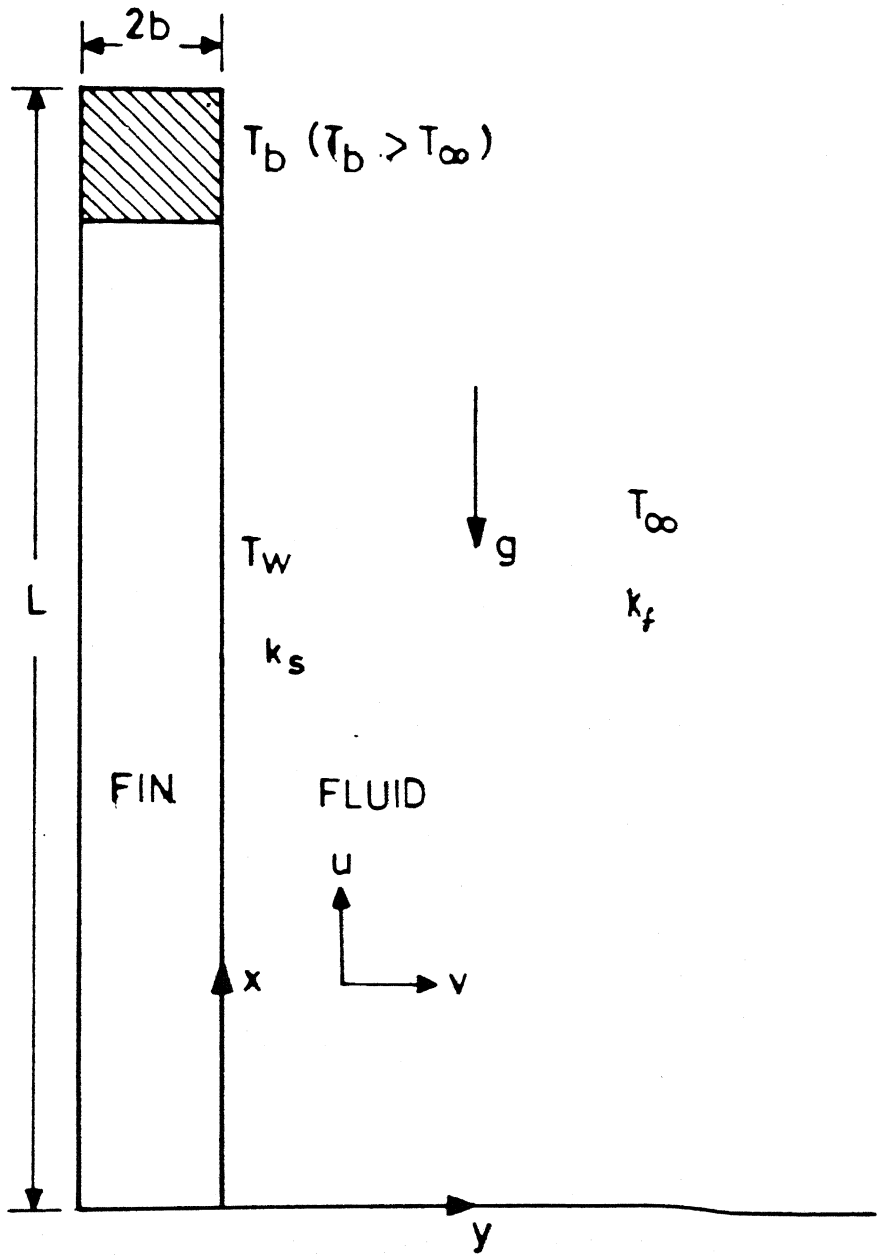

Figure 1 Fin Geometry

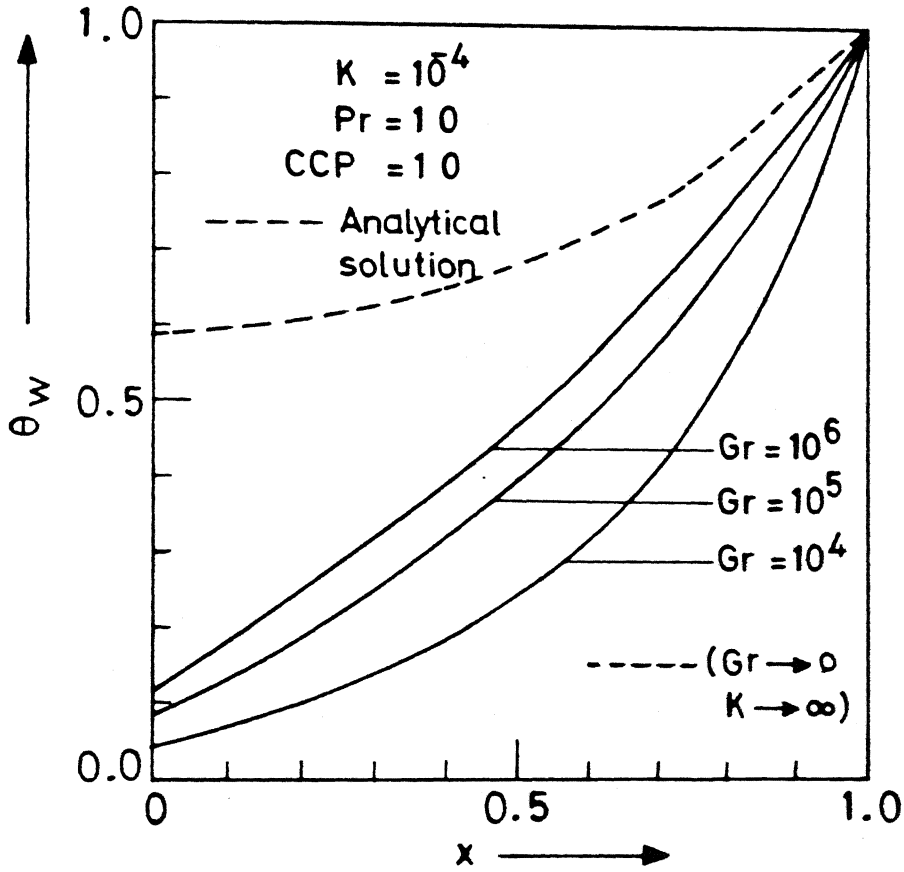

Figure 2 Wall Temperature versus x .

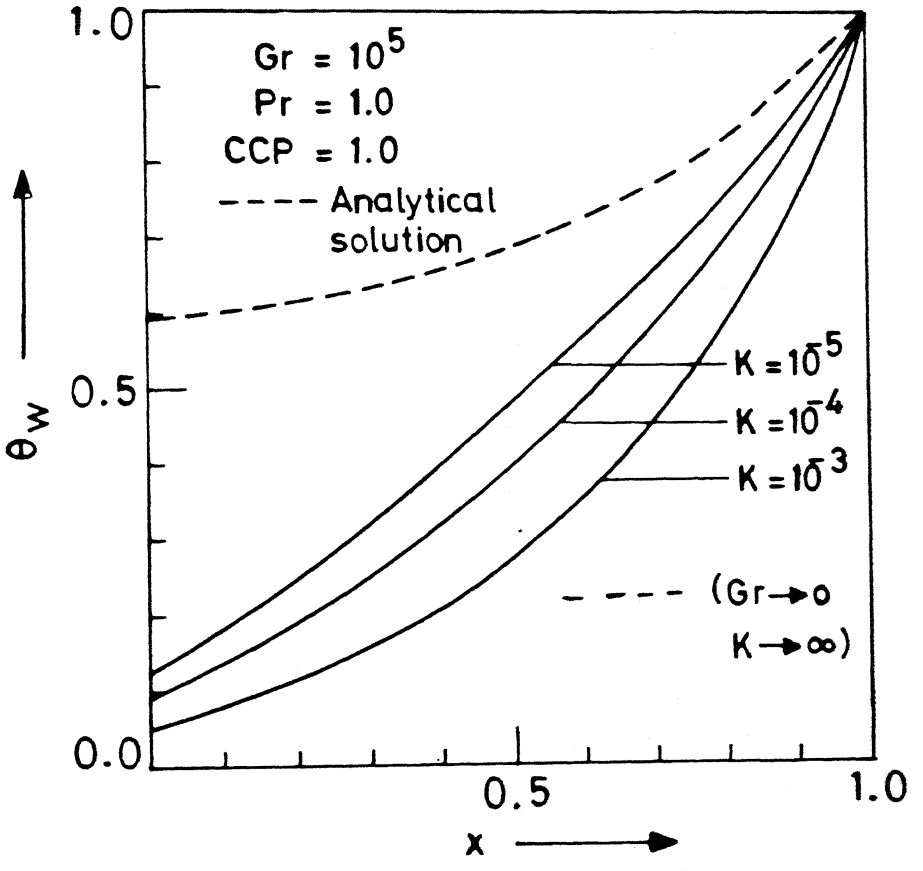

Figure 3 Wall Temperature versus x.

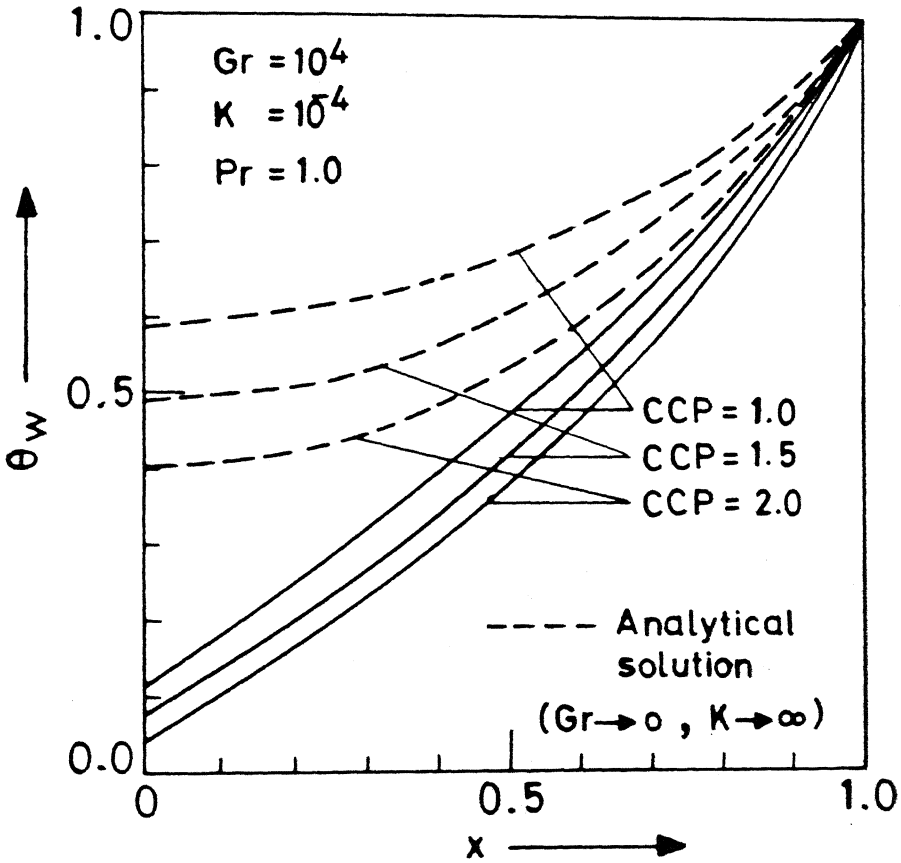

Figure 4 Wall Temperature versus x.

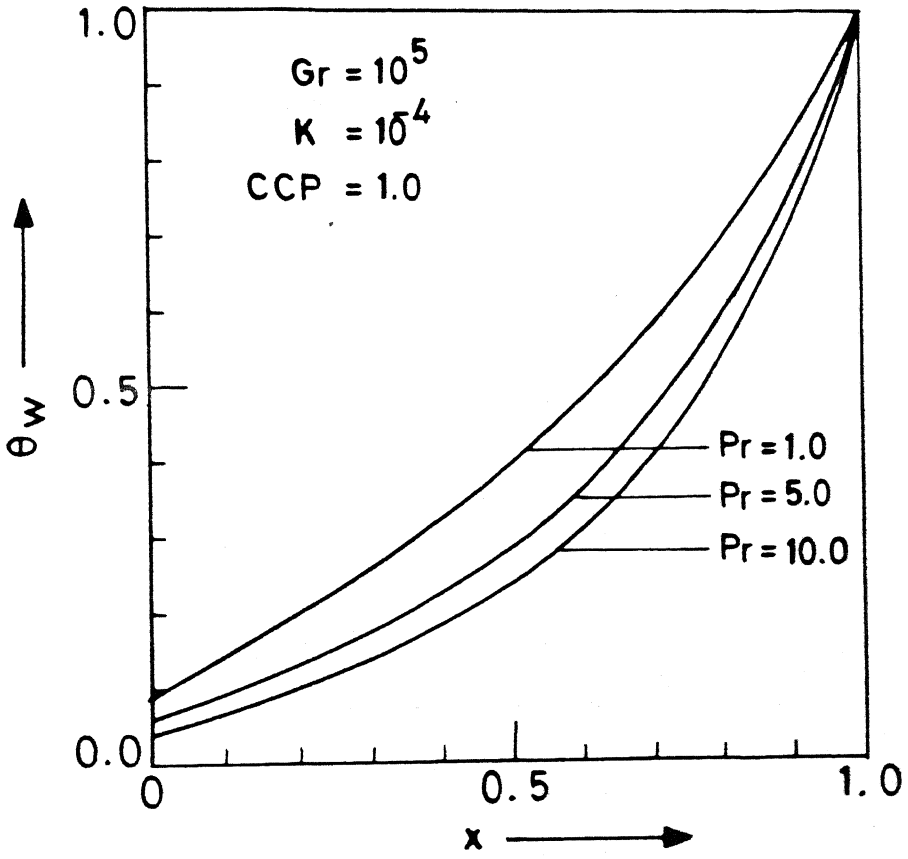

Figure 5 Wall Temperature versus x .

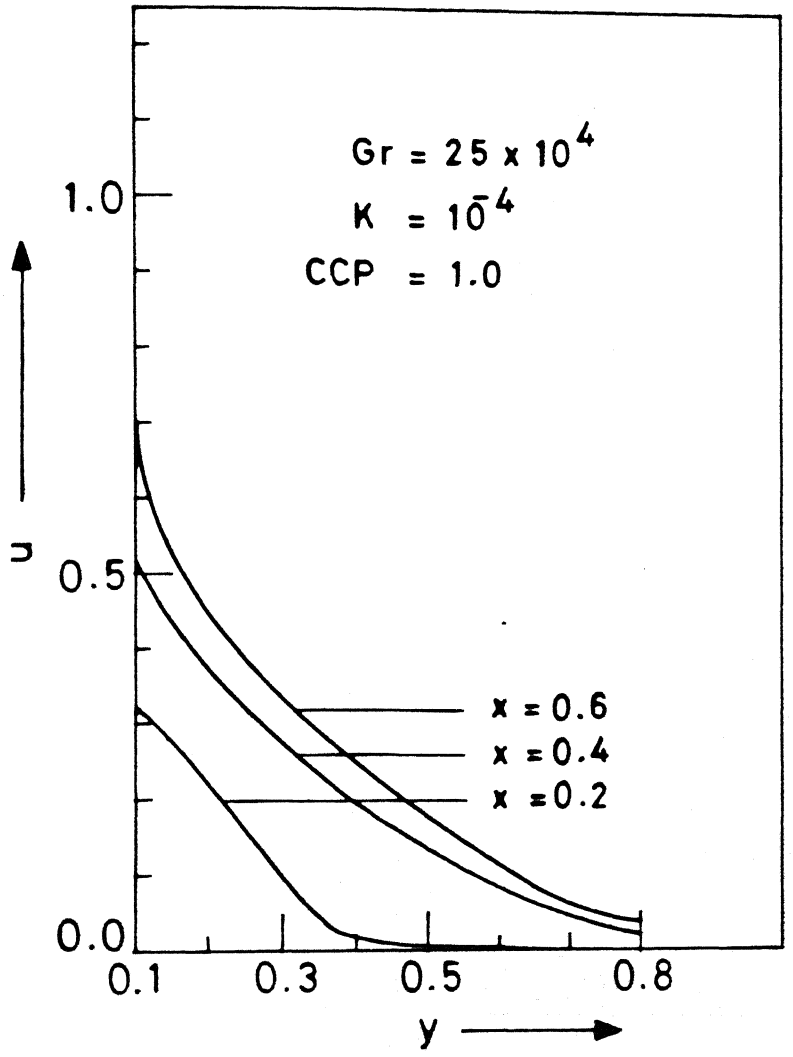

Figure 7 Velocity distribution versus y.

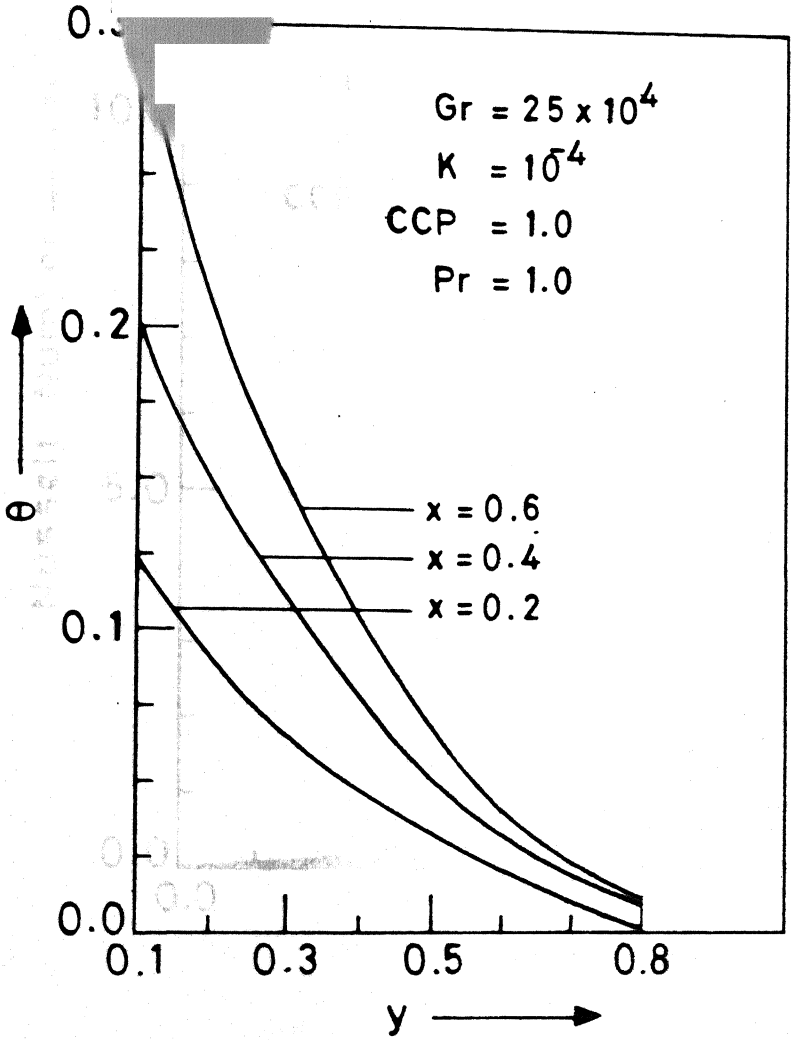

Figure 8 Fluid Temperature versus y.

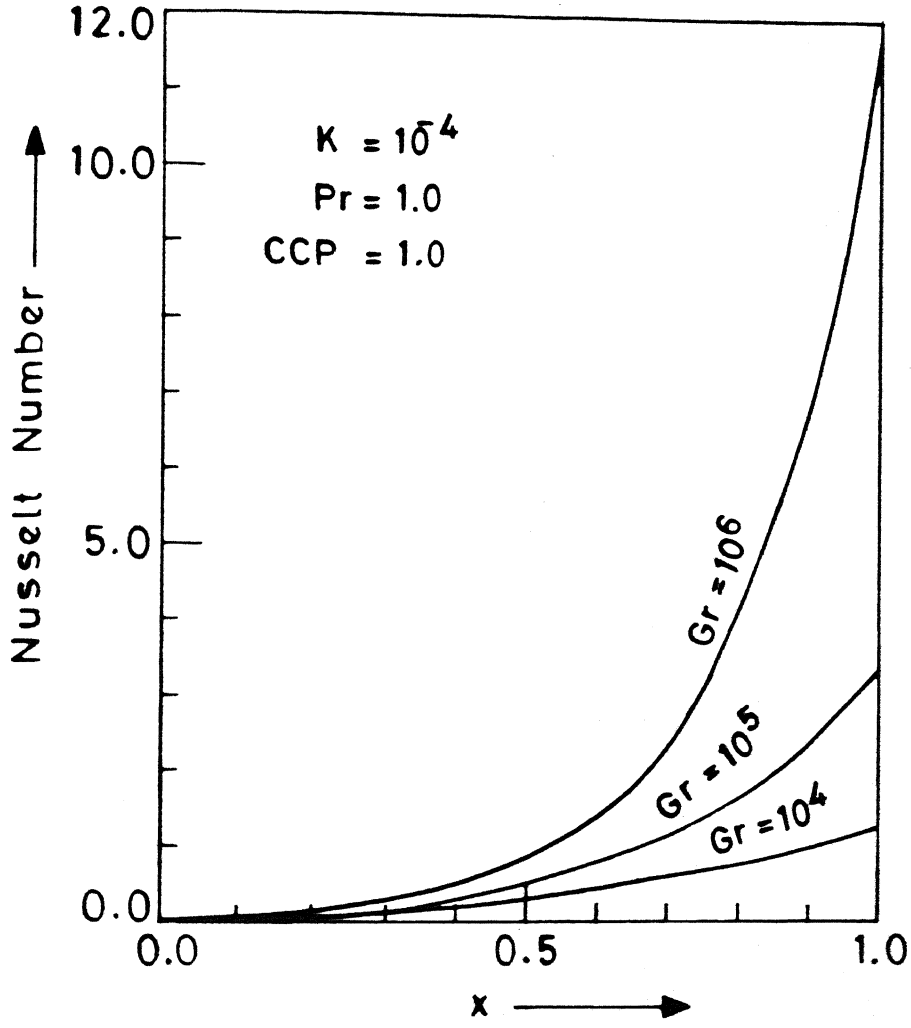

Figure 9 Nusselt Number versus x.

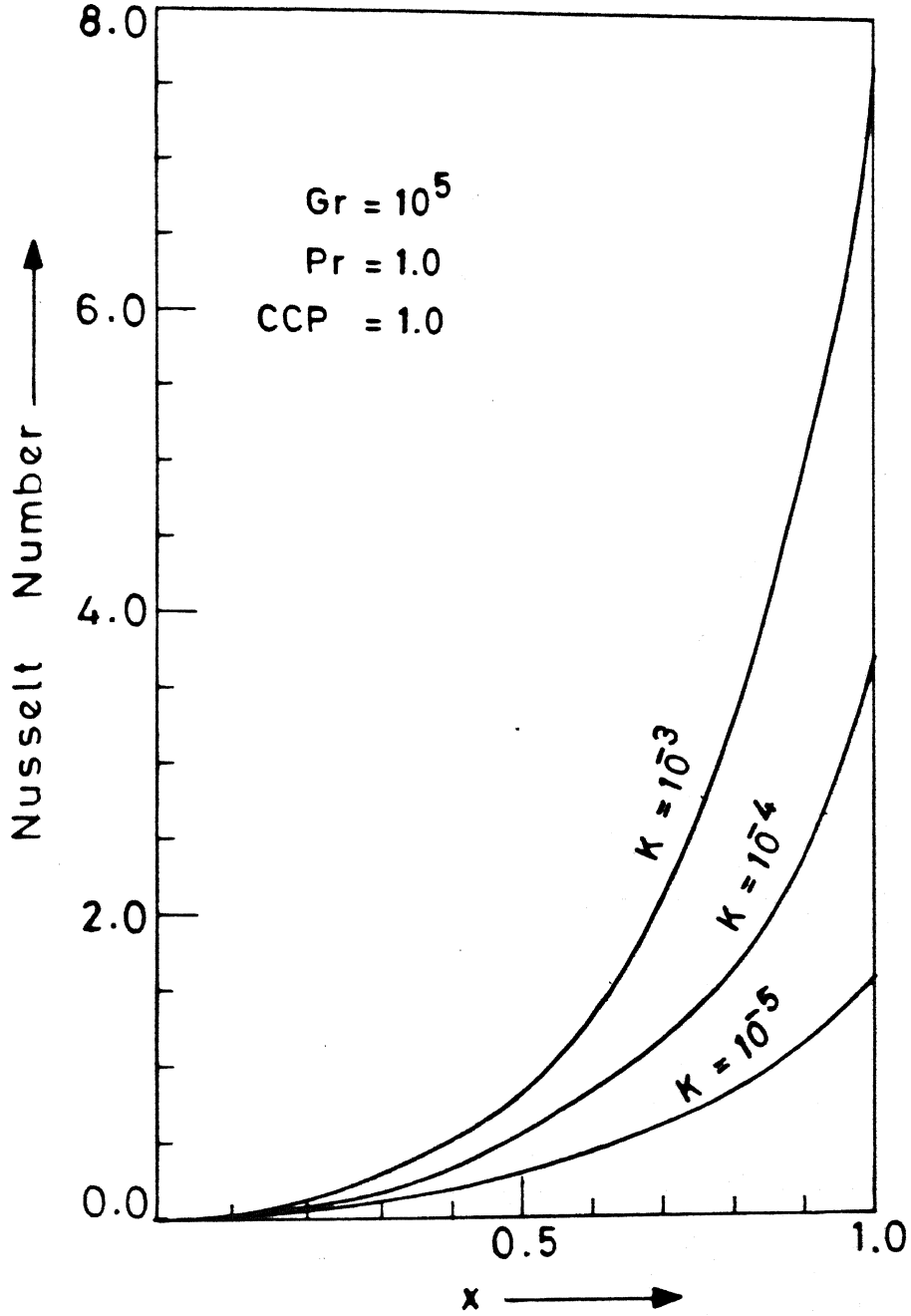

Figure 10 Nusselt Number versus x .

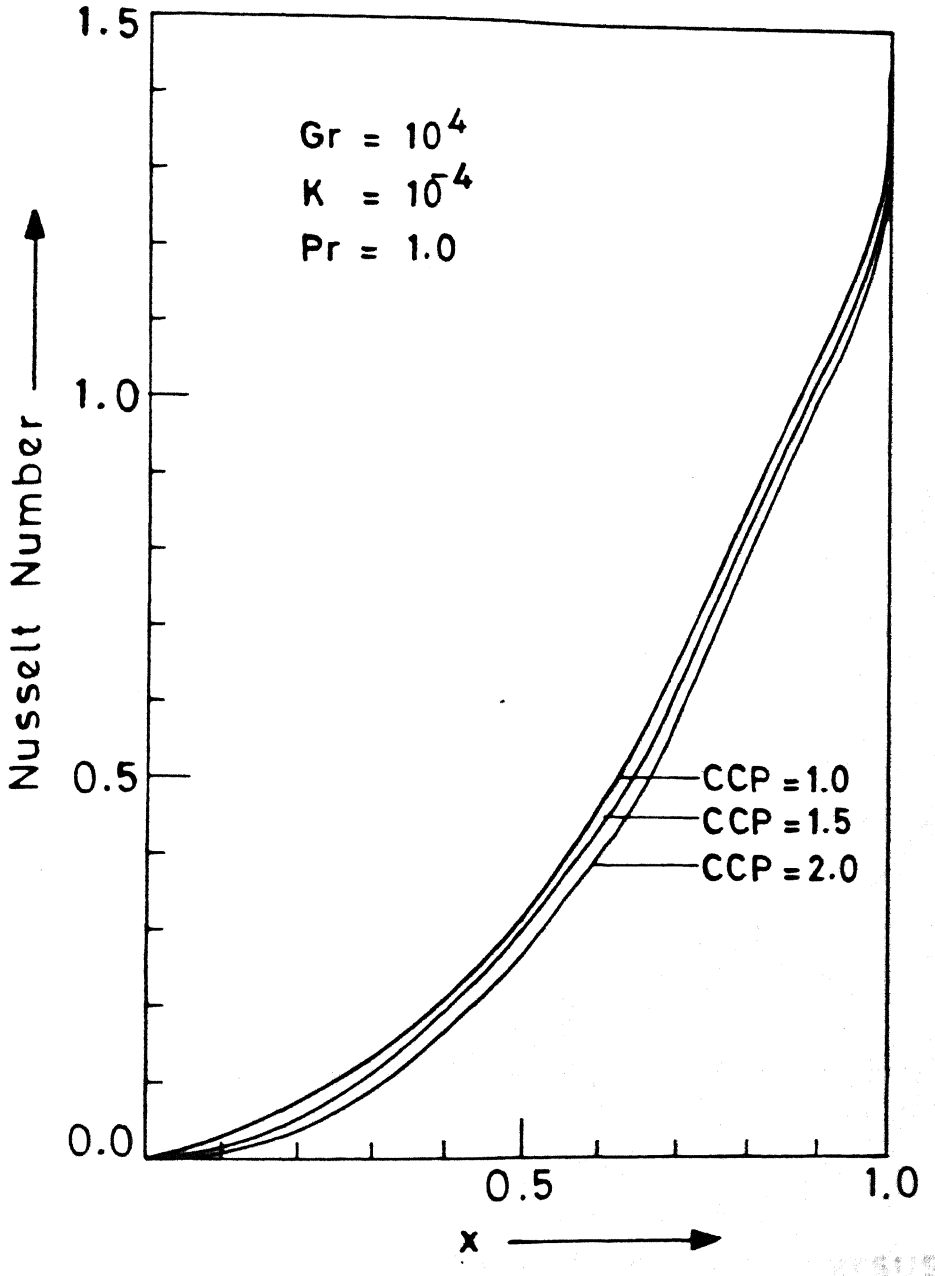

Figure 11 Nusselt Number versus x.

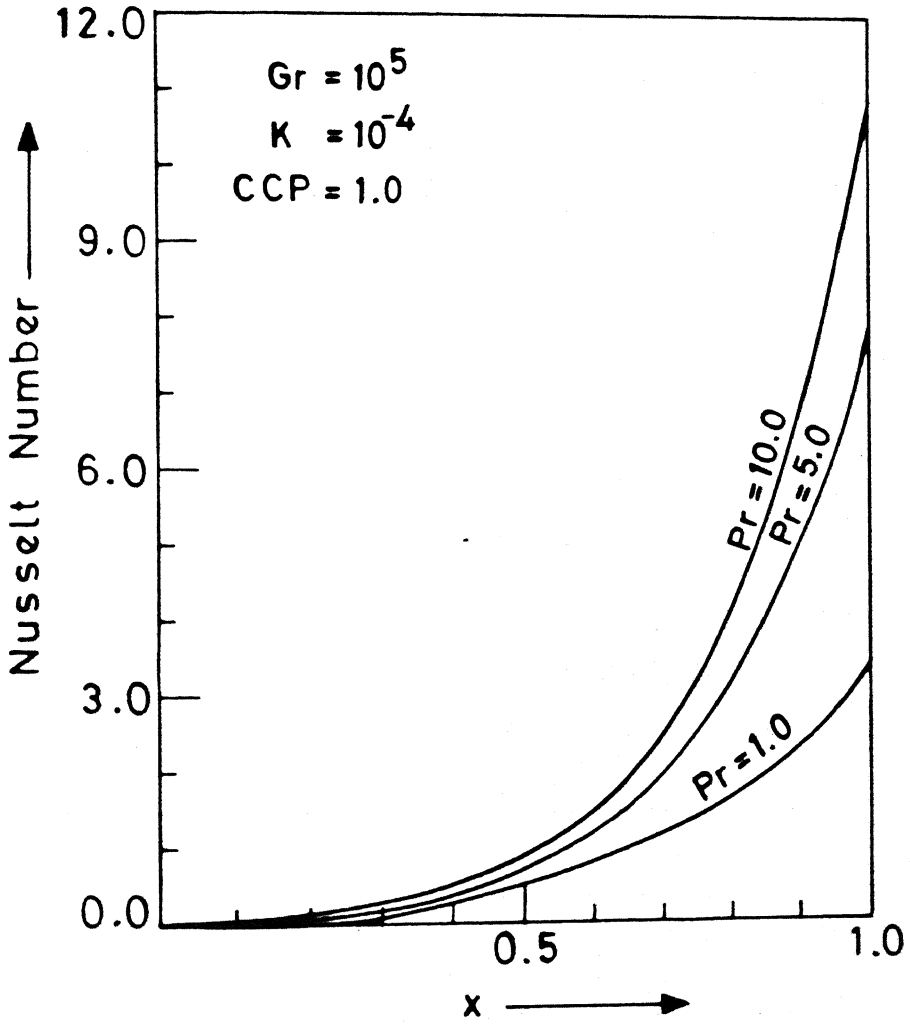

Figure 12 Nusselt Number versus x.

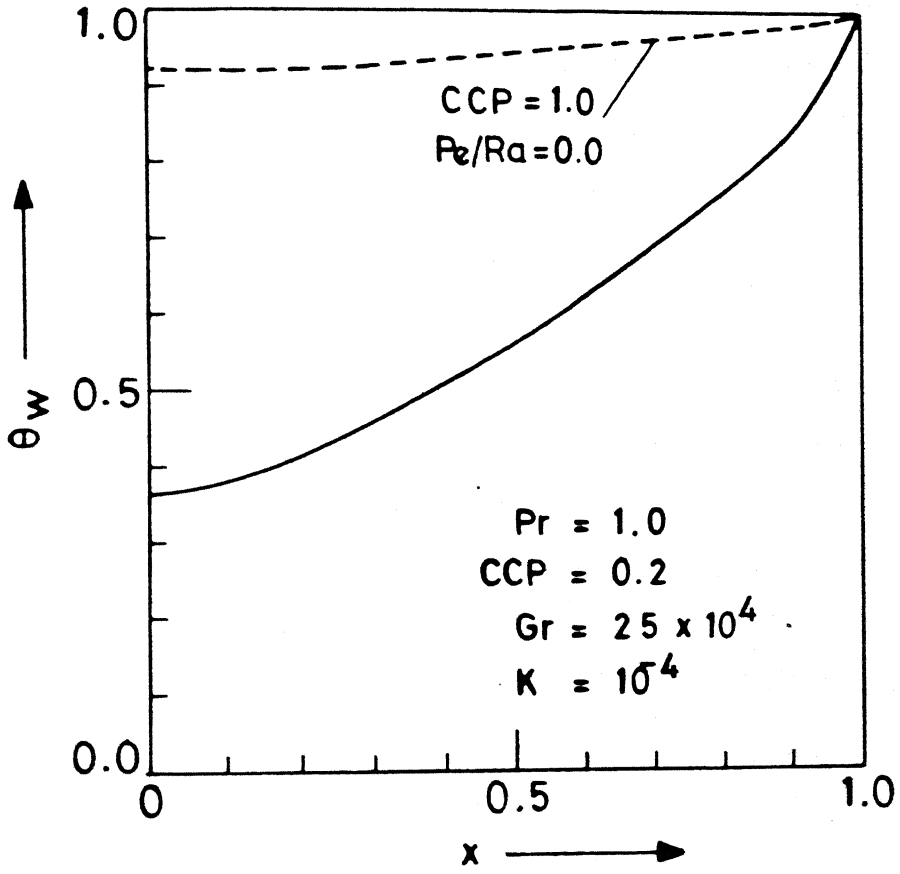

Figure 13 Comparison with [13].

CHAPTER IV

UNSTEADY NATURAL CONVECTION IN AN ENCLOSURE

4.1 INTRODUCTION

Natural convective heat transfer in enclosed porous media is a fundamental problem that pertains to many practical engineering situations. Applications include thermal insulation systems, nuclear waste storage devices and porous heat pipes, just to name a few.

The present study deals with the problem of natural convection in an enclosure which surrounds a saturated porous medium. The enclosure is made up of two isothermal vertical surfaces and two adiabatic horizontal surfaces. The walls of the enclosure are impermeable. The need for studying such problems had arisen from the common application such as the utilization of air gaps for effective insulation in the construction of buildings. It is a common practice to build brick walls separated by an unventilated air gap of few inches while constructing dwellings. For many years, heating engineers have been concerned with the calculation of heat transfer across this air gap. The problem of this type was first formulated in two-dimensional form by Batchelor in 1954 [1].

An appreciable insulating effect may be achieved by placing a porous material (fibre glass) in the unventilated air gap between vertical walls. This is due to the fact that multicellular convection does not occur in this case as shown theoretically by Gill [2] for a porous slab of finite height. Experimental

observations made by Klarsfeld [3] and Bories and Combarnous [4], and the numerical predictions of Chan et al. [5], also indicate that a unicellular motion exists inside the porous gap.

The problem of thermal convection in a confined porous medium has also been of some interest to geophysicists. In many naturally occurring situations, fluid motion results from the variation in the buoyancy force, which is a consequence of temperature gradient in the fluid. This fact has led to the theoretical and experimental studies of natural convective flow inside enclosures of various shapes filled with saturated porous media. A substantial amount of work in this regard has been done on the rectangular enclosure, particularly when either the vertical or the horizontal walls are maintained at constant temperature,while the other walls are insulated. Convective heat transfer in a rectangular porous enclosure, whose vertical walls are maintained at two different temperatures and horizontal walls are insulated, is a problem of fundamental interest in this area. This problem has been studied numerically by Chan et al. [5], Vlasuk [6], Holst and Aziz [7], Bankvall [8], Burns et al. [9], Hickox and Gartling [10], Prasad and Kulacki [11,12]. The boundary layer analysis of the problem has been presented by Weber [13], Walker and Homsy [14], and Bejan [15], while Simpkins and Blythe [16] have presented integral solutions. Approximate solutions for the same problem have been obtained by Walker and Homsy [14], and Bejan and Tien [17]. Important experimental results are reported by Klarsfeld [3], Bories and Combarnous [4] and Seki et al. [18].

Most of the above analytical and numerical studies employ Darcy's law as the momentum equation and only a few researchers have considered non-Darcian flow behaviour in porous media. Chan et al. [5] have adopted the Brinkman model which includes viscous diffusion terms in the fluid. They inferred that the inclusion of viscous force term and no-slip condition on the impermeable enclosure walls give virtually the same result as a pure Darcy analysis for any reasonable value of Darcy number. Tong and Subramanian [19] gave a boundary layer analysis for natural convection in a vertical porous enclosure on the basis of Brinkman model. A numerical solution for a high value of the modified Rayleigh number was given by Tong et al. [20] using the Brinkman model. Inertial effects on buoyancy driven flow and heat transfer in a vertical porous cavity were examined by Prasad et al. [21] using the Forchheimer-extension of Darcy equation.

It is worthwhile to mention that generally, researchers have concentrated mainly on steady state natural convective flow in rectangular cavities with both vertical walls at uniform but different temperatures. Comprehensive reviews of the existing literature has been presented by Ostrach [22, 23] and Catton [24] for the free fluid case. However, transient development of heat transfer and flow may be of importance in many natural convective problems [25] in the porous media.

The objective of the work presented here is to study the two-dimensional unsteady natural convection inside a rectangular porous enclosure saturated with an incompressible fluid. The enclosure consists of two isothermal vertical walls and two adiabatic horizontal walls. The flow and temperature field

solutions are obtained using the finite difference technique. The upwind differencing procedure is applied for convection terms along with central differences for diffusion terms, for spatially discretizing the governing equations. The timewise discretization has been performed using a fully implicit scheme. The resulting equations are solved using the line-by-line technique coupled with the tridiagonal matrix-solver algorithm.

A parametric study is presented for various governing parameters of the problem such as the Rayleigh number, Ra, the Darcy number, Da, and the Prandtl number, Pr. Streamlines and isotherms are plotted for different times, to analyse the flow patterns inside the enclosure. The transient variation of the average Nusselt number at the hot wall has also been obtained in order to analyse the rate of heat transfer between the wall and the fluid trapped inside the porous matrix.

4.2 GOVERNING EQUATIONS

A rectangular, two-dimensional enclosure with isothermal vertical and adiabatic horizontal walls is considered (figure 1) 1. Initially the fluid is stationary and has the same temperature T_c as that of the walls. At time $t = 0$, the wall at $x = 0$ is suddenly brought to a temperature T_H ($T_H > T_c$) and is maintained at this temperature for $t > 0$. Thus, the heat conduction and thermal convection processes are automatically set-up in the fluid. The following assumptions are invoked to simplify the problem formulation:

a) The Boussinesq approximation is valid, so that the variation in density can be neglected except in the buoyancy term of the momentum equation. This is true if the temperature

difference between the isothermal walls and the height of the cavity are not very large.

b) The flow is two-dimensional and laminar.

c) The fluid under consideration is Newtonian and all properties except density are constants.

d) The compression work and viscous dissipation are negligible.

e) The boundary walls of the enclosure are impermeable.

f) The enclosure is filled with a porous material which is saturated with fluid.

Thus the mass, momentum and energy equations for the flow inside the porous medium are,

$$\frac{\partial u}{\partial x} + \frac{\partial v}{\partial y} = 0 , \tag{4.1}$$

$$\rho\left(\frac{\partial u}{\partial t} + u \frac{\partial u}{\partial x} + v \frac{\partial u}{\partial y}\right) = - \frac{\partial P}{\partial x} + \mu \left(\frac{\partial^2 u}{\partial x^2} + \frac{\partial^2 u}{\partial y^2} \right) - \frac{\mu u}{K} , \tag{4.2}$$

$$\rho\left(\frac{\partial v}{\partial t} + u \frac{\partial v}{\partial x} + v \frac{\partial v}{\partial y}\right) = - \frac{\partial P}{\partial x} + \mu \left(\frac{\partial^2 v}{\partial x^2} + \frac{\partial^2 v}{\partial y^2} \right) - \frac{\mu v}{K} + \rho g \beta \, (T - T_c) , \tag{4.3}$$

$$\frac{\partial T}{\partial t} + u \frac{\partial T}{\partial x} + v \frac{\partial T}{\partial y} = \alpha \left(\frac{\partial^2 T}{\partial x^2} + \frac{\partial^2 T}{\partial y^2} \right). \tag{4.4}$$

The initial and boundary conditions of the problem are:

$t = 0 : \quad u = 0, \; v = 0, \; T = T_c , \quad (\text{for } 0 \le x \le A, \; 0 \le y \le B),$

$t > 0 : \quad u = 0, \; v = 0, \; T = T_H, \quad \text{at } x = 0, \text{ for } 0 \le y \le B ,$

$t > 0 : \quad u = 0, \; v = 0, \; T = T_c, \quad \text{at } x = A, \text{ for } 0 \le y \le B ,$

$t > 0 : \quad u = 0, \; v = 0, \; \frac{\partial T}{\partial y} = 0, \quad \text{at } y = 0 \text{ for } 0 \le x \le A ,$

$t > 0 : \quad u = 0, \; v = 0, \; \frac{\partial T}{\partial y} = 0, \quad \text{at } y = B \text{ for } 0 \le x \le A.$

where, u and v denote the velocity components in x and y directions respectively, P is the dynamic pressure, T is the fluid temperature, K is the permeability of the medium and g is

the acceleration due to gravity. The properties μ, α and β denote viscosity, thermal diffusivity and coefficient of thermal expansion respectively and ρ is the density. Also, T_H and T_c denote the temperatures of hot and cold walls and the constants A and B represent the horizontal and vertical dimensions of the enclosure.

The following dimensionless quantities are introduced,

$$u = \frac{uA}{\alpha}, \quad v = \frac{vA}{\alpha}, \quad p = \frac{PA^2}{\rho\alpha^2}, \quad \xi = \frac{x}{A}, \quad \eta = \frac{y}{A}, \quad \theta = \frac{T - T_c}{T_H - T_c},$$

$$Ra = \frac{g\beta\,(T_H - T_c)\,A^3}{\nu\alpha}, \quad Da = \frac{K}{A^2}, \quad \tau = \frac{t\alpha}{A^2}, \quad \nu = \frac{\mu}{\rho}, \qquad (4.6)$$

$$As = \frac{B}{A}, \quad Pr = \frac{\nu}{\alpha},$$

where, Ra and Da are the Rayleigh number and the Darcy number respectively, As is the aspect ratio and Pr is the Prandtl number.

The equations (4.1) - (4.4) may be written in their dimensionless form as,

$$\frac{\partial u}{\partial \xi} + \frac{\partial v}{\partial \eta} = 0, \qquad (4.7)$$

$$\frac{\partial u}{\partial \tau} + u\frac{\partial u}{\partial \xi} + v\frac{\partial u}{\partial \eta} = -\frac{\partial p}{\partial \xi} + Pr\left(\frac{\partial^2 u}{\partial \xi^2} + \frac{\partial^2 u}{\partial \eta^2}\right) - \frac{Pru}{Da}, \qquad (4.8)$$

$$\frac{\partial v}{\partial \tau} + u\frac{\partial v}{\partial \xi} + v\frac{\partial v}{\partial \eta} = -\frac{\partial p}{\partial \eta} + Pr\left(\frac{\partial^2 v}{\partial \xi^2} + \frac{\partial^2 v}{\partial \eta^2}\right) - \frac{Prv}{Da} + Ra\,Pr\,\theta, \qquad (4.9)$$

$$\frac{\partial \theta}{\partial \tau} + u\frac{\partial \theta}{\partial \xi} + v\frac{\partial \theta}{\partial \eta} = \frac{\partial^2 \theta}{\partial \xi^2} + \frac{\partial^2 \theta}{\partial \eta^2}. \qquad (4.10)$$

The equations (4.7) - (4.10) describing thermal convective flow inside the porous enclosure, are a set of simultaneous non-linear and elliptic partial differential equations. Complete analytical solutions for these equations are not possible and one

needs to take recourse to numerical solution techniques. In the present study the finite difference method based on stream function - vorticity flow formulation has been adopted for convenience in numerical simulation.

Eliminating p from equations (4.8) and (4.9), and introducing stream function ψ and vorticity ω, as

$$u = \frac{\partial \psi}{\partial \eta}, \quad v = -\frac{\partial \psi}{\partial \xi} \quad \text{and} \tag{4.11}$$

$$\omega = \frac{\partial u}{\partial \eta} - \frac{\partial v}{\partial \xi}, \tag{4.12}$$

the following set of equations is obtained:

$$\frac{\partial \omega}{\partial \tau} + \frac{\partial \psi}{\partial \eta}\frac{\partial \omega}{\partial \xi} - \frac{\partial \psi}{\partial \xi}\frac{\partial \omega}{\partial \eta} = Pr\left(\frac{\partial^2 \omega}{\partial \xi^2} + \frac{\partial^2 \omega}{\partial \eta^2}\right) - \frac{Pr}{Da}\omega - \frac{\partial \theta}{\partial \xi} Ra\, Pr, \tag{4.13}$$

$$\frac{\partial \theta}{\partial \tau} + \frac{\partial \psi}{\partial \eta}\frac{\partial \theta}{\partial \xi} - \frac{\partial \psi}{\partial \xi}\frac{\partial \theta}{\partial \eta} = \frac{\partial^2 \theta}{\partial \xi^2} + \frac{\partial^2 \theta}{\partial \eta^2}, \tag{4.14}$$

$$\omega = \frac{\partial^2 \psi}{\partial \xi^2} + \frac{\partial^2 \psi}{\partial \eta^2}. \tag{4.15}$$

The initial and boundary conditions to be satisfied by ψ, ω and θ are given as follows:

$$\tau = 0: \quad \psi = 0, \quad \omega = 0, \quad \theta = 0, \quad (0 \le \xi \le 1, \quad 0 \le \eta \le As)$$

$$\tau > 0, \ \xi = 0: \ \theta = 1, \ \psi = 0, \ \frac{\partial \psi}{\partial \xi} = 0, \tag{4.16}$$

$$\tau > 0, \ \xi = 1: \ \theta = 0, \ \psi = 0, \ \frac{\partial \psi}{\partial \xi} = 0,$$

$$\tau > 0, \ \eta = 0: \ \frac{\partial \theta}{\partial \eta} = 0, \ \psi = 0, \ \frac{\partial \psi}{\partial \eta} = 0,$$

$$\tau > 0, \quad \eta = As: \ \frac{\partial \theta}{\partial \eta} = 0, \ \psi = 0, \ \frac{\partial \psi}{\partial \eta} = 0.$$

The difficulty associated with the determination of pressure field has led to the stream function - vorticity method, which eliminates pressure from the governing equations. Moreover, in this formulation, instead of dealing with continuity equation and

two momentum equations, one needs to solve only two second order equations.

4.3 METHOD OF SOLUTION

The governing equations (4.13) - (4.15) for unsteady free convection are coupled, non-linear partial differential equations, the solution of which eventually converges to the steady state solution of the problem. A marching procedure in time is employed to determine the velocity and temperature distributions at various times. Using an implicit scheme the governing equations may be written in the difference form as follows:

$$\frac{\omega_{i,j}^{k+1} - \omega_{i,j}^{k}}{\Delta\tau} + \frac{|\Delta\psi_j|}{2\Delta\eta}\left(\frac{\omega_{i,j}^{k+1} - \omega_{i\pm1,j}^{k+1}}{\Delta\xi}\right) + \frac{|\Delta\psi_i|}{2\Delta\xi}\left(\frac{\omega_{i,j}^{k+1} - \omega_{i,j\pm1}^{k+1}}{\Delta\eta}\right)$$

$$= Pr\left(\frac{\omega_{i-1,j}^{k+1} - 2\omega_{i,j}^{k+1} + \omega_{i+1,j}^{k+1}}{(\Delta\xi)^2} + \frac{\omega_{i,j-1}^{k+1} - 2\omega_{i,j}^{k+1} + \omega_{i,j+1}^{k+1}}{(\Delta\eta)^2}\right)$$

$$- \frac{Pr}{Da}\omega_{i,j}^{k+1} - Ra\ Pr\left(\frac{\theta_{i+1,j}^{k+1} - \theta_{i-1,j}^{k+1}}{2\Delta\xi}\right), \qquad (4.17)$$

$$\frac{\theta_{i,j}^{k+1} - \theta_{i,j}^{k}}{\Delta\tau} + \frac{|\Delta\psi_j|}{2\Delta\eta}\left(\frac{\theta_{i,j}^{k+1} - \theta_{i\pm1,j}^{k+1}}{\Delta\xi}\right) + \frac{|\Delta\psi_i|}{2\Delta\xi}\left(\frac{\theta_{i,j}^{k+1} - \theta_{i,j\pm1}^{k+1}}{\Delta\eta}\right)$$

$$= \frac{\theta_{i-1,j}^{k+1} - 2\theta_{i,j}^{k+1} + \theta_{i+1,j}^{k+1}}{(\Delta\xi)^2} + \frac{\theta_{i,j-1}^{k+1} - 2\theta_{i,j}^{k+1} + \theta_{i,j+1}^{k+1}}{(\Delta\eta)^2}\Big) \text{ and} \qquad (4.18)$$

$$\frac{\psi_{i-1,j}^{k+1} - 2\psi_{i,j}^{k+1} + \psi_{i+1,j}^{k+1}}{(\Delta\xi)^2} + \frac{\psi_{i,j-1}^{k+1} - 2\psi_{i,j}^{k+1} + \psi_{i,j+1}^{k+1}}{(\Delta\eta)^2} = \omega_{i,j}^{k+1}. \qquad (4.19)$$

where, i and j are subscripts corresponding to ξ and η directions,

Also, $\Delta\psi_i = \psi_{i+1,j}^{k+1} - \psi_{i-1,j}^{k+1}$, $\Delta\psi_j = \psi_{i,j+1}^{k+1} - \psi_{i,j-1}^{k+1}$

and the superscript k represents the time level.

To obtain the difference equations of (4.17) and (4.18), upwind-differences for the convective terms and central differences for other terms have been employed. For obtaining equation (4.19), only central differencing has been used. In the upwind differencing scheme one uses the backward difference expression for a derivative term when velocity in the concerned direction is positive and a forward difference expression when it is negative. It is evident from above difference equations that they satisfy the "positive coefficient rule" required for stability [26] and therefore, the solution from the present numerical formulation is stable for all step-sizes $\Delta\xi$ and $\Delta\eta$ of spatial discretization. Moreover, since implicit scheme has been used for timewise marching, the solutions are stable for all time step sizes also [27]. The truncation error in the final solution is $0\ (\Delta\xi, \Delta\eta, \Delta\tau)$.

The resulting difference equations are solved by line-by-line method which is a popular technique for solving multi-dimensional problems [26]. In this procedure, the solution for a two dimensional problem is obtained by alternately applying horizontal and vertical sweeps to all the nodal equations over a couple of iterations, for each time step. During the horizontal sweep, all horizontal lines will be swept one by one using tridiagonal algorithm for fixed j. The terms corresponding to the nodes (i, j+1) and (i, j-1) will be transferred to the right hand side and these values will be assumed from the previous iteration or the most recently available values. Thus, after including the nodal equations for (1, j) and (N+1, j) from the boundary conditions, a pseudo tridiagonal system will be set up for each j.

which can be solved by tridiagonal algorithm. After sweeping all the horizontal lines except those with prescribed boundary conditions, if any, one can perform vertical sweeps in a similar fashion by transferring terms corresponding to (i+1, j) and (i-1, j) to right-hand side for each i. The line-by-line sweep can be done for the horizontal and vertical directions alternately until convergence for all grid points occurs.

The equations (4.17) - (4.19) can be rewritten in the triadiagonal form as follows, for applying the line-by-line procedure. Considering equation (4.17), at a point (i, j),

For Horizontal Sweep:

Case 1: $\Delta\psi_j > 0$ and $\Delta\psi_i > 0$

$$(-|\Delta\psi_j| - 2r_2\,Pr)\,\omega^{k+1}_{i-1,j} + (|\Delta\psi_i| + |\Delta\psi_j| + 4r_1Pr + 4r_2Pr + r_3 + 2\,\Delta\xi\,\Delta\eta\,\frac{Pr}{Da})\,\omega^{k+1}_{i,j} - 2r_2\,Pr\,\omega^{k+1}_{i+1,j} \qquad (4.20a)$$

$$= 2r_1\,Pr\,\omega^{k+1}_{i,j-1} + (|\Delta\psi_i| + 2r_1Pr)\,\omega^{k+1}_{i,j+1} + r_3\,\omega^{k}_{i,j} - \Delta\eta\;RaPr\,(\theta^{k+1}_{i+1,j} - \theta^{k+1}_{i-1,j}),$$

where, $r_1 = \frac{2\Delta\xi}{\Delta\eta}$, $r_2 = \frac{2\Delta\eta}{\Delta\xi}$ and $r_3 = \frac{2\,\Delta\xi\,\Delta\eta}{\Delta t}$.

Case 2: $\Delta\psi_j < 0$ and $\Delta\psi_i < 0$

$$-2r_2Pr\,\omega^{k+1}_{i-1,j} + (|\Delta\psi_i| + |\Delta\psi_j| + 4r_1Pr + 4r_2Pr + r_3 + 2\,\Delta\xi\,\Delta\eta\,\frac{Pr}{Da})\,\omega^{k+1}_{i,j} + (-|\Delta\psi_j| - 2r_2Pr)\,\omega^{k+1}_{i+1,j} \qquad (4.20b)$$

$$= (|\Delta\psi_i| + 2r_1Pr)\omega^{k+1}_{i,j-1} + 2r_1Pr\omega^{k+1}_{i,j+1} + r_3\omega^{k}_{i,j} - \Delta\eta\;Ra\,Pr\,(\theta^{k+1}_{i+1,j} - \theta^{k+1}_{i-1,j}),$$

Case 3: $\Delta\psi_j > 0$ and $\Delta\psi_i < 0$

$$(-|\Delta\psi_j| - 2r_2Pr)\,\omega^{k+1}_{i-1,j} + (|\Delta\psi_i| + |\Delta\psi_j| + 4r_1Pr + 4r_2Pr + r_3 + 2\,\Delta\xi\,\Delta\eta\,\frac{Pr}{Da})\,\omega^{k+1}_{i,j} - 2r_2Pr\,\omega^{k+1}_{i+1,j} \qquad (4.20c)$$

$$= (|\Delta\psi_i| + 2r_1Pr)\,\omega^{k+1}_{i,j-1} + r_3\,\omega^{k}_{i,j} + 2r_1Pr\,\omega^{k+1}_{i,j+1} - \Delta\eta\ Ra\ Pr\ (\theta^{k+1}_{i+1,j} - \theta^{k+1}_{i-1,j}),$$

Case 4: $\Delta\psi_j < 0$ and $\Delta\psi_i > 0$

$$-2r_2Pr\,\omega^{k+1}_{i-1,j} + (|\Delta\psi_i| + |\Delta\psi_j| + 4r_1Pr + 4r_2Pr + r_3 + 2\,\Delta\xi\,\Delta\eta\,\frac{Pr}{Da})\,\omega^{k+1}_{i,j} + (-|\Delta\psi_j| - 2r_2Pr)\,\omega^{k+1}_{i+1,j} \qquad (4.20d)$$

$$= 2r_1Pr\,\omega^{k+1}_{i,j-1} + (|\Delta\psi_i| + 2r_1\,Pr)\,\omega^{k+1}_{i,j+1} + r_3\,\omega^{k}_{i,j} - \Delta\eta\ Ra\ Pr\ (\theta^{k+1}_{i+1,j} - \theta^{k+1}_{i-1,j}).$$

For Vertical Sweep

Case 1: $\Delta\psi_j > 0$ and $\Delta\psi_i > 0$

$$-2r_1\,Pr\,\omega^{k+1}_{i,j-1} + (|\Delta\psi_i| + |\Delta\psi_j| + 4r_1\,Pr + 4r_2\,Pr + r_3 + 2\,\Delta\xi\,\Delta\eta\,\frac{Pr}{Da})\,\omega^{k+1}_{i,j} + (-|\Delta\psi_i| - 2r_1Pr)\,\omega^{k+1}_{i,j+1} \qquad (4.20e)$$

$$= (|\Delta\psi_j| + 2r_2Pr)\,\omega^{k+1}_{i-1,j} + 2r_2Pr\,\omega^{k+1}_{i+1,j} + r_3\,\omega^{k}_{i,j} - \Delta\eta\ Ra\ Pr\ (\theta^{k+1}_{i+1,j} - \theta^{k+1}_{i-1,j}),$$

Case 2: $\Delta\psi_j < 0$ and $\Delta\psi_i < 0$

$$(-|\Delta\psi_i| - 2r_1Pr)\,\omega^{k+1}_{i,j-1} + (|\Delta\psi_i| + |\Delta\psi_j| + 4r_1Pr + 4r_2Pr + r_3 + 2\,\Delta\xi\,\Delta\eta\,\frac{Pr}{Da})\,\omega^{k+1}_{i,j} - 2r_1Pr\,\omega^{k+1}_{i,j+1} \qquad (4.20f)$$

$$= (|\Delta\psi_j| + 2r_2Pr)\,\omega^{k+1}_{i+1,j} + 2r_2Pr\,\omega^{k+1}_{i-1,j} + r_3\,\omega^{k}_{i,j}$$

$$- \Delta\eta \quad Ra\ Pr\ (\theta^{k+1}_{i+1,j} - \theta^{k+1}_{i-1,j}),$$

Case 3: $\Delta\psi_j > 0$ and $\Delta\psi_i < 0$

$$(-|\Delta\psi_i| - 2r_1 Pr)\ \omega^{k+1}_{i,j-1} + (|\Delta\psi_i| + |\Delta\psi_j| + 4r_1 Pr + 4r_2 Pr + r_3$$

$$+ 2\ \Delta\xi\ \Delta\eta\ \frac{Pr}{Da})\ \omega^{k+1}_{i,j} - 2r_1 Pr\ \omega^{k+1}_{i,j+1} \qquad (4.20g)$$

$$= (|\Delta\psi_j| + 2r_2 Pr)\ \omega^{k+1}_{i-1,j} + 2r_2 Pr\ \omega^{k+1}_{i+1,j} + r_3\ \omega^{k}_{i,j}$$

$$- \Delta\eta\ Ra\ Pr\ (\theta^{k+1}_{i+1,j} - \theta^{k+1}_{i-1,j}),$$

Case 4: $\Delta\psi_j < 0$ and $\Delta\psi_i > 0$

$$-2r_1\ Pr\ \omega^{k+1}_{i,j-1} + (|\Delta\psi_i| + |\Delta\psi_j| + 4r_1\ Pr + 4r_2\ Pr + r_3$$

$$+ 2\ \Delta\xi\ \Delta\eta\ \frac{Pr}{Da})\ \omega^{k+1}_{i,j} + (-2r_1\ Pr - |\Delta\psi_i|)\ \omega^{k+1}_{i,j+1} \qquad (4.20h)$$

$$= 2r_2 Pr\ \omega^{k+1}_{i-1,j} + (|\Delta\psi_j| + 2r_2 Pr)\ \omega^{k+1}_{i+1,j} + r_3\ \omega^{k}_{i,j}$$

$$- \Delta\eta\ Ra\ Pr\ (\theta^{k+1}_{i+1,j} - \theta^{k+1}_{i-1,j}).$$

The boundary conditions for ω are obtained as follows:

From the definition of vorticity, $\omega = \frac{\partial^2\psi}{\partial\xi^2} + \frac{\partial^2\psi}{\partial\eta^2}$. Using the no-slip conditions on the boundaries in the above equations for ω one can obtain the following expressions

$$\omega = \frac{\partial^2\psi}{\partial\xi^2} \text{ at } \xi = 0, \qquad \omega = \frac{\partial^2\psi}{\partial\eta^2} \text{ at } \eta = 0,$$

$$\omega = \frac{\partial^2\psi}{\partial\xi^2} \text{ at } \xi = 1, \qquad \omega = \frac{\partial^2\psi}{\partial\eta^2} \text{ at } \eta = As. \qquad (4.21)$$

The surface vorticity values can now be evaluated through the finite differences form of equation (4.21) for the concerned boundary.

(i) At $\xi = 0$:

Applying central difference scheme to $\frac{\partial^2 \psi}{\partial \xi^2}$, one obtains,

$$\omega_{1,j} = \frac{\psi_{2,j} + \psi_{0,j} - 2\psi_{1,j}}{(\Delta\xi)^2},$$

Since $\frac{\partial \psi}{\partial \xi} = 0$ and $\psi = 0$ at $\xi = 0$ (no-slip)

$$\psi_{0,j} = \psi_{2,j} \text{ and } \psi_{1,j} = 0$$

Thus, $\omega_{1,j} = \frac{2\psi_{2,j}}{(\Delta\xi)^2}$, $\forall$ j, (4.22a)

Similarly,

(ii) $$\omega_{N+1,j} = \frac{2\psi_{N,j}}{(\Delta\xi)^2}, \forall j, \quad (4.22b)$$

(iii) $$\omega_{i,1} = \frac{2\psi_{i,2}}{(\Delta\eta)^2}, \forall i, \quad (4.22c)$$

(iv) $$\omega_{i,M+1} = \frac{2\psi_{i,M}}{(\Delta\eta)^2}, \forall i. \quad (4.22d)$$

Let us now consider the line-by-line solution of eq. (4.18).

For Horizontal Sweep

Case 1: $\Delta\psi_j > 0$ and $\Delta\psi_i > 0$

$$(-|\Delta\psi_j| - 2r_2)\,\theta^{k+1}_{i-1,j} + (|\Delta\psi_i| + |\Delta\psi_j| + 4r_1 + 4r_2 + r_3)\,\theta^{k+1}_{i,j} - 2r_2\,\theta^{k+1}_{i+1,j} = 2r_1\,\theta^{k+1}_{i,j-1} + (|\Delta\psi_i| + 2r_1)\,\theta^{k+1}_{i,j+1} + r_3\,\theta^{k}_{i,j}, \quad (4.23a)$$

Case 2: $\Delta\psi_j < 0$ and $\Delta\psi_j < 0$

$$-2r_2\,\theta^{k+1}_{i-1,j} + (|\Delta\psi_i| + |\Delta\psi_j| + 4r_1 + 4r_2 + r_3)\theta^{k+1}_{i,j} + (-|\Delta\psi_j| - 2r_2)\,\theta^{k+1}_{i+1,j} \quad (4.23b)$$

$$= (|\Delta\psi_i| + 2r_1)\,\theta^{k+1}_{i,j-1} + 2r_1\,\theta^{k+1}_{i,j+1} + r_3\,\theta^{k}_{i,j},$$

Case 3: $\Delta\psi_j > 0$ and $\Delta\psi_i < 0$

$$(-|\Delta\psi_j| - 2r_2)\,\theta^{k+1}_{i-1,j} + (|\Delta\psi_i| + |\Delta\psi_j| + 4r_1 + 4r_2 + r_3)\,\theta^{k+1}_{i,j} - 2r_2\,\theta^{k+1}_{i+1,j} \qquad (4.23c)$$

$$= (|\Delta\psi_i| + 2r_1)\,\theta^{k+1}_{i,j-1} + 2r_1\,\theta^{k+1}_{i,j+1} + r_3\,\theta^{k}_{i,j},$$

Case 4: $\Delta\psi_j < 0$ and $\Delta\psi_i > 0$

$$-2r_2\,\theta^{k+1}_{i-1,j} + (|\Delta\psi_i| + |\Delta\psi_j| + 4r_1 + 4r_2 + r_3)\,\theta^{k+1}_{i,j} + (-|\Delta\psi_j| - 2r_2)\,\theta^{k+1}_{i+1,j} \qquad (4.23d)$$

$$= 2r_1\,\theta^{k+1}_{i,j-1} + (|\Delta\psi_i| + 2r_1)\,\theta^{k+1}_{i,j+1} + r_3\,\theta^{k}_{i,j}.$$

For Vertical Sweep

Case 1: $\Delta\psi_j > 0$ and $\Delta\psi_i > 0$

$$-2r_1\,\theta^{k+1}_{i,j-1} + (|\Delta\psi_j| + |\Delta\psi_i| + 4r_1 + 4r_2 + r_3)\,\theta^{k+1}_{i,j} + (-|\Delta\psi_i| - 2r_1)\,\theta^{k+1}_{i,j+1} \qquad (4.23e)$$

$$= (|\Delta\psi_j| + 2r_2)\,\theta^{k+1}_{i-1,j} + 2r_2\,\theta^{k+1}_{i+1,j} + r_3\,\theta^{k}_{i,j},$$

Case 2: $\Delta\psi_j < 0$ and $\Delta\psi_i < 0$

$$(-|\Delta\psi_i| - 2r_1)\,\theta^{k+1}_{i,j-1} + (|\Delta\psi_i| + |\Delta\psi_j| + 4r_1 + 4r_2 + r_3)\,\theta^{k+1}_{i,j} - 2r_1\,\theta^{k+1}_{i,j+1} \qquad (4.23f)$$

$$= 2r_2\,\theta^{k+1}_{i-1,j} + (|\Delta\psi_j| + 2r_2)\,\theta^{k+1}_{i+1,j} + r_3\,\theta^{k}_{i,j},$$

Case 3: $\Delta\psi_j > 0$ and $\Delta\psi_i < 0$

$$(-|\Delta\psi_i| - 2r_1)\,\theta^{k+1}_{i,j-1} + (|\Delta\psi_i| + |\Delta\psi_j| + 4r_1 + 4r_2 + r_3)\,\theta^{k+1}_{i,j} - 2r_1\,\theta^{k+1}_{i,j+1} \qquad (4.23g)$$

$$= (|\Delta\psi_j| + 2r_2)\,\theta^{k+1}_{i-1,j} + 2r_2\,\theta^{k+1}_{i+1,j} + r_3\,\theta^{k}_{i,j},$$

Case 4: $\Delta\psi_j < 0$ and $\Delta\psi_i > 0$

$$-2r_1\,\theta^{k+1}_{i,j-1} + (|\Delta\psi_i| + |\Delta\psi_j| + 4r_1 + 4r_2 + r_3)\,\theta^{k+1}_{i,j} + (-|\Delta\psi_i| - 2r_1)\,\theta^{k+1}_{i,j+1} \qquad (4.23h)$$

$$= 2r_2\,\theta^{k+1}_{i-1,j} + (|\Delta\psi_j| + 2r_2)\,\theta^{k+1}_{i+1,j} + r_3\,\theta^{k}_{i,j}.$$

The line-by-line procedure is applied to equation (4.19) as follows:

For Horizontal Sweep

$$\psi^{k+1}_{i-1,j} - 2(1+r^2)\,\psi^{k+1}_{i,j} + \psi^{k+1}_{i+1,j} = -r^2\,\psi^{k+1}_{i,j-1} - r^2\,\psi^{k+1}_{i,j+1} + (\Delta\xi)^2\,\omega^{k+1}_{i,j}. \qquad (4.24a)$$

For Vertical Sweep

$$r^2\,\psi^{k+1}_{i,j-1} - 2(1+r^2)\,\psi^{k+1}_{i,j} + r^2\,\psi^{k+1}_{i,j+1} = -\psi^{k+1}_{i-1,j} - \psi^{k+1}_{i+1,j} + (\Delta\xi)^2\,\omega^{k+1}_{i,j}. \qquad (4.24b)$$

where, $r = \left(\frac{\Delta\xi}{\Delta\eta}\right)^2$.

A suitable under-relaxation factor is used for each equation to increase the stability of the iteration scheme.

An important physical characteristic of the problem is the rate of heat transfer from the hot wall to the fluid. In the present problem, the Nusselt number on the hot wall of the enclosure is calculated by

$$Nu = -\left.\frac{\partial\theta}{\partial\eta}\right|_{\eta=0}. \qquad (4.25)$$

The wall gradient is calculated using a three-point formula. After obtaining the gradients at each grid point lying on the hot wall, the average Nusselt number is calculated by Simpson's integration formula.

The computational procedure adopted for obtaining the overall solution of the problem may be summarised as follows,

(a) Initially at $\tau = 0$, set $\theta \equiv 0$ and $\psi \equiv 0$, as given by the initial conditions of the problem.

(b) Set $\tau = \tau + \Delta\tau$, where $\Delta\tau$ is the time step.

(c) Guess the values of θ and ψ at the new time step.

(d) Get the nodal values of θ from equation (4.18).

(e) Calculate ω from equation (4.17), using the θ-values obtained in step (d).

(f) Obtain the values of ψ by substituting the values of ω from step (e), in equation (4.19).

(g) Iterate steps (d - f) for a few times.

(h) With the current values of θ, ω and ψ, proceed to the next time step (begin at Step (b)).

(i) Repeat the above process is repeated until steady state is reached.

(j) Calculate the local Nusselt number using a three-point formula for the temperature gradient at the hot wall and then evaluate the average Nusselt number by Simpon's 1/3 rule.

4.4 RESULTS AND DISCUSSION

Results have been presented for the temperature field, the flow pattern and the average Nusselt number at the hot wall, at different times and for various parameters.

In order to verify the accuracy of the finite difference discretization in space, the results were calculated using different step-sizes for the enclosure aspect ratio of 10. The value of the steady state Nusselt number was found to have no significant change for the meshes of 60 x 60, 80 x 80 and 100 x 100. Thus, it may be concluded that the finite difference spatial discretization is adequate. In the present analysis the 80 x 80 grid system has been used and a fixed aspect ratio of 10 has been considered, for all the calculations.

The flow patterns inside the enclosure at small and large times after the start of thermal convection inside the enclosure are shown in figures (2-5) for various sets of parameters. It is clearly seen from the plots that unicellular convection occurs for the chosen aspect ratio and range of parameters. Similar results have been reported for a vertical layer by Klarsfeld [3]. For smaller time the circulation vortex is closer to the hot wall since the convection starts at time $\tau = 0$, near the wall. Also the close spacing of streamlines adjacent to the hot wall for small times indicate that a boundary layer exists there. For later times due to vorticity diffusion into the interior portion of the enclosure, a circulation vortex which is almost symmetric about the midplane develops. The total dimensionless time to approach steady state depends on the modified Rayleigh number, Ra_o (= Ra x Da). It is observed that steady state is attained at a smaller value of time for small Ra_o.

At a fixed Darcy number the boundary layer near hot wall becomes steeper as Rayleigh number is increased. This can be easily understood from the fact that if the temperature potential

increases or fluid viscosity decreases, the boundary layer will become steeper. It is also seen from the values of stream functions in Figures (2-5) that the strength of the circulation vortex increases with Rayleigh number. For the range of Rayleigh numbers considered, this increase in vortex strength is almost propotional to the Rayleigh number. The shapes of circulation vortices indicate that near the corners of the enclosure the flow is virtually stagnant. For a fixed Rayleigh number, when Darcy number is reduced the strength of the vortex decreases and the boundary layer becomes less steep due to high resistance of the porous matrix. From the above trends it maybe concluded that for thermal convection problems in a porous medium, the product Ra x Da is more relevant than the Rayleigh number or Darcy number, individually. This feature has also been observed by Chan et al. [5] earlier.

The shapes of isotherms at small and large times are shown in Figures (6-9) for various values of the parameters. It is observed that for initial times the isotherms are closer to the hot wall since heat transfer is affected by contact with this wall at starting time, $\tau = 0$. For larger times the isotherms are more evenly distributed due to the heat transfer mechanisms of conduction and thermal convection. The shapes of the isotherms are almost vertical straight lines for small times, indicating that the heat transfer within the enclosure is dominated by conduction in the beginning, before thermal convection gains strength. In general, the isotherms are curved towards the hot wall at the bottom of the enclosure and curved away from the hot wall at top in exact correspondence with the direction of flow within the

enclosure. The effect of modified Rayleigh number upon the isotherm patterns is as follows. At low values of Ra_o, the steady state isotherm pattern also consists of evenly-spaced, nearly-straight lines, indicating that the effects of convection are minimal and the heat transfer is dominated by conduction. For larger values of Ra_o, the isotherm patterns become more and more distorted at large times, when thermal convection is fully set-up. This is clearly shown by the shift of the isotherms towards the hot wall at the bottom of the enclosure and away from the hot wall at the top. Thus, the shape of the isotherms is also determined by the modified Rayleigh number rather than Ra and Da individually, as seen in the case of flow patterns earlier.

In Figures (10, 11) the transient variation of the average Nusselt number at the hot wall is plotted for different Rayleigh and Darcy numbers. The effect of increasing Rayleigh number or increasing Darcy number is similar upon the Nusselt number variation, confirming the fact that Nusselt number is also determined by Ra x Da. At time $\tau = 0$, the Nusselt number is infinitely large due to an infinite gradient existing when the hot wall is suddenly brought into contact with the cold fluid. The Nusselt number decreases gradually with time (at low Ra or Da) upto the steady state value due to the continuous penetration of heat into the porous medium and the consequent decrease in the value of the wall temperature gradient. At high Ra or Da, the Nusselt number increases briefly after the initial sharp decrease when the wall comes into contact with the fluid. This increase in the Nusselt number may be attributed to the existence of strong convection currents adjacent to the hot wall when heat has not

penetrated completely into the porous layer. The strong buoyancy effects adjacent to the hot wall at high Ra (aided by the low resistance from the solid matrix at high Da) will generate a vortex flow of high strength adjacent to the hot wall for small times. This strong convection, in turn, tends to increase the wall temperature gradient and consequently an increase in the Nusselt number at the hot wall. When steady state is achieved, heat penetration through the fluid is complete in the entire enclosure and the strength of convection existing adjacent to the wall also slowly decreases due to the fluid mixing. This leads to the decrease in the wall temperature gradient and in the Nusselt number value.

A comparison between the present results and those of Bejan [15] are presented in Figure 12. The graphs have been plotted for Nusselt number versus modified Rayleigh number for the aspect ratio of 10. Weber's [13] results are also shown in the graph. It is observed that the present results are very close to that of Bejan and Weber for lower values of Rayleigh number. However, for larger values of Ra_o the results are a bit deviated from Bejan's results which are for the Darcy's law. This difference may be attributed to the inertial and viscous effects taken into account in the generalized Darcy's model of the present study.

REFERENCES

[1] Batchelor, G.K., Quart. J. Appl. Maths., 12, 209, 1954.

[2] Gill, A.E., The boundary layer regime for convection in a rectangular cavity, J. Fluid Mech., 26, 515, 1966.

[3] Klarsfeld, S., Champs de temperature associes aux mouvements de convection naturelle dans un milieu poreux limite, Revue Gen. Thermique, 9, 1403, 1970.

[4] Bories, S.A. and Combarnous, M.A., Natural convection in a sloping porous layer, J. Fluid Mech., 57, 63, 1973.

[5] Chan, B.K.C., Ivey, C.M. and Barry, J.M., Natural convection in enclosed porous media with rectangular boundaries, J. Heat transfer, 92, 21, 1970.

[6] Vlasuk, M.P., Transfer de chalem par convection dans une couche Poreuse, Proceedings, 4th all union heat and mass transfer conference, Minsk, 1972.

[7] Holst, P.H., and Aziz, K., A theoretical and experimental study of natural convection in a confined porous medium, Can. J. Chem. Engng., 50, 232, 1972.

[8] Bankvall, C.G., Natural convection in a vertical permeable space, Warme-und Stoffubertragung, 7, 22, 1974.

[9] Burns, P.J., Chow, L.C. and Tien, C.L., Convection in a vertical slot filled with porous insulation, Int. J. Heat Mass Transfer, 20, 919, 1976.

[10] Hickox, C.E. and Gartling, D.K., A numerical study of natural convection in a horizontal porous layer subjected to an end to end temperature difference, J. Heat Transfer, 103, 797, 1981.

[11] Prasad, V. and Kulacki, F.A., Natural convection in a vertical porous annulus, Int. J. Heat Mass Transfer, 27, 207, 1984.

[12] Prasad, V. and Kulacki, F.A., Convective heat transfer in a rectangular porous cavity - effect of aspect ratio on flow structure and heat transfer, 106, 158, 1984.

[13] Weber, J.E., The boundary layer regime for convection in a vertical porous layer, Int. J. Heat Mass Transfer, 18, 569, 1975.

[14] Walker, K.E. and Homsy, G.M., Convection in a porous cavity, J. fluid Mech., 97, 449, 1978.

[15] Bejan, A., On the boundary layer regime in a vertical enclosure filled with a porous medium, Letters in Heat and Mass Transfer, 6, 93, 1979.

[16] Simpkins, P.G. and Blythe, P.A., Convection in a porous layer, Int. J. Heat Mass Transfer, 23, 881, 1980.

[17] Bejan, A. and Tien, C.L., Natural convection in a horizontal porous medium subject to an end-to-end temperature difference, J. Heat Transfer, 100, 191, 1978.

[18] Seki, N., Fukusako, S. and Inaba, M., Heat transfer in a confined rectangular cavity packed with porous media, Int. J.Heat Mass Transfer, 21, 985, 1978.

[19] Tong, T.W. and Subramanian, E., A boundary layer analysis for natural convection in vertical enclosures containing a porous medium, Int. J. Heat Mass Transfer, 28, 563, 1985.

[20] Tong, T.W. and Orangi, S., A numerical analysis for high modified Rayleigh number natural convection in enclosures containing a porous medium, Proceedings of Heat Transfer Conference, 2647, 1986.

[21] Prasad, V. and Tuntomo, A., Inertia effects on natural convection in a vertical porous cavity, Numerical Heat Transfer, 11, 295, 1987.

[22] Ostrach, S., Natrual convection in cavities and cells, Proceedings 7th International Heat Transfer conference, V. Grigul et al. eds. Hemisphere, Washington D.C., 1, 365, 1982.

[23] Ostrach,S., Natural convection in Enclosures, Advances in Heat Transfer, Hartnett, J.P. and Irvine, T.E. eds., 8, 161, 1972.

[24] Catton,I., Natural convection in enclosures, Proceedings of 6th international conference, Rodgers, J.P., et al., eds. Hemisphere, Washington D.C., 6, 13, 1984.

[25] Christopher, D.M., Transient Natural Convection Heat transfer in a cavity filled with a fluid saturated porous medium, Proceedings of Heat Transfer Conference, 2659, 1986.

[26] Patankar, S.V., Numerical Heat Transfer and fluid Flow, Hemisphere, 1980.

[27] Jaluria, Y. and Torrance,K.E., Computational Heat Transfer, Hemisphere Publishing Corporation, 1986.

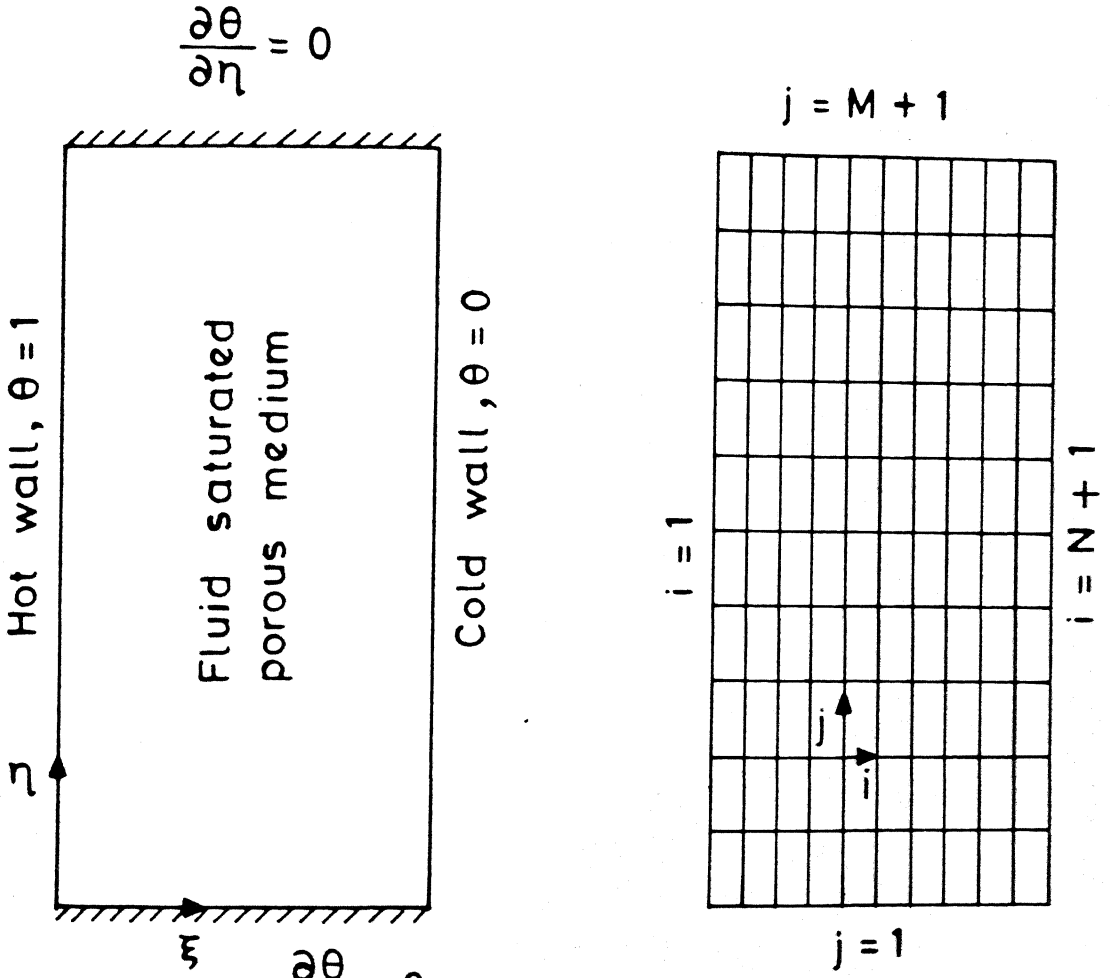

(i) Temperature boundary conditions for the problem

(ii) Finite difference mesh

Figure 1 Geometry of the system under consideration.

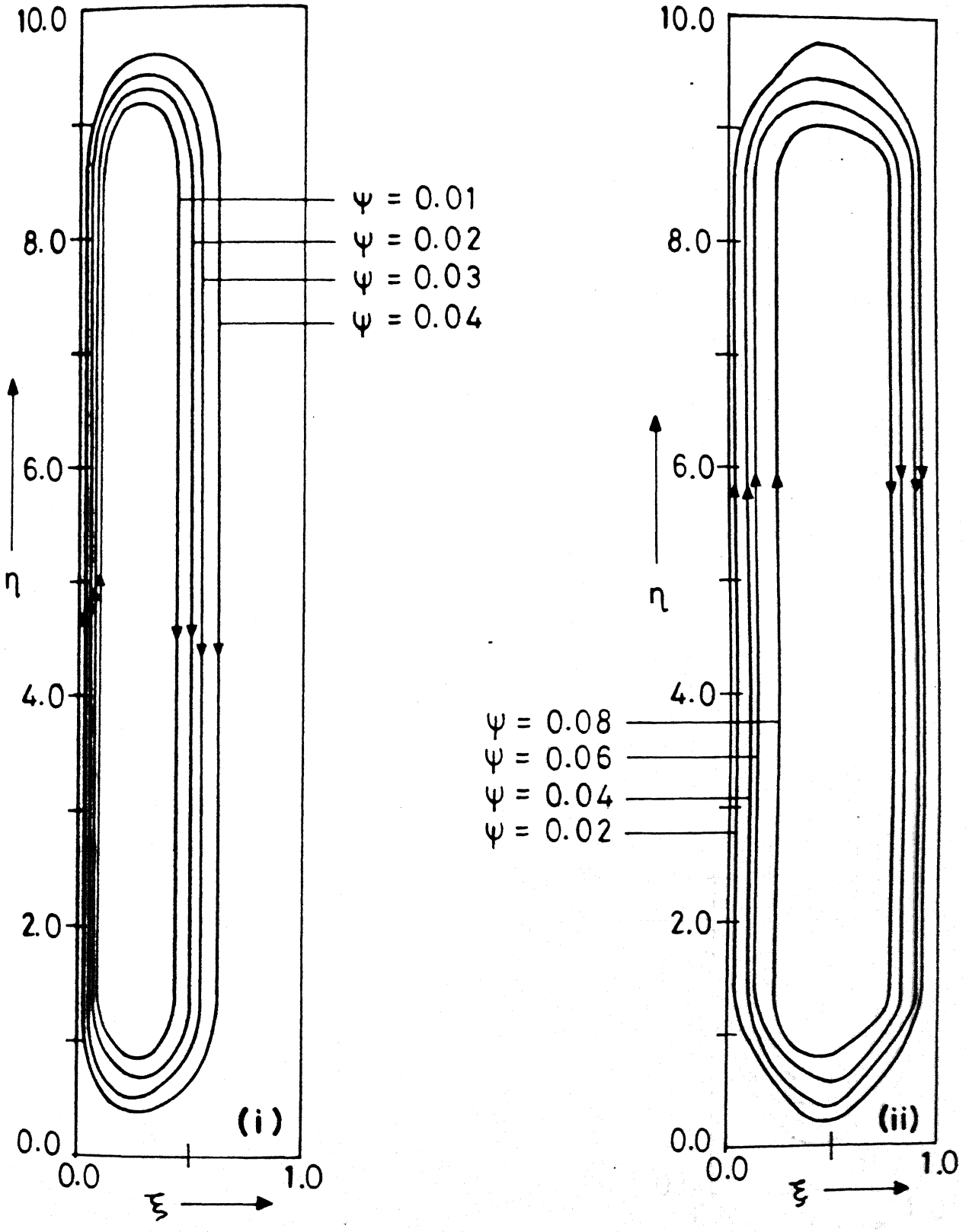

Figure 2 Streamlines for $Ra=10^6$, $Da=10^{-6}$, $As=10.0$, $Pr=1.0$.
(i) $\tau = 0.2$ (ii) $\tau = 1.8$

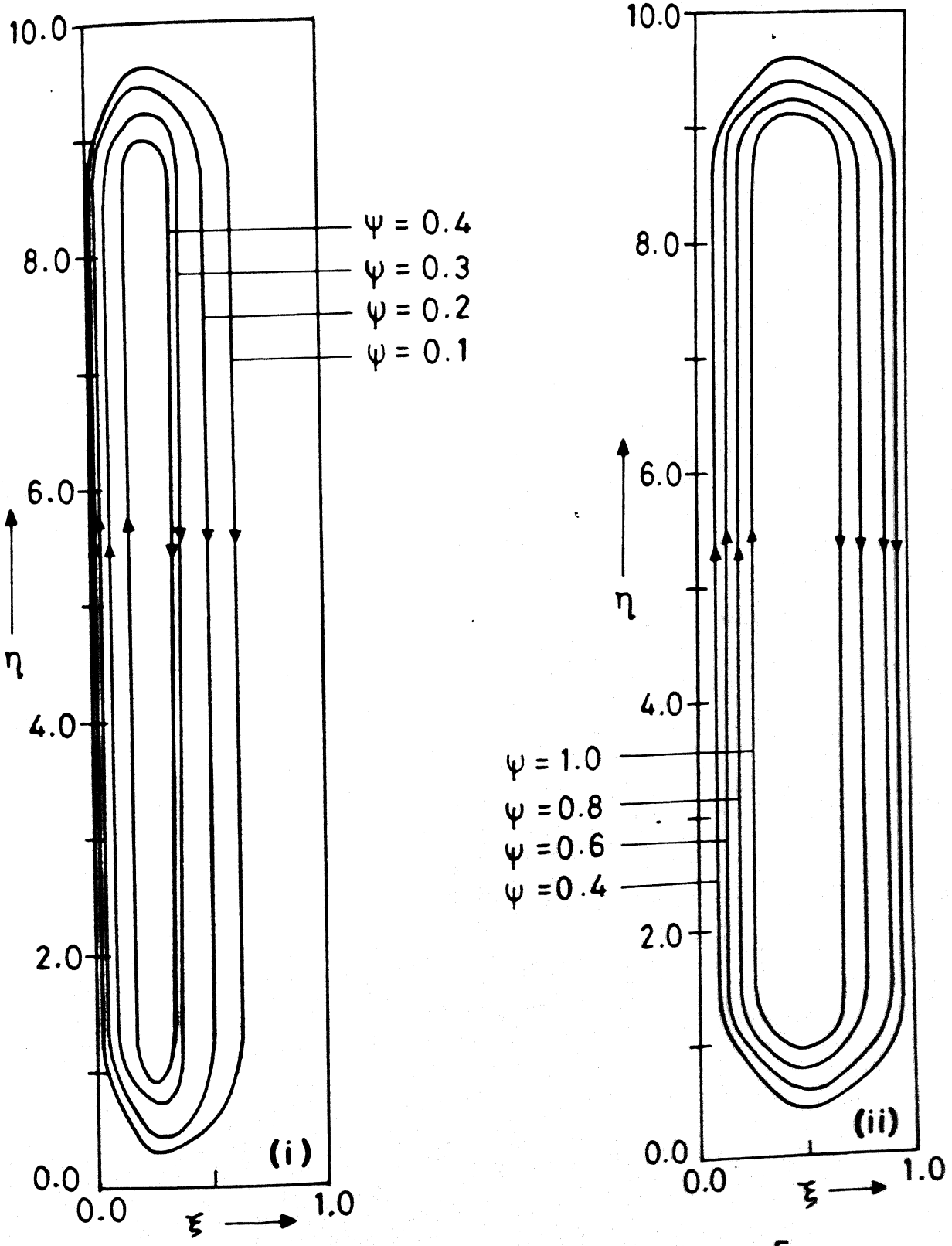

Figure 3 Streamlines for $Ra = 10^6$, $Da = 10^{-5}$, $As = 10.0$, $Pr = 1.0$. (i) $\tau = 0.2$ (ii) $\tau = 1.8$

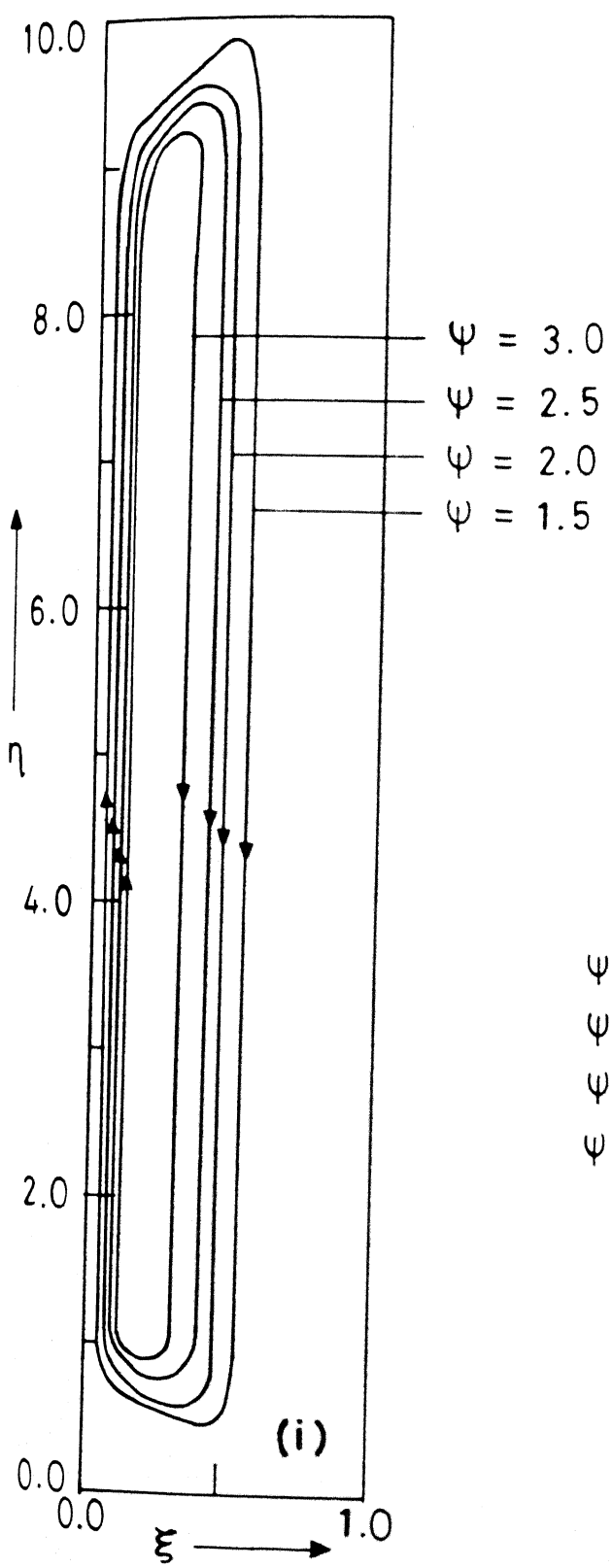

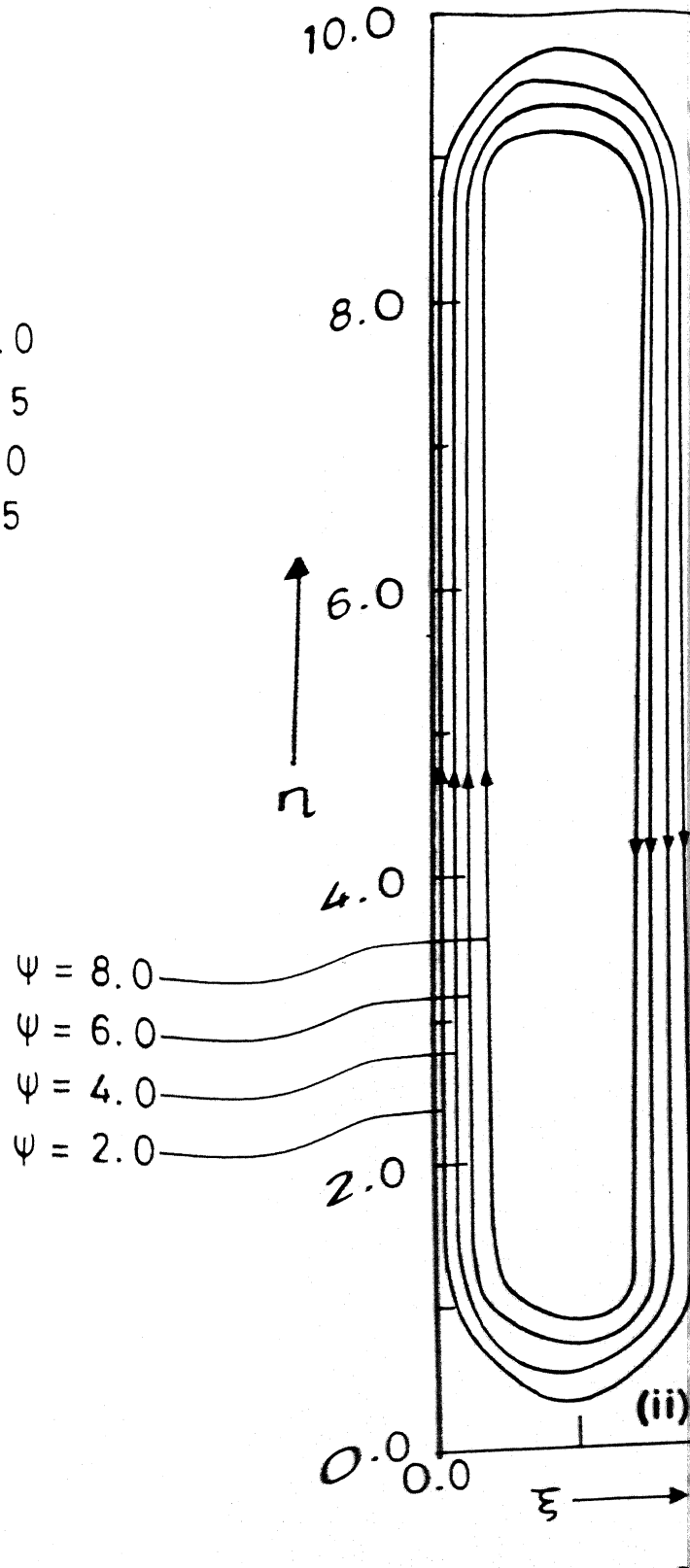

Figure 4 Streamlines for $Ra = 10^6$, $Da = 10^{-6}$, AS = 10.0, Pr = 1.0

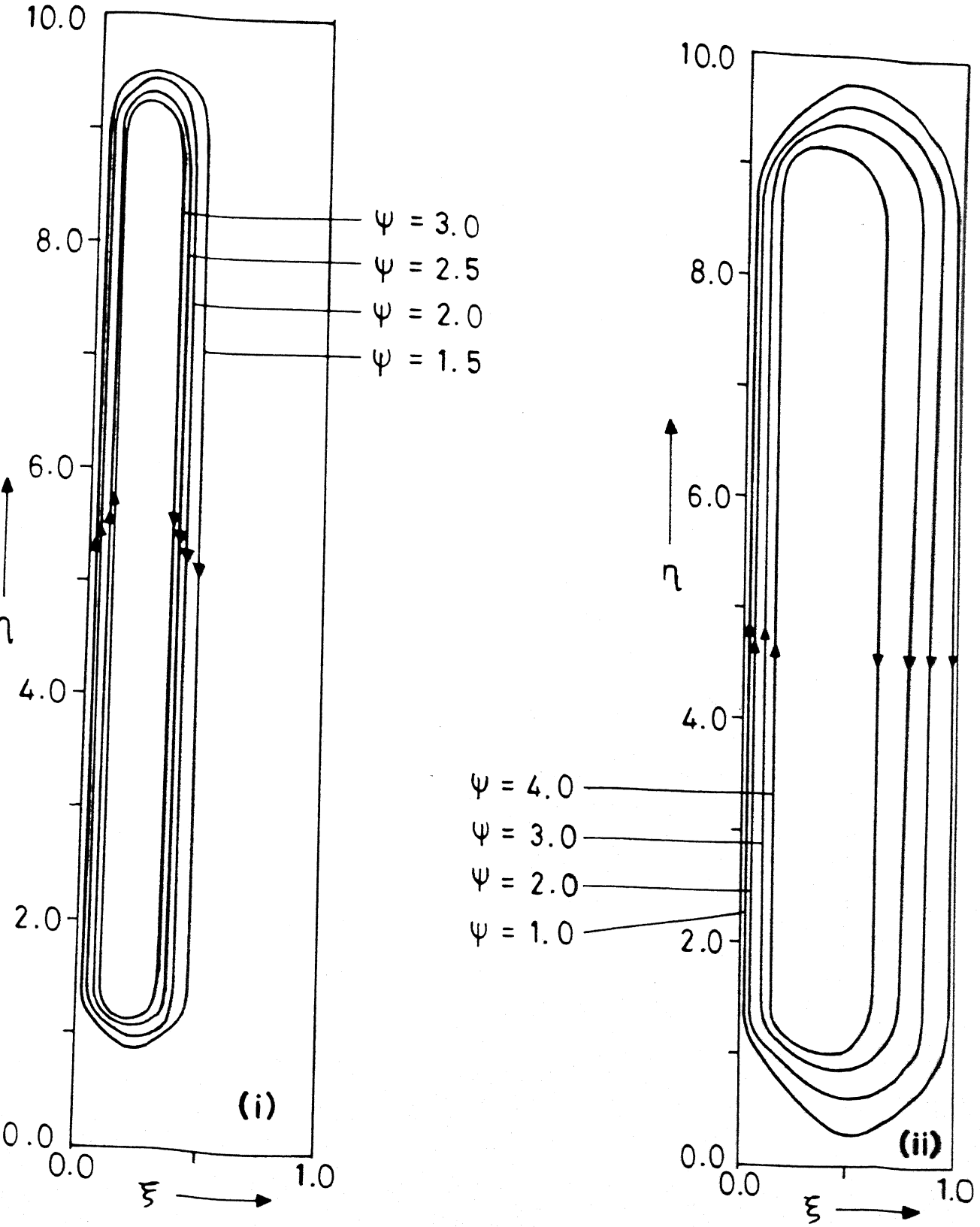

Figure 5 Streamline for $Ra=10^7$, $Da=10.0^{-4}$, $As=10.0$, $Pr=1.0$.
(i) $\tau = 0.2$ (ii) $\tau = 1.8$

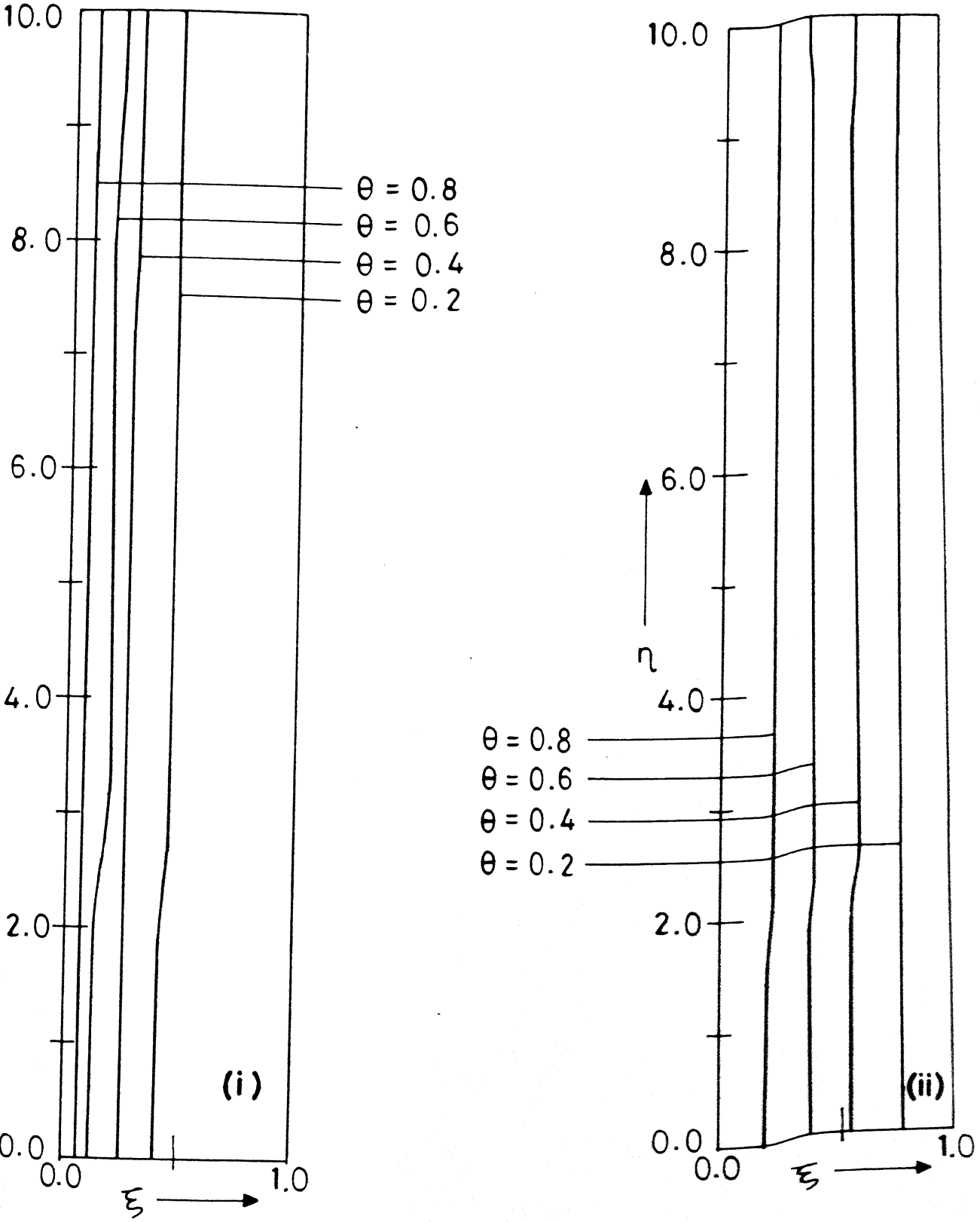

Figure 6 Isotherms for $Ra=10^6, Da=10^{-6}, As=10.0, Pr=1.0$

(i) $\tau = 0.2$ (ii) $\tau = 1.8$

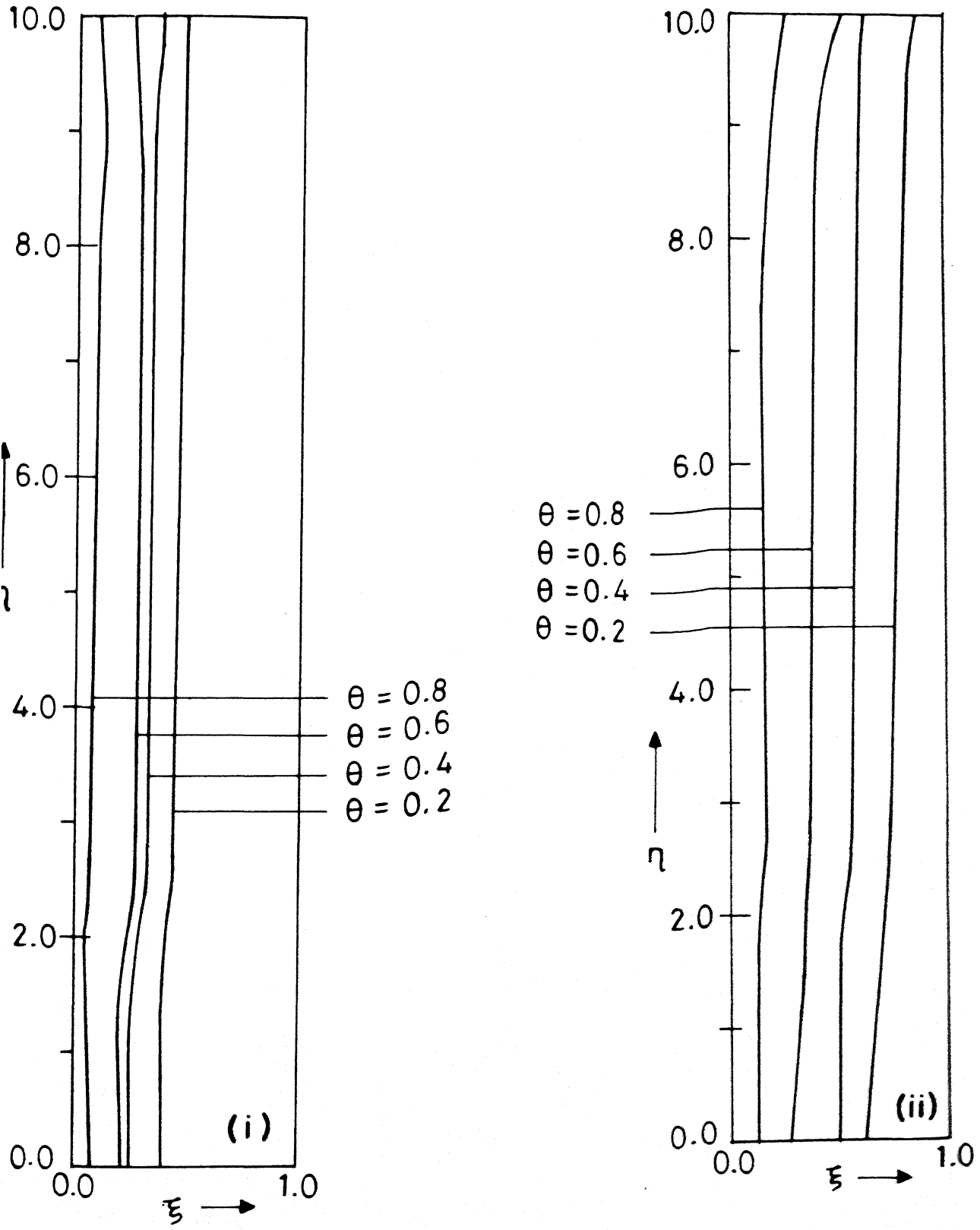

Figure 7 Isotherms for $Ra = 10^6$, $Da = 10^{-5}$, $As = 10.0$, $Pr = 1.0$ (i) $\tau = 0.2$, (ii) $\tau = 1.8$

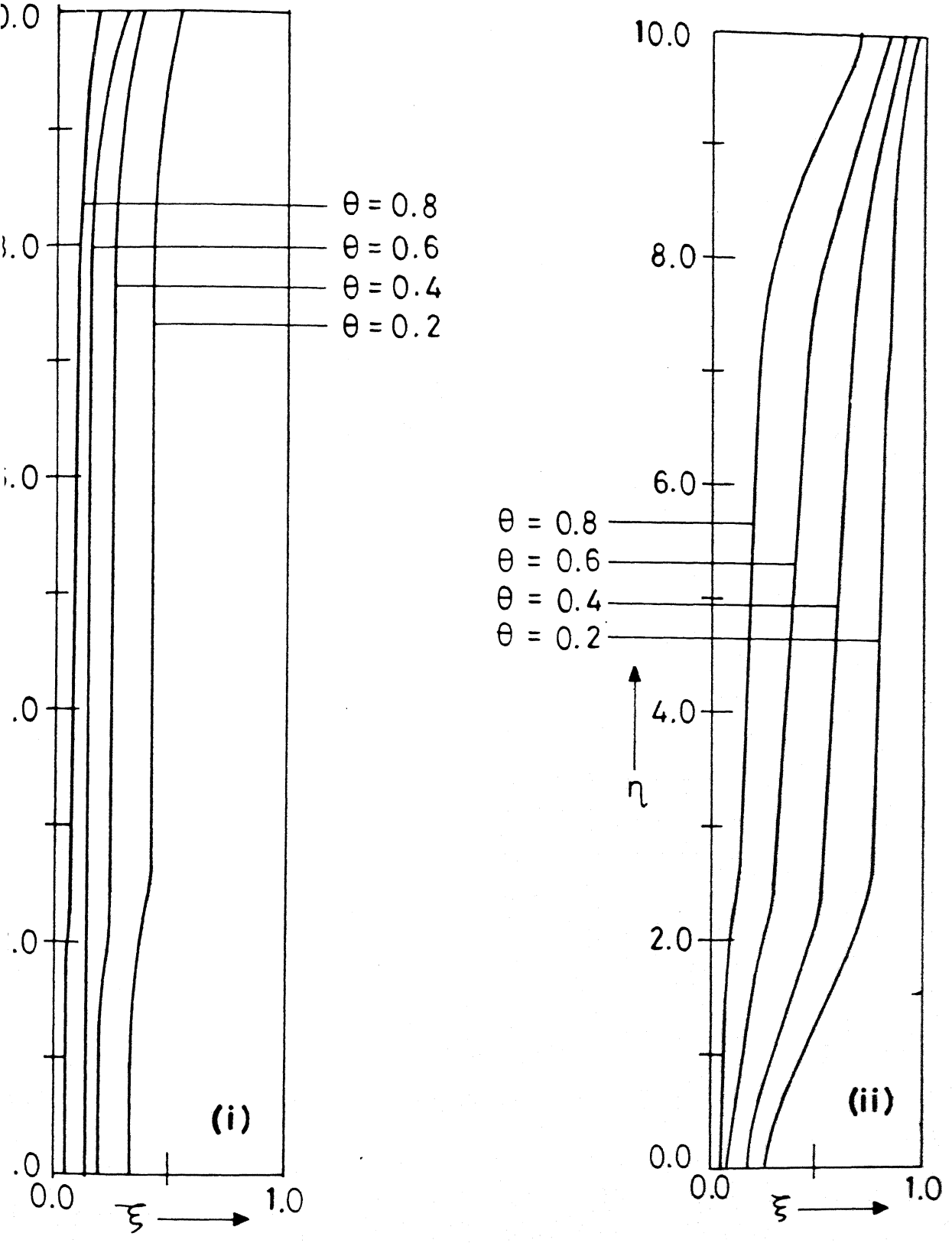

Figure 8 Isotherms for $Ra=10^6$, $Da=10^{-4}$, $As=10.0$, $Pr=1.0$.
(i) $\tau = 0.2$ (ii) $\tau = 1.8$

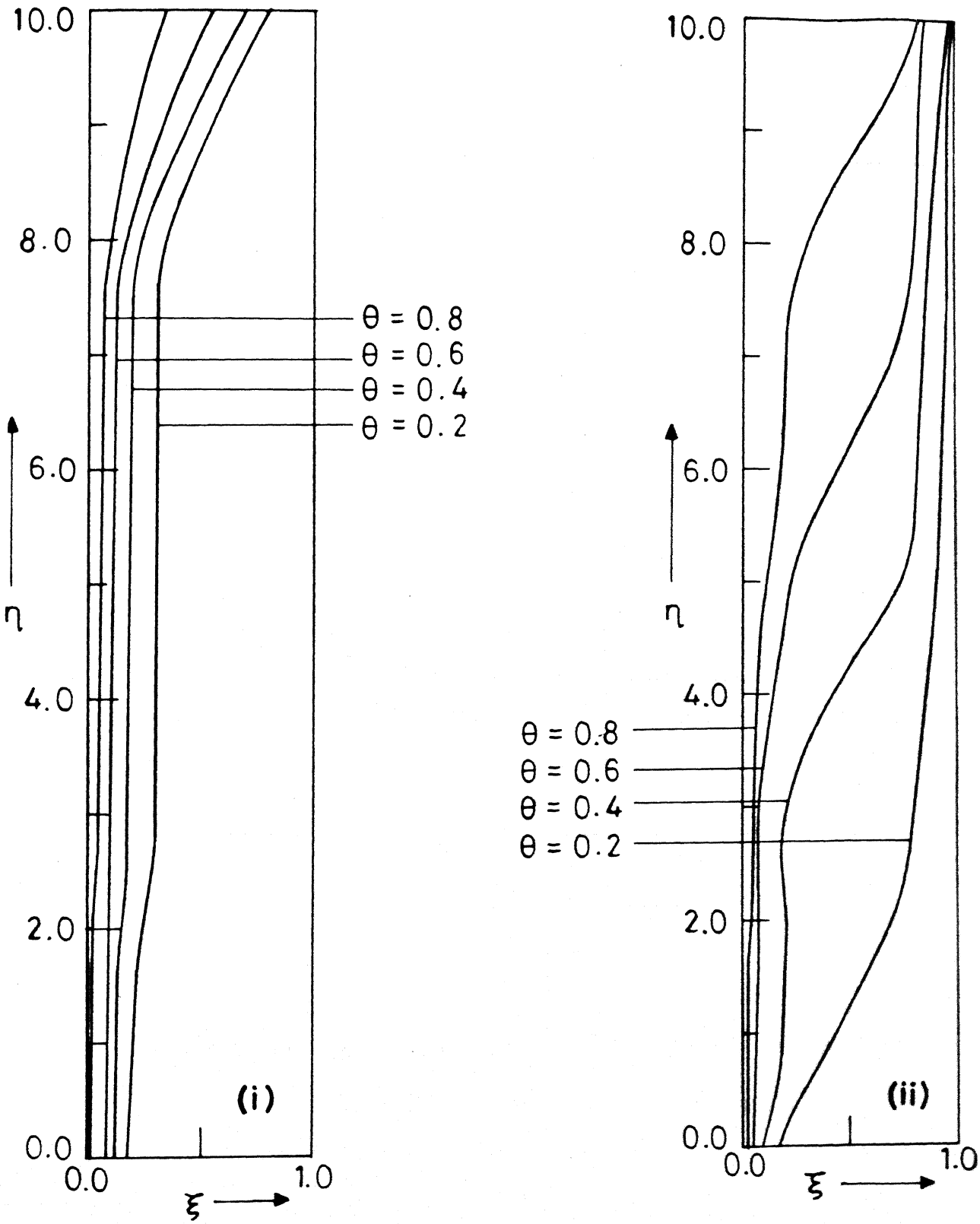

Figure 9 Isotherms for $Ra=10^7$, $Da=10^{-4}$, $As=10.0$, $Pr=1.0$.
(i) $\tau = 0.2$ (ii) $\tau = 1.8$

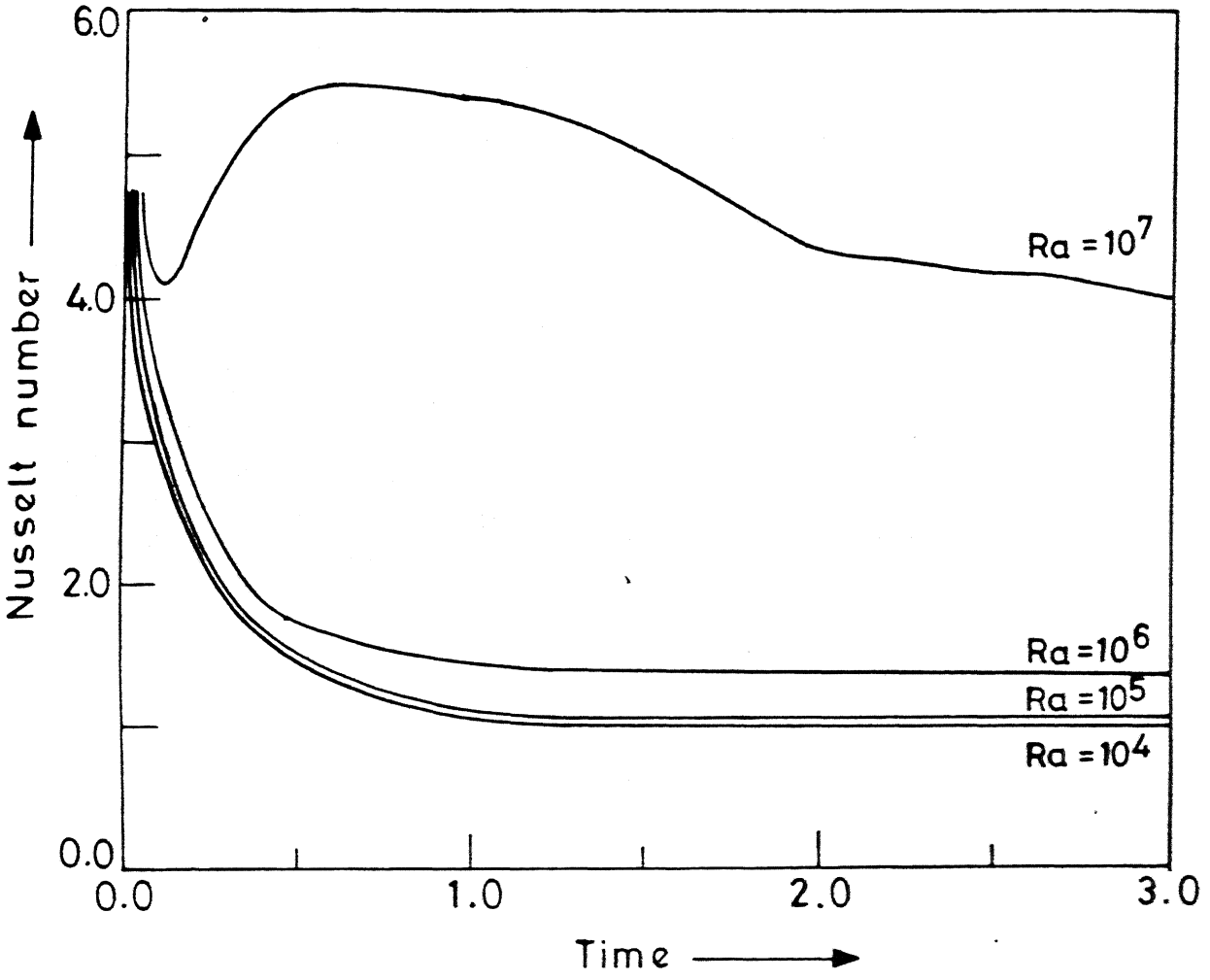

Figure 10 Nusselt number versus time for $Da = 10^{-4}$, As = 10.0, Pr = 1.0

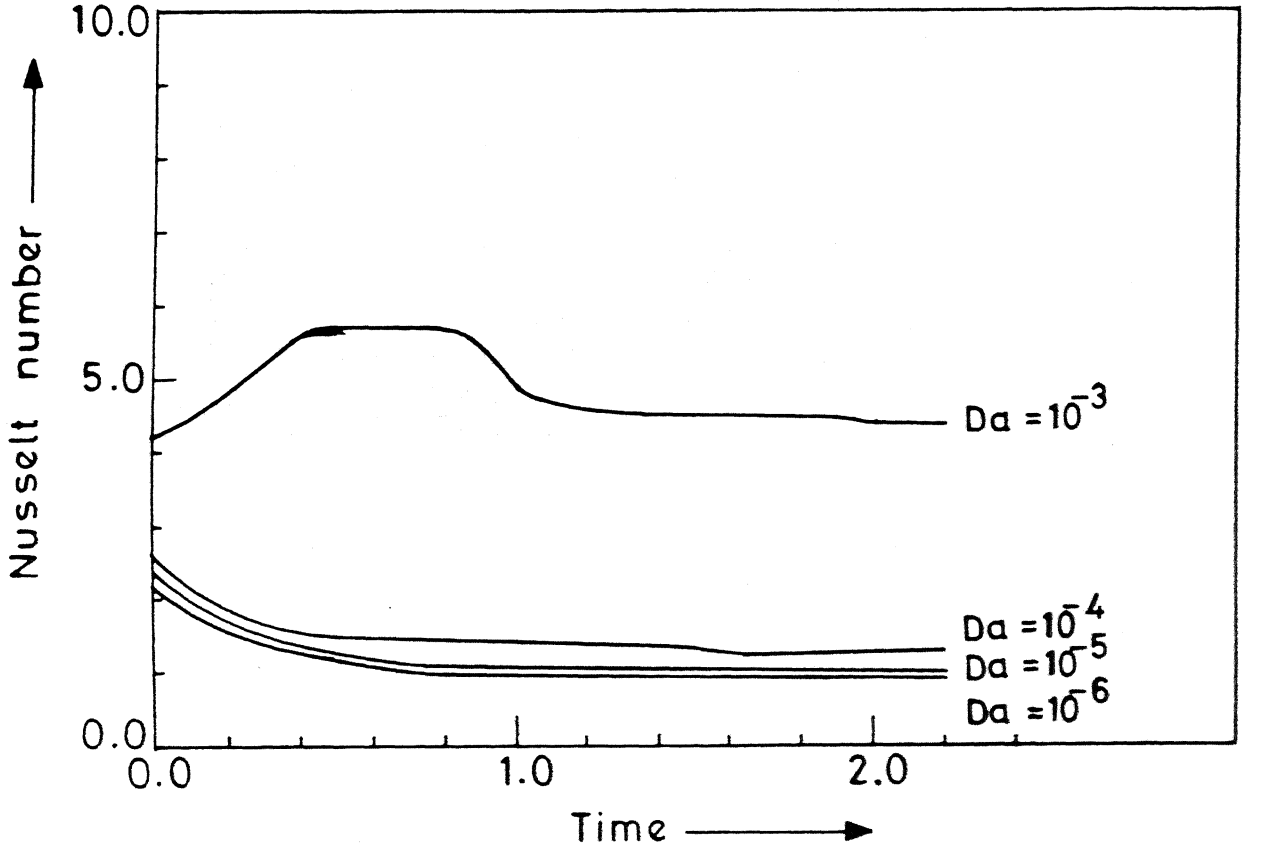

Figure 11 Nusselt number versus time for $Ra = 10^6$, $Pr = 1.0$, $As = 10.0$

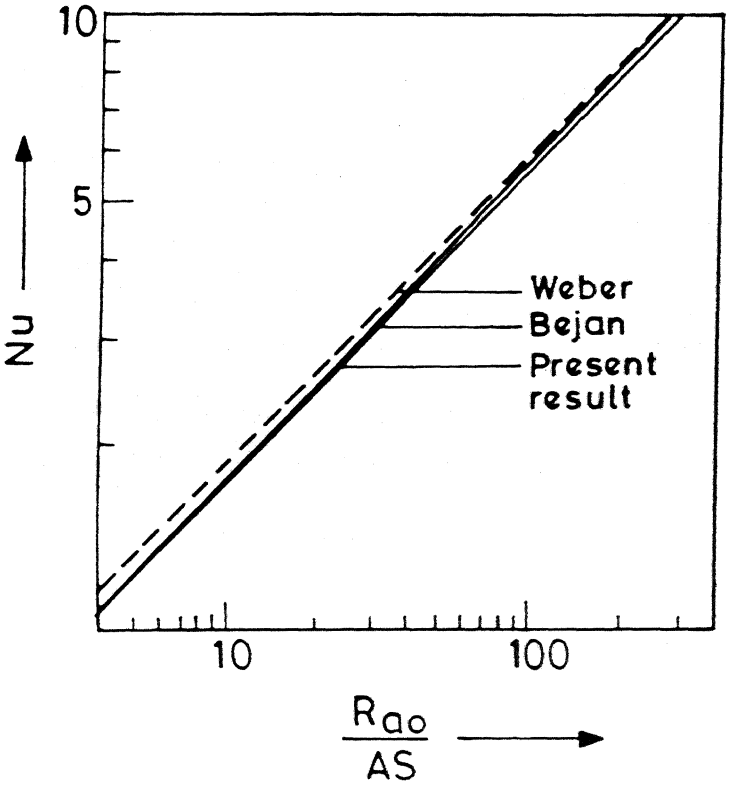

Figure 12 Nussult number (Nu) versus R_{ao}/AS.

CHAPTER V

FREE CONVECTION FLOW ALONG A MOVING VERTICAL WALL IN A POROUS MEDIUM

5.1 INTRODUCTION

Heat transfer from a vertical surface embedded in a saturated porous medium finds application in many branches of technology such as the power production from geothermal energy and the design of underground energy storage systems. The basic theory and much of the previous work in this area are found in the extensive review articles by Cheng [1] and Bejan [2]. Many of these studies deal with steady or unsteady boundary layer flows along vertical and horizontal surfaces.

The problem which deals with the flow of an incompressible, viscous fluid past an impulsively started infinite plate was first studied by Stokes [3] and the problem was later extended to bodies of different shapes as well as to viscous compressible fluids by a number of researchers. Closely related to the work reported in this chapter is the contribution of Soundalgekar [4], who has analysed the flow near an impulsively started infinite vertical plate, including the free convective effects caused by external heating or cooling of the plate.

The main aim of the present analysis is to study the flow of a viscous fluid through a saturated porous medium adjacent to a moving vertical infinite plate. Considering the wall temperature to be different from that of the fluid, the resulting

buoyancy-driven flow and the heat transfer in the fluid, are taken into account. The problem has an exact solution only for Pr $\geq$ 1. Therefore, the solution has been obtained here by the approximate momentum-integral method for Pr < 1 and numerically by the finite difference method based on the Crank-Nicolson scheme. The results obtained by the two methods compare well.

5.2 GOVERNING EQUATIONS

Consider unsteady flow of an incompressible viscous fluid through a porous medium bounded by an infinite vertical moving wall. A co-ordinate system is introduced with x-axis taken along the wall in the upward direction and y-axis perpendicular to it. The flow through the porous medium is assumed to be governed by the generalized Darcy's law. It is also assumed that the Boussinesq approximation is applicable to the present problem. The governing equations for the problem are,

$$\frac{\partial u}{\partial t} = g\beta\,(T - T_\infty) + \nu \frac{\partial^2 u}{\partial y^2} - \frac{\nu u}{K}\,, \tag{5.1}$$

$$\frac{\partial T}{\partial t} = \alpha \frac{\partial^2 T}{\partial y^2}\,, \tag{5.2}$$

where, u is the velocity in x-direction, t is the time, g is the acceleration due to gravity, β is the coefficient of volume expansion, K is the permeability of the porous medium, T is the temperature of the fluid, T_∞ is the ambient temperature of the fluid, ν is the kinematic viscosity and α is the thermal diffusivity.

The initial and boundary conditions are,

$$t = 0 \;:\; u = 0, \quad T = T_\infty; \quad y \geq 0,$$

$$y = 0 \;:\; u = u_0, \quad T = T_w; \quad t > 0, \tag{5.3}$$

$$y \to \infty \; : \; u \to 0, \quad T = T_\infty; \quad t > 0,$$

here, T_w and u_o are the temperature and the velocity of the plate espectively.

The following non-dimensional variables are introduced,

$$u = \frac{u}{u_o}, \quad y = \frac{y u_o}{\nu}, \quad t = \frac{t\, u_o^2}{\nu}, \quad \theta = \frac{T - T_\infty}{T_w - T_\infty},$$

$$Gr = \frac{\nu g \beta\, (T_w - T_\infty)}{u_o^3} \text{ (Grashof number)}, \tag{5.4}$$

$$Pr = \frac{\nu}{\alpha} \text{ (Prandtl number) and}$$

$$Da = \frac{u_o^2}{\nu^2} K \text{ (Darcy number).}$$

ubstituting (5.4) into (5.1) and (5.2), the non-dimensional quations are obtained as,

$$\frac{\partial u}{\partial t} = \frac{\partial^2 u}{\partial y^2} + Gr\, \theta - \frac{u}{Da}, \tag{5.5}$$

$$\frac{\partial \theta}{\partial t} = \frac{1}{Pr} \frac{\partial^2 \theta}{\partial y^2}. \tag{5.6}$$

ne initial and boundary conditions reduce to ,

$$\begin{aligned} &t = 0 : u = 0, \; \theta = 0, \; (y \geq 0), \\ &y = 0 : u = 1, \; \theta = 1, \; (t > 0), \\ &y \to \infty : u \to 0, \; \theta \to 0, \; (t > 0). \end{aligned} \tag{5.7}$$

.3 METHOD OF SOLUTION

Equation (5.6) has exact solution for all values of Pr, nereas the momentum equation (5.5) has exact solution for only Pr 1. Using Laplace transform technique, the solution of these quations is obtained [6] as follows:

$$\theta = \text{erfc}\left(\frac{y\sqrt{Pr}}{2\sqrt{t}}\right), \tag{5.8}$$

$$u = \frac{1}{2}(1 - Gr\ Da)\left(\exp\left[-y\sqrt{\frac{1}{Da}}\right]\operatorname{erfc}\left(\frac{y}{2\sqrt{t}} - \sqrt{\frac{t}{Da}}\right)\right.$$

$$\left. + \exp\left[y\sqrt{\frac{1}{Da}}\right]\operatorname{erfc}\left(\frac{y}{2\sqrt{t}} + \sqrt{\frac{t}{Da}}\right)\right) + \frac{GrDa}{2}\exp\left[\frac{t/Da}{Pr-1}\right]$$

$$x\left(\exp\left[-y\sqrt{\frac{Pr}{Da\,(Pr-1)}}\right]\left(\operatorname{erfc}\left(\frac{y}{2\sqrt{t}} - t\sqrt{\frac{Pr}{Da\,(Pr-1)}}\right)\right.\right.$$

$$\left.\left. - \operatorname{erfc}\left(\frac{y}{2}\sqrt{\frac{Pr}{t}} - \sqrt{\frac{t}{Da\,(Pr-1)}}\right)\right) + \exp\left[y\sqrt{\frac{Pr}{(Pr-1)\,Da}}\right]\right.$$

$$\left. x\left(\operatorname{erfc}\left(\frac{y}{2\sqrt{t}} + \sqrt{\frac{Pr\ t}{Da\,(Pr-1)}}\right) - \operatorname{erfc}\left(\frac{y}{2}\sqrt{\frac{Pr}{t}} + \sqrt{\frac{t}{Da\,(Pr-1)}}\right)\right)\right)$$

$$+ Gr\ Da\ \operatorname{erfc}\left(\frac{y}{2}\sqrt{\frac{Pr}{t}}\right), \quad \text{for } Pr \neq 1 \text{ and} \qquad (5.9)$$

$$u = \frac{1}{2}(1 - Gr\ Da)\left[\exp\left[-y\sqrt{\frac{1}{Da}}\right]\operatorname{erfc}\left(\frac{y}{2\sqrt{t}} - \sqrt{\frac{t}{Da}}\right)\right.$$

$$\left. + \exp\left[y\sqrt{\frac{1}{Da}}\right]\operatorname{erfc}\left(\frac{y}{2\sqrt{t}} + \sqrt{\frac{t}{Da}}\right)\right]$$

$$+ Gr\ Da\ \operatorname{erfc}\left(\frac{y}{2\sqrt{t}}\right), \text{ for } Pr = 1. \qquad (5.10)$$

For $Pr < 1$, the equation (5.5) has no exact solution. Thus, the main interest of the present study is to give the complete solution of these equations. Consequently, the governing equations are solved by finite difference method and the momentum integral method for $Pr < 1$.

(a) Integral Method

In this method, the velocity and temperature profiles are chosen so as to vary smoothly from the prescribed values at the surface and blend into the free stream values at the edge of the boundary layer. A non-dimensional shape profile is assumed and integrated over the boundary layer thickness, so that the local inaccuracies do not play a significant role.

Let δ_1 be the thickness of thermal boundary layer and δ_2 be the thickness of viscous boundary layer. Since the situation

under consideration pertains to Pr < 1, it may be concluded that $\delta_1 > \delta_2$.

Integrating equation (5.5) with respect to y, from y = 0 to δ_2, one gets,

$$\int_0^{\delta_2} \frac{\partial u}{\partial t}\, dy = -\left(\frac{\partial u}{\partial y}\right)_{y=0} + Gr \int_0^{\delta_1} \theta\, dy - \frac{1}{Da} \int_0^{\delta_2} u\, dy. \qquad (5.11)$$

A third order profile is assumed for u in the form

$$u = b_o + b_1\eta + b_2\eta^2 + b_3\eta^3, \qquad (5.12)$$

where, $\eta = y/\delta_2$. The coefficients b_o, b_1, b_2 and b_3 are, in general, functions of t and are to be determined with the help of boundary and initial conditions (5.7) and the smoothness condition $\frac{\partial u}{\partial y} = 0$ at $y = \delta_2$. In addition to this, we use the following condition,

$$\frac{\partial^2 u}{\partial y^2} + Gr\,\theta - \frac{u}{Da} = 0, \qquad (5.13)$$

which is obtained by evaluating the momentum equation at y = 0.

The expression for u, thus takes the final form,

$$u = \left(1 - \frac{3}{2}\eta + \frac{1}{2}\eta^3\right) - \frac{A\delta_2}{4}\left(\eta - 2\eta^2 + \eta^3\right), \qquad (5.14)$$

where, $A = \frac{1 - GrDa}{Da}$.

For θ, a third order profile is assumed which can be expressed as:

$$\theta = 1 - \frac{3}{2}\frac{y}{\delta_1} + \frac{1}{2}\frac{y^3}{\delta_1^3}, \qquad (5.15)$$

where, $\delta_1 = 2\sqrt{2}\ \sqrt{t/Pr}$.

The above profile satisfies the temperature conditions of equation (5.7), the smoothness condition $\frac{\partial\theta}{\partial y} = 0$ at $y = \delta_1$ and an

additional condition $\frac{\partial^2\theta}{\partial y^2} = 0$, at y = 0 which results from evaluating equation (5.6) at y = 0.

Substituting (5.14) and (5.15) in (5.11) and integrating, one gets:

$$\frac{d\delta_2}{dt}(18 - 3A\,\delta_2^2) = \frac{1}{\delta_2}(72 + 12\,A\,\delta_2^2) + 36\,Gr\sqrt{2t/Pr} - \frac{\delta_2}{Da}(18 - A\,\delta_2^2) . \qquad (5.16)$$

This equation can be reduced to the form,

$$\frac{dz}{dt} = \{(144+24Az) + 101.82337\,Gr\sqrt{\frac{zt}{Pr}} - \frac{z}{Da}(36-2Az)\}/(18-3Az), \qquad (5.17)$$

where, $z = \delta_2^2$.

The values of z are obtained by the fourth-order Runge Kutta method. The expression for skin-friction, τ, at the wall is given by:

$$\tau = -(\frac{\partial u}{\partial y})_{y=0} = \frac{3}{2\delta_2} + \frac{A\delta_2}{4} . \qquad (5.18)$$

(b) Finite Difference Method

To obtain the solution by finite difference method, a region adjacent to the wall which is sufficiently large to include both the viscous and the thermal boundary layers is taken as the solution domain. This domain is divided into steps of equal size Δy in the y-direction, with grid points placed at the wall as well as the far stream boundary. In order to obtain the transient variation in the solution, time is incremented in equal steps of Δt. Since the dependent variables u and θ are functions of two independent variables y and t, two subscripts are used to specify

the value of u and θ at a given point at any time, say for instance, $u(x_i, t_j) = u_{j,j}$.

The difference equations corresponding to (5.5) and (5.6) are,

$$\frac{u_{i,j+1} - u_{i,j}}{\Delta t} = \frac{1}{2}\left[\frac{u_{i-1,j} - 2u_{i,j} + u_{i+1,j}}{(\Delta y)^2} + \frac{u_{i-1,j+1} - 2u_{i,j+1} + u_{i+1,j+1}}{(\Delta y)^2}\right] + Gr\ \theta_{i,j} - \frac{1}{2Da}\left[u_{i,j} + u_{i,j+1}\right], \tag{5.19}$$

$$\frac{\theta_{i,j+1} - \theta_{i,j}}{\Delta t} = \frac{1}{2Pr}\left[\frac{\theta_{i-1,j} - 2\theta_{i,j} + \theta_{i+1,j}}{(\Delta y)^2} + \frac{\theta_{i-1,j+1} - 2\theta_{i,j+1} + \theta_{i+1,j+1}}{(\Delta y)^2}\right]. \tag{5.20}$$

These equations lead to the following relationships between the values of u and θ at six points (in space-time domain),

$$-\lambda_1 u_{i-1,j+1} + (1+2\lambda_1 + \frac{\Delta t}{2Da})\, u_{i,j+1} - \lambda_1 u_{i+1,j+1} = \lambda_1 u_{i-1,j} + (1-2\lambda_1 - \frac{\Delta t}{2Da})\, u_{i,j} + \lambda_1 u_{i+1,j} + Gr\ \theta_{i,j}\, \Delta t, \tag{5.21}$$

$$-\lambda_2 \theta_{i-1,j+1} + (1+2\lambda_2)\, \theta_{i,j+1} - \lambda_2 \theta_{i+1,j+1} = \lambda_2 \theta_{i-1,j} + (1-2\lambda_2)\, \theta_{i,j} + \lambda_2 \theta_{i+1,j}, \tag{5.22}$$

where, $\lambda_1 = \dfrac{\Delta t}{2(\Delta y)^2}$, $\lambda_2 = \dfrac{\Delta t}{2Pr\ (\Delta y)^2}$.

The initial and boundary conditions take the following form,

$$u_{i,o} = 0 \quad \text{and} \quad \theta_{i,o} = 0; \quad \text{for all } i,$$

$$u_{o,j} = 1 \quad \text{and} \quad \theta_{o,j} = 1; \quad \text{for all } j \neq 0, \tag{5.23}$$

$$u_{M,j} = 0 \quad \text{and} \quad \theta_{M,j} = 0; \quad \text{for all } j.$$

where M is the grid point on the far stream boundary.

At any time level, the above difference equations will be solved once for each point $1 \leq i \leq M-1$, resulting in a system of M-1 simultaneous equations in M-1 unknowns, for each of the variables u and θ. The equations exhibit a tridiagonal structure as follows:

$$(1+2\lambda_1 + \frac{\Delta t}{2Da})\, u_{1,j+1} - \lambda_1\, u_{2,j+1}$$
$$= \lambda_1\, u_{o,j+1} + \lambda_1\, u_{o,j} + (1-2\lambda_1 - \frac{\Delta t}{2Da})\, u_{1,j}$$
$$+ \lambda_1\, u_{2,j} + Gr\, \Delta t\, \theta_{1,j}, \tag{5.24}$$

$$-\lambda_1\, u_{i-1,j+1} + (1+2\lambda_1 + \frac{\Delta t}{2Da})\, u_{i,j+1} - \lambda_1\, u_{i+1,j+1}$$
$$= \lambda_1\, u_{i-1,j} + (1-2\lambda_1 - \frac{\Delta t}{2Da})\, u_{i,j} + \lambda_1\, u_{i+1,j}$$
$$+ Gr\, \Delta t\, \theta_{i,j}, \quad \text{for } 2 \leq i \leq M-2 \text{ and} \tag{5.25}$$

$$-\lambda_1\, u_{M-2,j+1} + (1+2\lambda_1 + \frac{\Delta t}{2Da})\, u_{M-1,j+1}$$
$$= \lambda_1\, u_{M,j+1} + \lambda_1\, u_{M-2,j} + (1-2\lambda_1 - \frac{\Delta t}{2Da})\, u_{M-1,j}$$
$$+ \lambda_1\, u_{M,j} + Gr\, \Delta t\, \theta_{M-1,j}. \tag{5.26}$$

$$(1+2\lambda_2)\, \theta_{1,j+1} - \lambda_2\, \theta_{2,j+1}$$
$$= \lambda_2\, \theta_{o,j+1} + \lambda_2\, \theta_{o,j} + (1-2\lambda_2)\, \theta_{1,j} + \lambda_2 \theta_{2,j}, \tag{5.27}$$

$$-\lambda_2\, \theta_{i-1,j+1} + (1+2\lambda_2)\, \theta_{i,j+1} - \lambda_2\, \theta_{i+1,j+1}$$
$$= \lambda_2\, \theta_{i-1,j} + (1-2\lambda_2)\, \theta_{i,j} + \lambda_2\, \theta_{i+1,j}, \text{ for } 2 \leq i \leq M-2 \tag{5.28}$$

$$-\lambda_2\, \theta_{M-2,j+1} + (1+2\lambda_2)\, \theta_{M-1,j+1} = \lambda_2\, \theta_{M,j+1}$$
$$+ \lambda_2\, \theta_{M-2,j} + (1-2\lambda_2)\, \theta_{M-1,j} + \lambda_2\, \theta_{M,j}. \tag{5.29}$$

The above system of equations have been solved by applying the tridiagonal matrix algorithm, once for the θ-equations and then for the u-equations.

5.4 RESULTS AND DISCUSSION

For the problem under consideration, the solution domain extends from y = 0 to ∞, in reality. However, calculations can be restricted to a smaller domain by observing that the analytical solutions of equations (5.5) and (5.6) which exist for Pr $\geq$ 1 are close tozero around y $\simeq$ 4.0, and at all points after this. Similar results are also found in most of the flow problems over infinite plates. Reference in this regard may be made to the works of Soundalgekar [4] and Georgantopoulas et al. [5]. Therefore, although any value of y greater than 4.0 can be chosen to represent ∞, in order to save computational time, it would be better to take an acceptably small value of y at which both u and θ reduce to zero. In the present calculations, y_{max} = 5.0 is considered as the far-stream boundary.

In the computations, Δy and Δt have been taken as 0.1 and 0.005, respectively. Transient calculations have been continued till t = 1.0. The parameter values considered are:

Pr = 0.71, 1.0, 7.0, Da = 0.25, 1.0, 4.0 and Gr = 1.0, 2.0.

To check the correctness of taking y_{max}= 5.0 as infinity, the program was run for y_{max} = 6.0 and 7.0 and very little changes were observed in the temperature and velocity profiles, for the time values considered in the problem. To judge the accuracy of the results predicted, different values of Δy and Δt have been considered and it was verified that the step sizes employed in our calculations produce sufficiently accurate results. The

convergence of the numerical scheme is thus tested. Finally, the skin - friction at the wall has been calculated by numerical differentiation, using Newton's interpolation formula.

Figure 1, shows the results obtained by the momentum integral method and the finite difference method using Crank-Nicolson scheme. The flow velocity along the plate has been plotted with respect to t, at differnt y-locations. The results obtained by the two methods compare well. It is also observed that the velocity tends to reach a steady value with time, although the time taken for such a stage increases with y.

Raptis and Singh [6] have obtained the velocity field using explicit differencing. Since it is well known that the explicit differencing in finite difference method produces only results which have an accuracy of $O(\Delta t)$, we have used the Crank-Nicolson scheme which is semi-implicit in nature. The Crank-Nicolson scheme produces results which are $O(\Delta t^2)$ accurate. There are, however, time step restrictions for both procedures to achieve numerically stable results.

Figure 2, shows the velocity field, for different values of Da and Gr. Positive values of Gr have been considered which correspond to the case of heating of the plate. As expected, the velocity of the fluid increases with Gr, due to the greater role played by buoyancy forces. The velocity of the fluid increases with an increase in the value of permeability parameter also, since pore space increases with Da offering less resistance to flow.

In figure 3, the variation in the velocity field for various values of Pr are shown. It is clear from the graph that the

velocity at a point is increased as the value of Pr is decreased. This may be attributed to the fact that at a lower value of Pr, the penetration of thermal effects is deeper due to larger thermal diffusivity. The increased thermal penetration results in an enhanced role for the buoyancy forces. As a consequence, the velocity values are larger.

In figure 4, the transient velocity variation is shown for various Prandtl numbers. The value of velocity for every Pr starts from a minimum value and then increases with time as the fluid adjacent to the wall gets heated up.

Table 1: Numerical values of skin-friction for Gr = 1.0, Pr = 0.71

t	Da	τ (Ref.[6])	τ (Finite difference)	τ (integral method)
0.2	1.0	1.2447	1.2360	1.1654
0.2	4.0	1.0596	1.0828	0.9574
0.4	1.0	0.8664	0.8631	0.8117
0.4	4.0	0.6030	0.6331	0.5171

The values of skin-friction (dimensionless shear stress) obtained by various methods are compared in Table 1, for Gr = 1.0, Pr = 0.71 and for different values of t and Da. The skin-friction obtained by the integral method differs from finite difference values by about 6% for Da = 1.0 while this difference becomes about 10% for Da = 4.0.

It is observed that the value of τ increases as Da decreases. This is due to the fact that the resistance to flow offered by the porous medium is higher at lower values of permeability, which in turn, results in steeper boundary layers leading to higher skin-friction. It is also observed that the skin-friction

decreases with time, since the boundary layer thickness increases.

5.5 CONCLUSION

The free convection effects are studied on flow due to the impulsive motion of an infinite vertical plate embedded in a porous medium. The problem has exact solution for $Pr \geq 1$, but for $Pr < 1$, there is no exact solution. Here, results for $Pr < 1$ have been predicted by the approximate momentum-integral method and in general, by the finite difference method. The integral method solution is seen to be sufficiently accurate for low value of Darcy number.

REFERENCES

[1] Cheng, P., Heat transfer in geothermal systems, Advances in Heat Transfer,14, 1, 1978.

[2] Bejan, A., Progress in Heat Transfer report CUMER 80-1, Department of Mechanical Engineering, University of Colarado, Boulder.

[3] Stokes, G.C., Camb. Phil. Trans., Ix, 8, 1951.

[4] Soundalgekar, V.M., J. Heat Transfer, 99, 499, 1977.

[5] Georgantopoulos, G.A., Douskos, G.A., Kafousis, C.A. and Goudas, C.L., Hydrodynamic free convection effect on the Stokes problem for an infinite vertical plate, Letters in Heat and Mass Transfer, 6, 397, 1979.

[6] Raptis, A.A. and Singh, A.K., Free Convection flow past an impulsively started vertical plate in a porous medium by finite difference method, Astrophysics and Space Science, 112, 259, 1985.

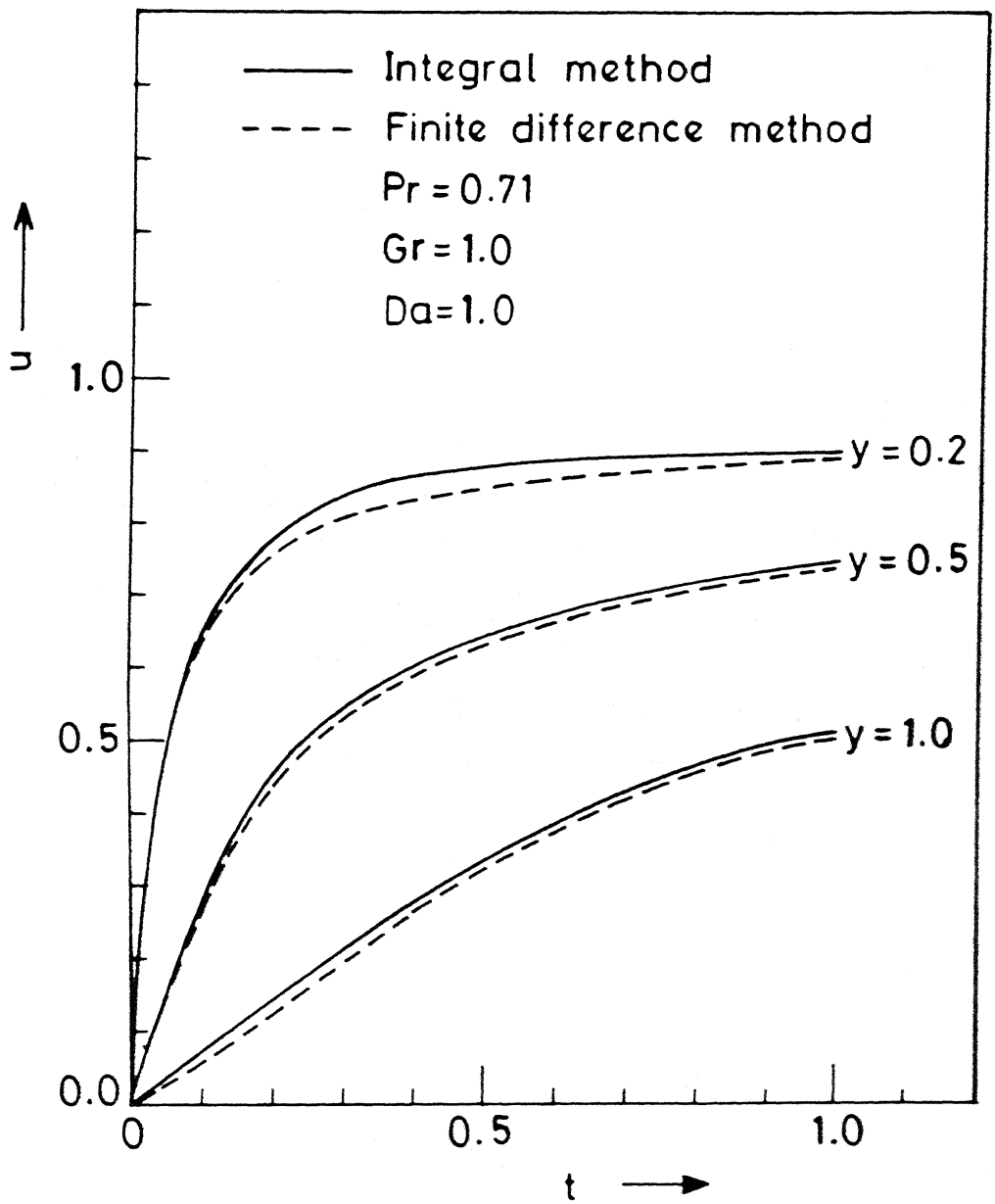

Figure 1 Comparison of velocity profile by two methods.

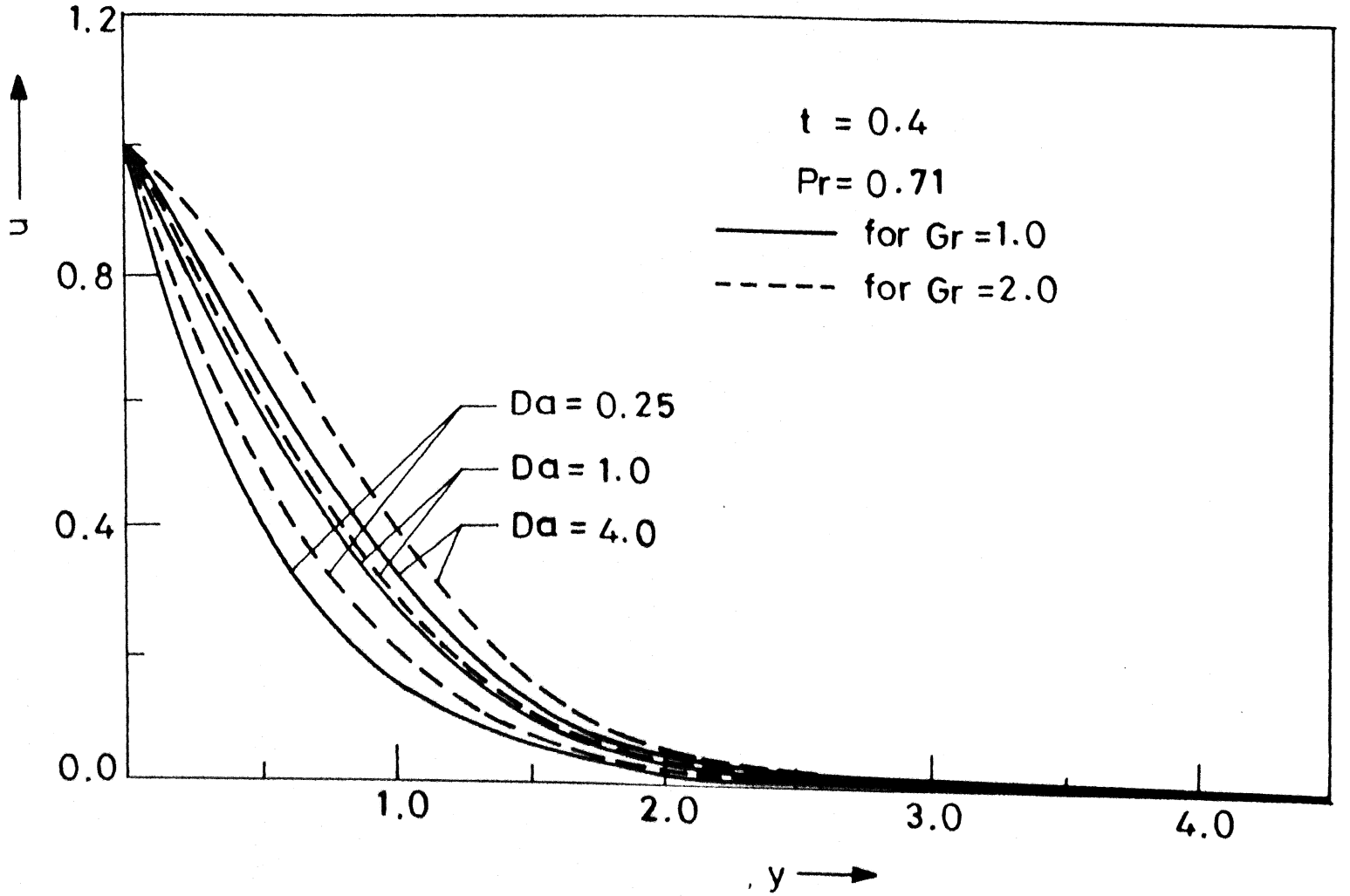

Figure 2 Velocity Profiles for Pr=0.71 and for various values of Da.

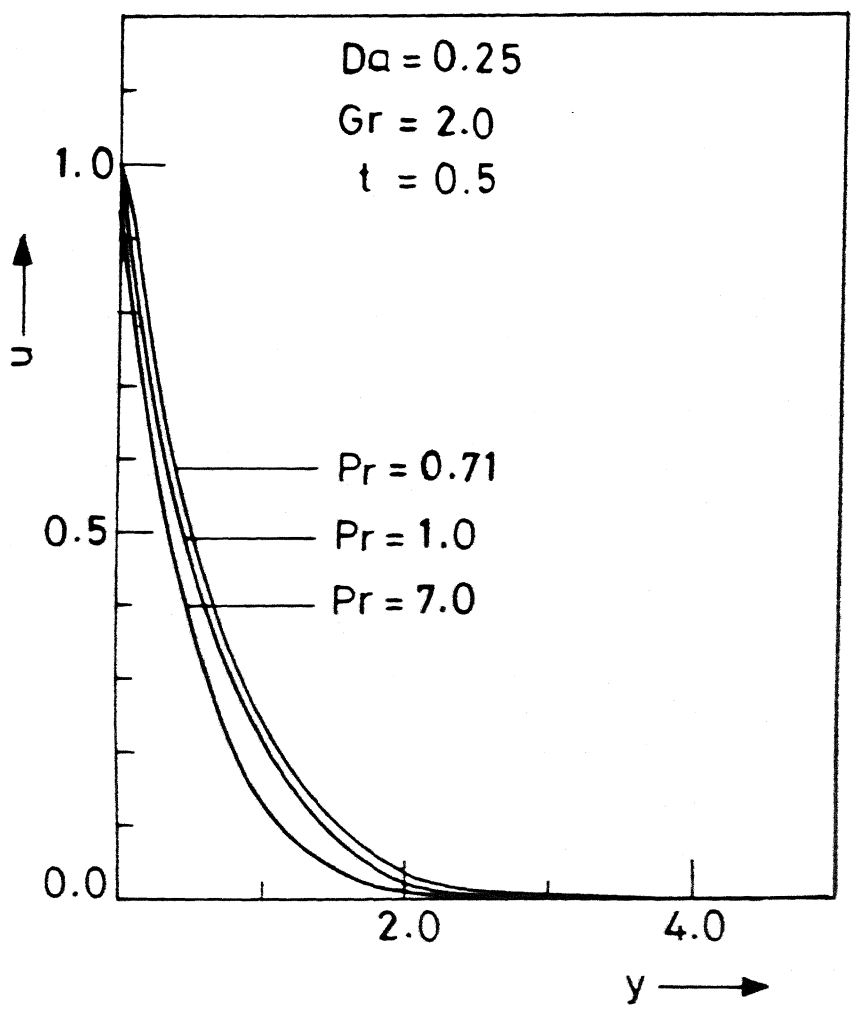

Figure 3 Velocity Profiles for various values of Pr.

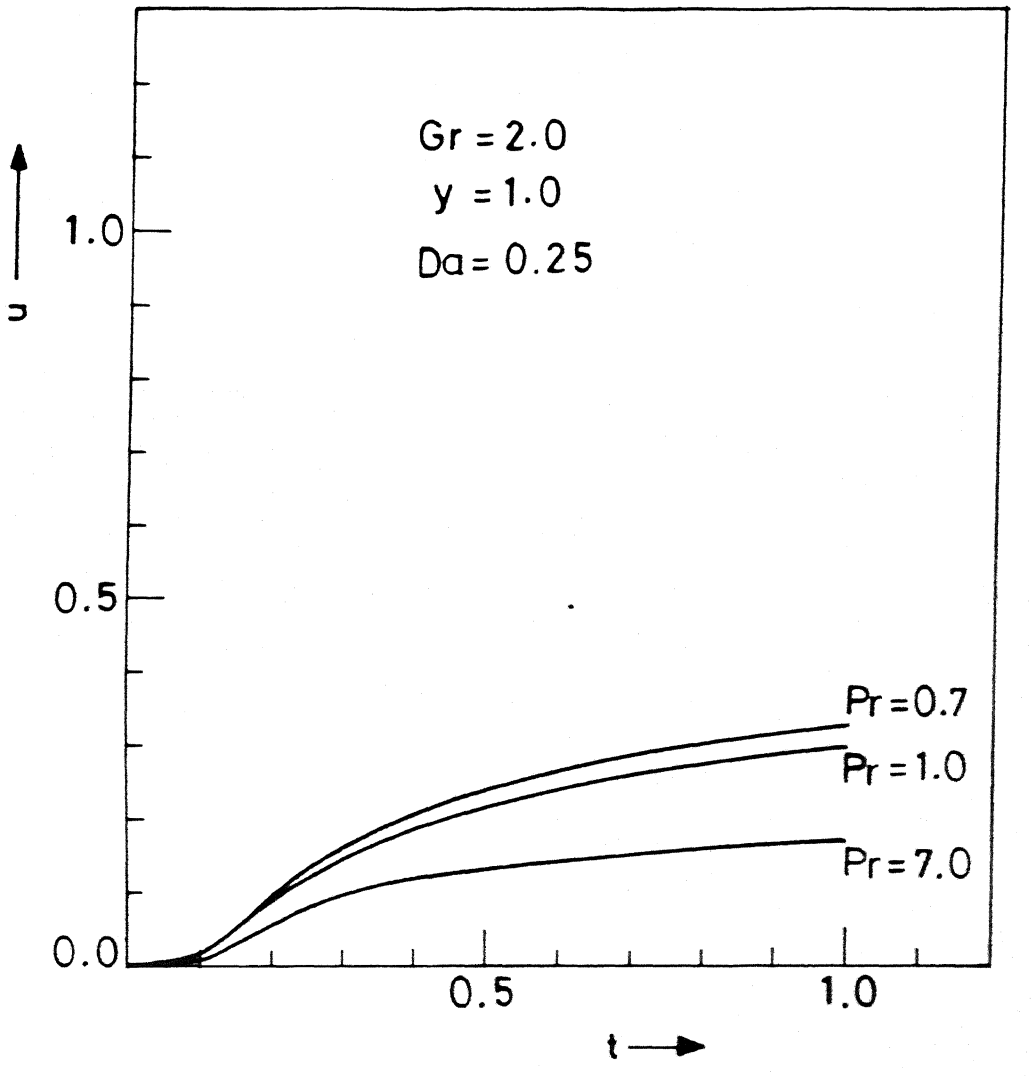

Figure 4 Velocity Profiles for various values of Pr.